# Nonuniform sampling of time-limited signals using time-scale localisation properties of wavelet transforms

*A Thesis Submitted*

*in Partial Fulfillment of the Requirements*

*for the Degree of*

*Doctor of Philosophy*

*by*

*Chaveli Ramesh*

*to the*

DEPARTMENT OF
ELECTRICAL ENGINEERING
INDIAN INSTITUTE OF TECHNOLOGY, KANPUR

*April, 1997.*

# CERTIFICATE

This is to certify that the work contained in the thesis entitled *Nonuniform sampling of time-limited signals using time-scale localisation properties of wavelet transforms* by Chaveli Ramesh, has been carried out under our supervision and that this work has not been submitted elsewhere for a degree.


Dr. P. R. K. Rao
Professor (Retd.)
Department of Elect. Engg.
Indian Institute of Technology,
Kanpur.

Dr. G. Sharma
Professor
Department of Elect. Engg.
Indian Institute of Technology,
Kanpur.


Date:

EE- 1997- D-CHA-NON

# Synopsis

Name of student: Chaveli Ramesh Roll No. 9220462

Degree for which submitted: Ph D Department: Electrical Engineering

Thesis title: Nonuniform sampling of time-limited signals using time-scale localisation properties of wavelet transforms

Name of thesis supervisors

1. Dr. Govind Sharma

2. Dr. P. R. K. Rao

Month and year of thesis submission: April, 1997

Sampling is an indispensable operation in signal processing and digital communications. The conventional approach of collecting samples of an analog signal is uniform sampling, which collects samples at equal intervals. The uniform sampling approach is not always the best in terms of the number of samples required for the same reconstruction error, therefore, the possibility of collecting samples of an analog signal at nonuniform intervals has to be explored. Given any signal, what is the best way to take the samples or at what intervals the samples are to be taken so that the whole process is efficient (requires least number of samples to represent an analog signal for a given error and a given reconstruction

method), is the basic problem of nonuniform sampling. The objective of this thesis is to make some contributions towards the above described problem of nonuniform sampling.

The uniform sampling is based on Shannon's sampling theorem. In uniform sampling the signal is sampled at a rate greater or equal to the twice the bandwidth of the signal. This technique is not suitable in the following cases- (a) When the signal is not band-limited, (b) When an estimate of the bandwidth of the signal is not available. It is for these cases that nonuniform sampling can serve as an alternative. *The time-limited signals are not band-limited and so uniform sampling is not applicable in this case.* Moreover, signals found in practice are always time-limited, therefore, the time-limited class of signals is important; and hence, in this thesis, nonuniform sampling techniques for time-limited signals are developed.

In this thesis, two nonuniform sampling problems for time-limited signals have been formulated and algorithms which provide solutions to these problems are presented. Given any time-limited signal, what is the nonuniform placement of a finite number of samples in the domain of the signal such that the fractional mean square reconstruction error is minimised? This is the first problem that is attempted in this thesis. The basic drawback of the type of nonuniform sampling strategy that results from solving this problem is, that it requires the storage of the sampling instants as well. Therefore, another nonuniform sampling problem is proposed. Given a time-limited signal, what is the optimal distribution of a finite number of samples in the partitions of a time-limited signal? The optimality criterion is to minimise the fractional mean square reconstruction error. In this problem, in each of the partitions the samples are placed uniformly. Further, the reconstruction error minimisation has to be performed with respect to the partition lengths as well. It is more efficient in terms of the storage requirements, to sample uniformly in the different partitions at dissimilar rates rather than sampling completely nonuniformly, as in the case of the first problem. Because, in this scheme only the instant of the first sample in each of the partition, the partition length and the number of samples in the partition have to be noted down.

To solve both these problems, the excellent time-scale localisation properties of wavelet

transform have been used. Therefore, in this thesis, before presenting the solution to these problems, the wavelet transforms are discussed; further a novel concept, termed as *scale-limitedness* is introduced with reference to continuous wavelet transforms.

The wavelet transform of a signal is the inner product between the signal and the function $\frac{1}{\sqrt{a}}\psi\left(\frac{t-b}{a}\right)$. Here $a$ is the scale parameter, and the shift parameter, denoted by $b$, shifts the wavelet to $t = b$, therefore, the wavelet transform gives the behaviour of the signal at $t = b$. At lower scales the wavelet transform gives the fast varying component present in the signal. Therefore, the wavelet transform is enhanced at lower scales, in regions, wherein, the signal is varying fast. This has been illustrated through simulations.

The concept of scale-limitedness, introduced in this thesis, can be used for quantifying signal variations. A signal is called scale-limited, if its wavelet transform is zero for all scales below a certain scale value and for all shifts. Another definition, termed as $\delta_0$-practical scale-limitedness is also introduced. A signal is called $\delta_0$-practically scale-limited to $a_l$, if $a_l$ is the largest scale value below which the fraction of the energy, for all shifts, is less than $\delta_0$. Next some examples are presented, in which the signals are plotted and their $\delta_0$-scale-limits are computed. It can be inferred from these examples, that the signals which have faster varying component have smaller scale-limits. Further, eliminating fast varying components, it is possible to construct signals which are scale-limited.

Next we discuss the relation between the higher order vanishing moment property and scale-limitedness. Any real square integrable function qualifies as a wavelet if its zeroth moment vanishes; there exist wavelets for which the higher order moments vanish. It has been shown that, signals which are slower varying have relatively larger scale-limits because of the vanishing moment property of the wavelet. A few theorems have been stated and proved next. It has been shown that, a signal which is band-limited is also scale-limited. Moreover, it has been proved that there exist time-limited signals which are scale-limited and obviously, not band-limited. Further it is shown that, signals which have smaller scale-limits have larger upper bound on their differentials. Next it is shown that the Lagrangian interpolation function is $\delta_0$-practically scale-limited. Finally it is shown that, signals which

are in the successive approximation spaces associated with the multiresolution analysis, are scale-limited.

As an application of scale-limitedness, a sampling rate estimation method for signals is proposed. For estimating the sampling rate, a theorem is proved, which states that signals with smaller scale-limits should be sampled at a relatively faster rate for the same error bound. This method proceeds by, first over sampling the signal, then finding the scale-limit using the multiresolution analysis. And finally, given a bound on the error, reduction in the number of samples is found such that the error remains less than the bound. The method gives a sampling rate reduction of a multiple of $2^j$, where $j$ is an integer greater than or equal to zero.

The first nonuniform sampling problem is the optimal sample placement problem. Given any time-limited signal, what is the nonuniform placement of a finite number of samples in the domain of the signal such that the fractional mean square reconstruction error is minimised? The sampling algorithm developed here is based on the observation that if the error in the transform domain is bounded, then the error in the time domain is also bounded. Theorems have been presented, which give the bounds on the fractional mean square error. It can be inferred from these theorems, that the bound on the fractional mean square error is more sensitive to the value of the fractional mean square error in the transform domain at lower scales as compared to that at higher scales. Therefore, to make the fractional mean square error smaller, the error in the transform domain should be made relatively smaller at lower scales. Another observation is that, the mean square error in the transform domain can be made small by placing the samples at those points in the transform domain, at which the wavelet transform maxima occur.

The algorithm for solving this problem proceeds by first sampling the signal at the highest possible rate. Then the samples are picked in the time domain at a value denoted by $t_i$, if the wavelet transform attains maximum in the transform domain at $t_i$. This gives the initial set of samples, if all the maxima are exhausted and still samples can be taken then rest of the samples are taken in the neighbourhood of the samples in the initial set. Using the

optimal samples the original set of samples is reconstructed using an interpolation method. It is assumed that the interpolation is done using local functions shifted to the sample value. Further, the interpolation method should be such that, at the known values of the signal the interpolated value should be same as the known value. Simulation results which demonstrate the algorithm have been presented.

The second nonuniform sampling problem attempted in the thesis is the following- Given a time-limited signal, what is the optimal distribution of a finite number of samples in the partitions of a time-limited signal such that the fractional mean square error is minimum? In each of the regions, uniform sampling is done. The regions are obtained by partitioning the signal depending upon local variations. In the sampling strategy, proposed here, the rate of sampling adapts to local variations. In the algorithm, first the signal is partitioned into dissimilar regions. Each of the regions is characterised by a scale-limit, which is distinct from the values of the scale-limits of the neighbouring regions. Then, in each region the optimal number of samples are distributed, which is a fraction of the total number of samples to be distributed. It has been proved in the thesis, that segments with smaller scale-limits should be sampled at a higher sampling rate. In each of the regions the uniform sampling is done. Therefore the solution to the second problem leads to a multirate sampling strategy.

The algorithm proposed for multirate sampling is as follows. First a low value of the threshold is set, then the optimal sample distribution is found; using this optimal distribution the signal is sampled uniformly in the different segments. Next these samples are used to reconstruct the signal back and finally the fractional mean square error is found. This is repeated for successively higher values of the threshold and that sample distribution is selected, for which, the minimum fractional mean square error is obtained. The fractional mean square error versus the threshold value is found to have many local minima, therefore, the global minimum has to be selected. The simulation results also have been presented. The main conclusion is that, in order to keep the bound on the fractional mean square error low, the number of samples in any segment should be inversely proportional to a positive power of the scale-limit.

To summarise, in this thesis, two nonuniform sampling problems have been formulated. Given any time-limited signal what is the placement of a finite number of samples such that the fractional mean square error is minimum? It has been proved, that in order to minimise the fractional mean square reconstruction error, the samples should be placed at and in the neighbourhood of those points at which the wavelet transform maxima occur and also more samples should be placed using the information of the maxima at the lower scales. An algorithm for nonuniform sampling has also been presented. Given any time-limited signal, how to partition the signal into regions of dissimilar variation and what is the rate of sampling in each region, when uniform sampling is done in each region? This is the second problem attempted in this thesis. This problem has been solved by partitioning the signal into regions of dissimilar variation using the concept of scale-limitedness introduced with reference to the continuous wavelet transforms. The signals have been partitioned into regions such that each region has a scale-limit which is different from the scale-limits of the neighbouring regions. It has been established in this thesis, that the error bound is minimised when more samples fall in the regions of smaller scale-limits.

Conclusions based on the results obtained in the present work are given below-

- In regions of time domain, wherein, the wavelet transform gets enhanced at lower scales, the signal is faster varying as compared to regions where signal is slower varying.
- Signals which are faster varying, have relatively smaller scale-limits.
- Scale-limited signals satisfy the following properties-
  - Signals which are band-limited are also scale-limited.
  - There exist time-limited signals which are scale-limited as well.
  - Signals having smaller scale-limits have larger upper bounds on their differentials.
  - The Lagrangian interpolating function is $\delta_0$-practically scale-limited.
  - Signals which are in successive approximation spaces associated with multiresolution analysis are scale-limited.

- It has been shown that, for the same error performance, the signals with smaller scale-limits should be sampled at a higher rate.
- For placing the samples nonuniformly, in order to keep the mean square error low, the strategy of sampling is to place the samples at and in the neighbourhood of the maxima of the wavelet transform.
- For region based sampling, when samples are placed uniformly in each of the regions at different rates, more samples should fall in regions of smaller scale-limits.

*To*
*Bhagawan*
*Satya Sai Baba*

# Acknowledgements

I thank my supervisors, Professor P. R. K. Rao and Professor Govind Sharma for suggesting me the problem for the research work, their valuable guidance, sustained interest and enlightening discussions. They freely gave me time whenever I needed.

During my stay at IIT Kanpur, many of my friends have been a source of encouragement, in particular, I would like to mention the names of Kailash, Anand, Ashish Jadhav, Amit, Shailendra, Manoj Srivastav, Chandrashekhar, Shishir, Shafi and Appaji Rao.

I am thankful to Professor M. U. Siddiqui, former Head, Department of Electrical Engineering, IIT Kanpur for his help in my going abroad to Perth, Australia, to present a paper, which forms part of this thesis.

I thank Professors V. P. Sinha, P. Sircar, S. K. Mallick, R. Sharan and C. Dasgupta, faculty members, Department of Electrical Engineering, who have been eagerly enquiring about the progress of my work.

I thank Professors P. C. Das, V. Raghvendra and Shanmugraj, faculty members, Department of Mathematics, for their valuable discussions during the course of the investigation.

I thank Professor and Mrs. T. V. Prabhakar for maintaining spiritually enlightening atmosphere through their Chinmaya mission activities, which gave strength to me.

I thank Giri, Sudipto and S. C. Mishra, for being instrumental in my taking part in the ISKON activities, which were mentally refreshing to me.

Finally, I thank my parents and my sister for their encouragement and support during the thesis period.

# Contents

# List of Figures

# List of Tables

# Nomenclature

| | |
|---|---|
| $g(t)$ | The signal under study. |
| $\psi(t)$ | The mother wavelet. |
| $\Psi(f)$ | Fourier transform of $\psi(t)$. |
| a | Scale parameter. |
| b | Shift parameter. |
| $\psi\left(\frac{t-b}{a}\right)$ | Shifted and scaled versions of the wavelet. |
| $x \in X$ | $x$ belongs to $X$ |
| $a \subset A$ | $a$ is a subset $A$ |
| $W_{g,\psi}(a,b)$ | The wavelet transform. |
| E | Energy of the signal $g(t)$. |
| R | Set of real numbers |
| $<,>$ | Inner product. |
| $F_t[]$ | $\int_{-\infty}^{\infty} . e^{-j2\pi ft}\, dt$, the Fourier transform operator. |
| $\Gamma(x)$ | Gamma function |
| $\Pi_{i=1}^{N} x_i$ | $x_1 x_2 ... x_N$ |
| $Sinc(x)$ | $\frac{sin(\pi x)}{\pi x}$ |
| $k!$ | $k\ (k-1)\ ...\ 2\ 1$ |
| $\dot{g}(t)$ | $\frac{dg(t)}{dt}$ |

| | |
|---|---|
| $\mathcal{K}$ | The class of bandlimited square integrable signals. |
| $J_m(t)$ | Bessels function of second kind |
| $\forall k$ | For all $k$ |
| $L^2(R)$ | Class of square integrable functions |
| $L^1(R)$ | Class of absolutely integrable functions |
| $W_{g,\psi}(a,b)$ | $< g(t),\ \psi\left(\frac{t-b}{a}\right) >$ |
| $M^n$ | n-vanishing moment space |
| $\hat{g}(t)$ | The reconstruction of $g(t)$. |

# Chapter 1

# Introduction

This thesis deals with the problem of nonuniform sampling. The problem consists of finding an optimal algorithm for nonuniformly sampling a signal so that the samples can be used to reconstruct back the original signal. Nonuniform sampling can be classified into two categories. Firstly nonuniform sampling of signals on the whole of real line, and secondly, nonuniform sampling of time-limited signals. Here the problem of nonuniform sampling of time-limited signals is dealt with and optimal solutions are provided.

## 1.1 Motivation

Sampling is an indispensable operation in signal processing and digital communications. Modern digital computers can deal only with a finite set of numbers and there is no possibility of operation on analog signals. Although there are analog computers which operate upon analog signals, due to practical constraints like- difficulty in implementing

all types of operations, low speeds, problem in storing the results and application specific nature of the computer (for different applications different computers have to be designed), they have not become popular. In contrast, the digital computers do not have the above mentioned difficulties but they cannot operate on analog signals directly. Therefore, the analog signals have to be sampled and then only the discrete set of numbers, which represent the amplitude of the signal at different points of space and time, can be processed using the digital computers.

The following are some important questions which one comes across while dealing with sampling.

- What should be the rate of sampling?
- What is the sample placement strategy?
- How to reconstruct a signal from its samples?

The answers to these questions are dependent on the characteristics of the signal being sampled. Generally the samples are placed uniformly, which leads to uniform sampling. This technique was formally introduced by Shannon [Sha49]. Shannon based his arguments on Whittekar-Kotelnikov theorem and proposed his technique for band-limited signals. Once it is decided that the samples be placed uniformly, the only problem left is to find the rate of sampling required. The W-K theorem, which is now known as S-W-K theorem states, that for a signal band-limited to $[-W,\ W]$ a rate of $2W$ samples per second is sufficient to reconstruct the signal back from the samples.

The uniform sampling has become very popular in signal processing mainly due to the following reasons.

- Easy to implement.
- Simplicity in the processing of uniform samples.

In the case of uniform sampling, the only requirement is that the signal bandwidth be known apriori. In practice, however, for many cases this does not pose any problems because an antialiasing filter (AAF) is used as the preprocessing unit to band-limit the incoming signal. Then the rate of sampling is decided according to the bandwidth of the AAF. The bandwidth of the AAF has to be selected judiciously. Very small bandwidth of the AAF, although leads to lower sampling rate, in the process, may lead to loss of vital information related to the signal. Alternatively, larger bandwidth of AAF leads to larger sampling rate, which in turn leads to redundancy in the representation and at the same time leads to higher computational costs.

An alternative approach to uniform sampling is to have nonuniform sampling. In nonuniform sampling, the samples are placed at unequal spacings. Since the restriction that samples be placed uniformly is removed, the need to develop optimal sampling strategy arises. A general nonuniform sampling problem is one in which a finite duration signal is given and the optimal placement of a finite number of samples has to be found. The strategy adopted in nonuniform sampling is to analyse the incoming signal and place more samples in regions of faster variation.

Consider the case in which a finite duration signal has to be sampled at a finite number of points. The best criterion for deciding the position of the samples is to minimise the error between the original signal and the reconstructed signal using the samples with respect to the sample positions. But there are drawbacks to the above mentioned method. To reach the optimum may be difficult. Another problem is that the method does not explain why more samples get placed in certain regions.

In this thesis, an algorithm for optimal nonuniform sampling is proposed. Further, using a new signal variation measure, which is well suited for finite duration signals, a region based sampling strategy has been proposed. These strategies avoid the exhaustive search for an optimal sample placement.

## 1.2 The Nonuniform Sampling Problems

Here two problems have been formulated and solved, namely, sample number distribution problem and sample placement problem.

### The Sample Placement Problem

Given a finite duration signal, what is the nonuniform placement of a finite number of samples in the domain of the signal such that the fractional mean square error is minimised? To solve this problem, the wavelet transform description of the signal has been used. It has been shown that if the interpolation is done using functions which are shifted to sample point and multiplied by the sample value and further these functions are local (Most of the energy is concentrated around the origin.), then, the samples should fall in the same regions, in which, the wavelet transform values are relatively large in the domain of the shift parameter. Another constraint on the sample point is that sampling instant should be in the domain of the original signal. Using the above mentioned properties of the optimal sampling instants, an algorithm for optimal sampling has been proposed. The basic drawback of the type of nonuniform sampling strategy, that results from solving this problem is, that it requires the storage of the sampling instants as well. Therefore, another nonuniform sampling problem is proposed.

### The Sample Number Distribution Problem

Given any time-limited signal, what is the optimal distribution of a finite number of samples in the partitions of the signal? The problem is solved by segmenting the signal into regions of different variations and distributing the samples in the regions in an optimal fashion. In each of the regions, however, the samples are placed uniformly. To solve the problem a multirate sampling strategy for time-limited signals has been developed.

This problem has two aspects: the first aspect is to segment the signal into different regions such that the variations of the signal remains same throughout a region, while the second aspect is to decide the rate of sampling in each of the regions.

The problem of segmentation has been solved using a signal variation measure which is defined with reference to wavelet transforms. Further a theorem has been established which proves that relatively more samples should fall in regions of faster variation in order to minimise the error between the original signal and the reconstructed signal using the samples.

The reason for formulating this problem is, that in the case of sample placement all the sampling instants have to be stored which would require a lot of storage space. But the solution to the second problem leads to an algorithm, in which, the starting instant of a partition, the partition length and the number of samples in the partition only have to be noted down, to locate all the samples.

## 1.3 Strategies for Solving the Problems

For solving the sample placement problem, it is shown that the maxima of the wavelet transform at different scales have to be taken into consideration for deciding the optimal placement of the samples. Further, it can be inferred from the theorems, that more samples should be distributed using the information at lower scales. Using these results, an algorithm for sample placement has been presented. This algorithm assumes certain specific properties of the interpolation method used. Simulation results have also been presented. For solving the two distinct problems- the sample number distribution problem and the sample placement problem, the time-scale localisation properties of the wavelet transforms are exploited.

For solving the sample number distribution problem, a measure called scale-limitedness with reference to wavelet transforms, is introduced and utilised. The wavelet transform of a signal is an inner product between the signal and shifted and scaled versions of certain functions known as wavelets. Wavelets are finite energy functions with good decay properties.

Let a wavelet be denoted by $\psi(t)$, then $\psi\left(\frac{t}{a}\right)$ is the scaled version of the wavelet. A shift also can be introduced and the modified wavelet is given by $\frac{1}{\sqrt{a}}\psi\left(\frac{t-b}{a}\right)$. It can be observed, that at relatively lower scales, the support of the wavelet reduces. The support of the wavelet is the subset of the domain in which it has significant energy. Therefore, it can be concluded that, at low scales, the wavelet transform gives the behaviour of the signal at and around $t = b$. This has significance because, using wavelet transformed domain description of a signal, it is possible to get important information about the local behaviour of a signal. A signal is said to be scale-limited, if its wavelet transform is zero for all scales below certain value and for all shifts. This

value is called the scale-limit of the signal.

Using the concept of scale-limitedness, the given signal is segmented into disjoint regions, where each region is characterised by its own scale-limit. After segmenting the signal, for which an algorithm is provided, the only problem left out is to decide the sampling rate in each of the segments. Theorems have been stated and proved, which establish that regions wherein the scale-limit is low, the sampling rate should be relatively high, in order to keep the overall reconstruction error low, if the total number of samples that have to be distributed is fixed. Simulation results using various test signals have been presented.

## 1.4 Organisation of the Thesis

In Chapter 2, literature related to sampling theory has been reviewed. Mainly the focus is on nonuniform sampling.

Since the solution of the problems formulated in the thesis require certain time-scale localisation properties of the wavelet transform, therefore, before presenting the nonuniform sampling problems and their solution the wavelet transform is discussed. In Chapter 3, scale-limitedness is introduced with reference to wavelet transforms. A signal is called scale-limited if the wavelet transform is zero for all values of the scale below a certain value and for all shifts. The practical considerations due to which this concept has emerged have also been discussed. It has been shown through simulations that signals with smaller scale-limits have faster variation.

Scale-limitedness is similar to band-limitedness, but has some additional properties

which makes it very useful. As an extension $\delta_0$-practical scale-limitedness has been defined. Finally, a few properties of scale-limited signals have been established. It is shown that all band-limited signals are scale-limited with respect to a class of wavelet families. Further, the existence of time-limited signals which are also scale-limited is established. Moreover, it is proved that, the larger the value of the scale-limit, the smoother is the signal. The class $M^n$ is defined and it is shown that the Lagrangian interpolation for '$n$' points is $\delta_0$-practically scale-limited with respect to a wavelet family whose mother wavelet is in $M^n$ space.

In the same chapter, as an application of scale-limitedness, an algorithm for estimating the required sampling rate for any signal, for a given error performance is proposed; an expansion in terms of the samples is also presented. Scale-limitedness with reference to wavelet transforms is used as the measure of variation. The proposed algorithm proceeds by sampling the signal initially at a high rate, then recursively subsampling depending upon the required error performance.

In Chapter 4, the optimal sample placement problem is formulated. Theorems have been provided which serve as guidelines for optimal sample placement. An algorithm for sample placement has been provided. Simulation results have also been presented.

In Chapter 5, the sample number distribution has been formulated. The solution to the problem leads to a multirate sampling strategy for time-limited signals. The sampling strategy is based on the local variations. The strategy proceeds by segmenting the signal using the wavelet transformed domain description. Further, sampling in each segment is done depending upon the scale-limits of the partitions.

In the final and the sixth chapter, summary of the work carried out in the thesis, the conclusions and recommendations for future work are also given.

# Chapter 2

# Nonuniform Sampling: A Review

In this chapter, the literature related to sampling theory is reviewed. The main emphasis will be on nonuniform sampling. The whole chapter is organised into two sections, namely- uniform sampling and nonuniform sampling.

Traditionally signals have been subjected to uniform sampling, the reasons have been listed out in Chapter 1. These are- it is easy to obtain uniform samples; processing of uniform samples is easy and efficient techniques can be developed.

Intuitively, however, the nonuniform sampling appears to be the natural and rational way of discrete representation of a continuous signal. Because if the relatively faster varying portions of a signal are sampled at a higher rate then the samples would give a better representation of the original signal (in terms of lesser reconstruction error). Likewise, a signal might require lesser number of samples to represent it, if sampled nonuniformly, compared to uniform sampling, for the same error performance. Consequently, the nonuniform sampling can lead to economy in the storage space requirements and lower processing time. Moreover, lower amount of data would mean faster

communication or lower bandwidth for digital transmission.

These observations have led to certain interesting applications of nonuniform sampling, such as, ECG data compression [SA94] and nonuniform tapped delay lines [Yen57]. Another area of application is the error correcting codes, where over sampling and discarding the erased or erroneous samples is a potential alternative to error correcting codes [Mar90].

Further nonuniform reconstruction techniques are also important in the demodulation of frequency modulated [RGWW77], phase and pulse modulated [Kon89] and delta modulated signals [Gam89]. The problem of processing nonuniform samples also occurs in the context of astronomy [Mie79], [Pon] and in geophysical sciences [Stu83].

Other areas where nonuniform sampling occurs are: Computer assisted tomography [Sou88], [Sou89], Nuclear magnetic resonance [YS87], calibration of large space-borne antennas [RSC87] and very long-baseline interferometers [JJCL85]. There are certain reasons due to which the nonuniform sampling has not become popular. The main reasons are as follows-

- There are no efficient techniques for nonuniform sampling.

- Not much work is done in the field of processing the nonuniform samples.

Next we review the uniform sampling.

## 2.1 Uniform Sampling

The purpose of sampling is to represent an analog signal by a discrete sequence of its samples. In this context, the Shannon's sampling theorem specifies the lowest rate of sampling required to reproduce the original signal.

**Definition 2.1.1** *Shannon's sampling theorem: A band-limited signal of finite energy which has no frequency components higher than $W$ hertz, is completely described by specifying the values of the signal at instants of time separated by $1/2W$ seconds [Sha49]. The interpolation formula is given by*

$$g(t) = \sum_{n=-\infty}^{\infty} g(T)\ sin(2\pi Wt - n\pi)/(2\pi Wt - n\pi), \tag{2.1}$$

*where $g(t)$ is band-limited to $[-W, W]$ and $T = \frac{1}{2W}$.*

This implies that any signal band-limited to $[-W,\ W]$ can be represented in terms of its samples taken at rate of $2W$ samples per second.

### 2.1.1 Error Analysis in Sampling Representation

In this section, the errors that arise in the practical implementation of the Shannon's theorem are discussed. Due to the practical limitations in the implementation of the sampling theorem, the following types of errors can arise in the reconstruction of the original signal -

- Truncation error - When a finite number of samples are used to reconstruct the signal then the error that arises is called Truncation error.

- Aliasing error - This error arises when the sampling rate is less than the rate specified by the sampling theorem.
- Jitter error - This occurs due to the violation of the sampling instants from the uniform sampling points.
- Amplitude or round off error - This error occurs as a result of the uncertainty in measuring the amplitude of the sample values.

A comprehensive treatment of the errors have been presented by Thomas and Liu [TL64] and Popoulis [Pou68], [Pou66].

#### 2.1.1.1 The Truncation Error and its Bounds:

In this section, we will be discussing the truncation error bounds on a band-limited signal. The signal to be reconstructed using its uniform samples is denoted by $g(t)$ and it is band-limited to $[-W, W]$. The truncation error can be defined by the following partial sum

$$\mathcal{E}_T(t) = \sum_{|n|>N} g(nT) sinc(\frac{t}{T} - n). \tag{2.2}$$

Where $T$ is the interval between two consecutive samples, $T = \frac{1}{2W}$ and $g(nT)$ are the sample values at the time $nT$ for $n$ taking values on the integer set. Tsybako and Iakovlev [TI59] have given the following truncation error bound-

$$|\mathcal{E}_T(t)| \leq \frac{\sqrt{2}}{\pi} |sin\frac{\pi t}{\delta t}| \sqrt{\frac{T\delta t}{(T^2 - t^2)}}, \tag{2.3}$$

Where $E$ is the energy of the signal, $-T \leq t \leq T$ and $\delta t < \frac{1}{W}$.

Helms and Thomas [HT62] gave the following bound-

$$|\mathcal{E}_T(t)| \leq \frac{4M}{\pi^2 N(1-r)}. \tag{2.4}$$

Here $g(t)$ is band-limited to $rW < W$, where $0 < r < 1$ and $M = max\ |g(t)|$. A similar bound was given by Jordan [Jor61]

$$\mathcal{E}_T(t) \leq \frac{4M|sin(2\pi Wt)|}{\pi N(1-r)}. \tag{2.5}$$

If the $g(t)$ is approximated by the asymmetrical partial sum-

$$g_{N_1,\,N_2}(t) = \sum_{n=K-N_1}^{K+N_2} g\left(\frac{n}{2W}\right) \frac{sin(2W\pi - n\pi)}{(2W\pi - n\pi)}, \tag{2.6}$$

then the truncation error is also shown to be bounded by,

$$|\mathcal{E}_T(t)| \leq \frac{2M}{\pi^2(1-r)}\left[\frac{1}{N_1} + \frac{1}{N_2}\right]. \tag{2.7}$$

Many other bounds have been given by various researchers [deF67], [RB72].

#### 2.1.1.2 The Aliasing Error and its Bounds:

This type of error results when a band-limited signal is sampled at a lower rate than that specified by the Nyquist theorem. The aliasing error is given by

$$\mathcal{E}_A(t) = g(t) - g_s(t).$$

Where $g(t)$ is the original signal and $g_s(t)$ is the result of applying the sampling theorem representation with samples taken at rate of $2W$ samples per second, when the signal is not necessarily band-limited to $[-W, W]$. Weiss [Wei63] considered the aliasing error when the value of $G(f)$ differs from zero for $|f| > W$. The function $G(f)$ has the following properties $G(f) \in L^1(-\infty, \infty)$, $G(f) = \overline{G}(f)$, $G(f)$ is of bounded variation

and $2G(f) = G(f+0)+G(f-0)$. Let $g_s(t)$ be the reconstruction using the samples at a rate of $2W$ samples per second and the interpolation in 2.1. Weiss gave the following upper bound-

$$\begin{aligned} \mathcal{E}_A(t) &= |g(t) - g_s(t)|, \\ &\leq \frac{2}{\pi}\int_W^\infty |G(f)|df. \end{aligned}$$

Several other bounds are available in literature [Pou66], [JLB67], [Sta67], [Sti67].

#### 2.1.1.3 The Jitter and Round off Errors:

The Jitter error occurs due to the uncertainty in the sampling instants. If the signal has to be sampled at $nT$, then due to practical limitations (finite accuracy of the instruments), the actual sampling instants turn out to be $t_n = nT + \gamma_n$, where $\gamma_n$ is randomly chosen. The Jitter and Round off errors are similar and require similar treatment[TL64].

Popoulis [Pou66] has found the bound for the round off error for a signal which is band-limited to $[-W_1,\ W_1]$. He proposed the following general expansion-

$$g(t) = \sum_{-\infty}^{\infty} g(nT)\ \frac{sin(W_0(t-nT))}{W_2(t-nT)}, \tag{2.8}$$

where, $W_2 = (\frac{\pi}{T}) \geq W_1$, $W_1 \leq W_0 \leq 2W_2 - W_1$. Using this cardinal series with $W_0 = W_1$ and the actual recorded or sampled values he constructed the function $g_r(t)$, which differs from $g(t)$ by the total round-off error $\mathcal{E}_r(t)$. He showed that the error $\mathcal{E}_r(t)$ is bounded by its own total energy: that is,

$$|\mathcal{E}_r(t)| \leq \left(\frac{W_1\ E_r}{\pi}\right), \tag{2.9}$$

where,

$$E_r = \int_{-\infty}^{\infty} \mathcal{E}_r^2(t)\, dt \tag{2.10}$$

For the error free reconstruction of band-limited signal from its jittered samples, Higgins [Hig76] has presented two series representations. Beutler [Beu61], [Beu66] has presented the basic theoretical treatment of the problem.

## 2.2 Nonuniform Sampling

When sampling is done on the set $\{t_k\}$, where $t_k$'s are not necessarily $kT$s, where $k$ is an integer and $T$ is a real quantity whose value is equal to the interval of sampling, then the sampling is called nonuniform sampling. The nonuniform sampling will be discussed under two subsections, namely-

- Nonuniform sampling of signals on $R$:
- Nonuniform sampling of time-limited signals:

### 2.2.1 Nonuniform Sampling of Signals on $R$

Band-limited as well as nonband-limited signals can be subjected to nonuniform sampling. But so far research has been mainly concentrated on studying nonuniform sampling of band-limited signals. In the case of nonuniform sampling, arbitrary sampling of a band-limited signal at the Nyquist rate, does not ensure that the signal can be uniquely reconstructed from the samples. This fact can be observed from the following

example. Suppose a band-limited signal is sampled at the Nyquist rate at sampling instants $\{t_k\}$. Suppose that it is possible to to interpolate a band-limited signal with zero crossings at the points $\{t_k\}$. If the interpolated signal is added to the original signal, then another signal is obtained, which has the same bandwidth as the original signal and moreover it has the same sample values at the instants $\{t_k\}$. Therefore the samples taken at the instants $\{t_k\}$ do not uniquely represent the original signal. In other words, it is not possible to interpolate the original signal form the samples taken at such $\{t_k\}$. The set of samples which provide unique reconstruction is defined as *sampling set.*

Due to the previous arguments, the following Lemma has been inferred [Req80].

**Lemma 2.2.1** *If the nonuniform sample locations $\{t_k\}$ satisfy the Nyquist rate on the average, they uniquely represent a band-limited signal if the sample locations are not the zero crossings of a band-limited signal of the same bandwidth.*

The following corollary can be inferred from the Lemma.

**Corollary 2.2.1** *If the average sampling rate of the set of sampling instants $\{t_k\}$ is more than the Nyquist rate, then the samples taken at $t_k$'s uniquely specify a band-limited signal and $\{t_k\}$ is a* sampling set.

**Proof:** The average density of zero crossings (real zeros) of a signal band-limited to $[-W,\ W]$ is less than or at the most equal to the Nyquist rate ($2\ W$), for deterministic [Tit39] and random signals [Ric45]. Therefore when a signal band-limited to $[-W,\ W]$ is sampled at a rate more than $2W$, then the sampling positions cannot be the zero crossings of a signal band-limited to $[-W,\ W]$. Hence the samples, so taken, form a unique *sampling set.*

First we discuss the general nonuniform schemes, subsequently the methods of recovery of signals from their nonuniform samples are discussed. The time varying system interpretation of interpolation is also discussed. Further the problem of spectrum estimation from nonuniform samples is also reviewed.

## 2.2.2 Nonuniform Sampling Schemes

### 2.2.2.1 Sampling with a Gap in an Otherwise Uniform Distribution:

In this scheme of nonuniform sampling, a signal $g(t)$, band-limited to $[-W,\ W]$, is sampled uniformly for $t \leq 0$ and it is also ensured that a sample falls at $t = 0$, but for $t > 0$ the first sample is taken at $\delta + \frac{1}{2W}$. The subsequent samples are taken at $\delta + \frac{n}{2W}$, $n > 0$ for $t > 0$. Hence a gap of $\delta$ is introduced for the first sample for $t > 0$. In other words,

$$t_n = \begin{cases} nT, & n \leq 0 \\ \delta + nT, & n > 0 \end{cases} . \tag{2.11}$$

If $\delta < T$, then the samples $\{t_n\}$ uniquely specify the signal $g(t)$. Under these conditions Yen has proved the following theorem [Yen56].

**Theorem 2.2.1** *If $g(t)$, band-limited to $[-W,\ W]$ is sampled at $t_n$ specified by 2.11, then the signal can be reconstructed using the following interpolating formula,*

$$g(t) = \sum_{n=-\infty}^{\infty} g(t_n)\psi_n(t) \tag{2.12}$$

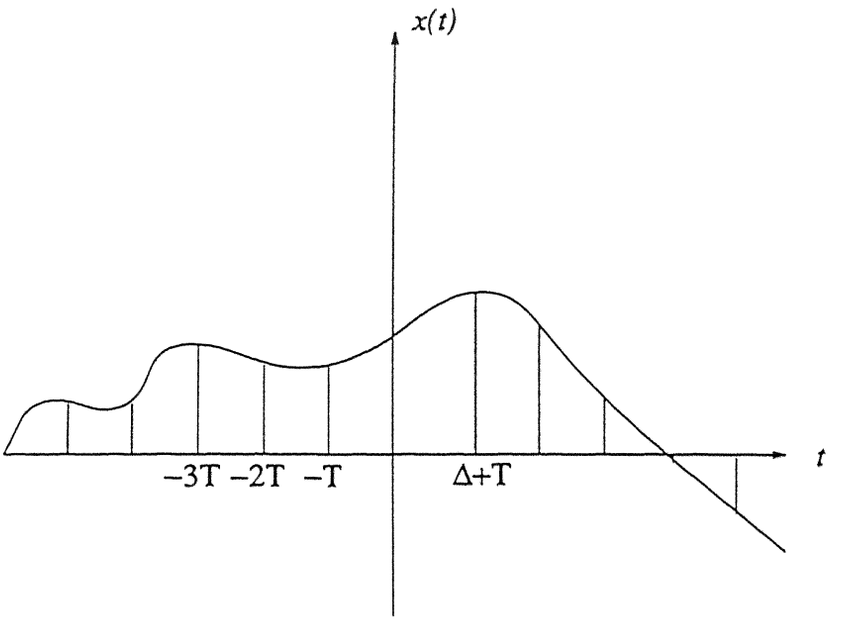


Figure 2.1: A signal sampled with a gap in an otherwise uniform distribution

*where,*

$$\begin{aligned}\psi_n(t) &= \frac{(-1)^n\Gamma(2W\Delta+n)}{\Gamma(2Wt)\Gamma[2W(\Delta-t)]n!} \times (n+2Wt)^{-1},\ n \leq 0 \\ &= \frac{(-1)^n\Gamma(2W\Delta+n)}{\Gamma(2Wt)\Gamma(2W(\Delta-t))n!} \times [n+2W(\delta-t)]^{-1},\ n > 0.\end{aligned}$$

This case has been shown in the Figure 2.1.

#### 2.2.2.2 Periodic Nonuniform Sampling:

In this sampling scheme, $N$ nonuniformly spaced points repeat with a period of $NT$. Let the delays of the one particular set of $N$ points be $\{\tau_k\}$. Then the sampling instants of all the points can be represented by the following general formula.

$$t_{nk} = nNT + \tau_k; \quad \left.\begin{array}{rcl} k & = & 1, 2, 3, \ldots, N \\ n & = & 0, \pm 1, \pm 2, \pm 3, \ldots \\ T & = & \frac{1}{2W}. \end{array}\right\} \tag{2.13}$$

Figure 2.2 shows the periodic nonuniform sampling scheme.

The reconstruction of the signal from the samples can be done by applying the following interpolating Equation [Pou77].

$$g(t) = \sum_{n=-\infty}^{\infty} \sum_{k=1}^{N} g(t_{nk}) \psi_{nk}(t) \tag{2.14}$$

*where,*

$$\psi_{nk}(t) = \frac{N \prod_{i=1}^{N} sin\left(\frac{2\pi W}{N}(t - t_{ni})\right)}{2\pi W (t - t_{nk}) \prod_{i=1,\ i \neq k}^{N} sin\left(\frac{2\pi W}{N}(\tau_k - \tau_i)\right)} \tag{2.15}$$

#### 2.2.2.3 Jittered Sampling:

When the samples are placed around the uniform samples ($nT$), then they are called jittered samples. These samples might be clustered either deterministically or randomly. A typical example is when the samples get jittered due to the uncertainty at the receiver end.

For deterministic jitter Popoulis [Pou66] has proposed a method for reconstructing the original signal from the samples. Let $g(t_n)$ be the samples of the signal which is band-limited to $[-W,\ W]$. We construct a signal $x(t)$ which has the uniform sample values equal to $g(t_n)$. In other words, $x(t)$ is a function such that $x(nT) = g(t_n)$.

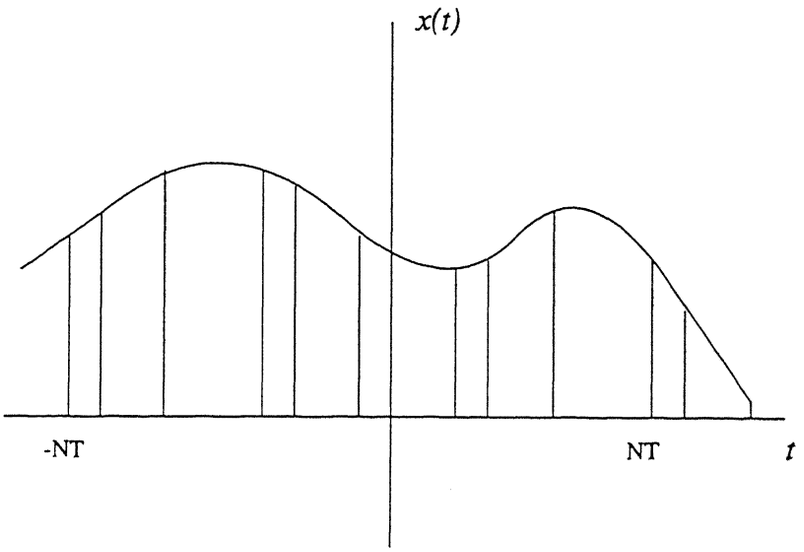


Figure 2.2: Periodic nonuniform sampling of a signal

Let there exist a function $\theta(t)$ such that, $\theta(nT) = t_n$. And let $\theta(t)$ be band-limited to $[-W_1, W_1]$, such that $W_1 < \frac{1}{2T}$ then,

$$\theta(t) = \sum_n t_n Sinc\left(\frac{t}{T} - n\right)$$

Therefore $x(t) = g(\theta(t))$ and $x(nT) = g(\theta(nT)) = g(t_n)$. Further if $x(t)$ is band-limited, then,

$$x(t) = \sum_n g(t_n)\ Sinc\left(\frac{t}{T} - n\right)$$

Finally if $\theta(t)$ is an invertible function then, $g(t) = x(\theta^{-1}(t))$, which leads to,

$$g(t) = \sum_n g(t_n)\ Sinc\left(\frac{\theta^{-1}(t)}{T} - n\right) \tag{2.16}$$

If $|nT - t_n|$ is small then the assumption that $x(t)$ is band-limited is valid. If $g(t)$ is band-limited then, in general, $x(t)$ is not band-limited, and therefore 2.16 is only an

approximation. But if $x(t)$ is band-limited, the $g(t)$ cannot be band-limited, hence 2.16 is an exact representation for this class of nonband-limited signals.

Clark et al. [JJCL85] have suggested that this method can be used for reconstructing a certain class of nonband-limited signals.

#### 2.2.2.4 Implicit Sampling:

In this type of sampling the signal is sampled at instants at which the signal takes a predefined value. For instance, $t_n$ may be selected such that $g(t_n) = 0$ or the $t_n$ is selected at the crossings of the function $g(t)$ with $A\ cos(2\omega t_n)$. The first implicit sampling was considered by Bond and Cahn [BC58]. They considered the case when $g(t)$ is a function band-limited to $[-W,\ W]$ and represented the function in terms of the zero crossings. They extended '$t$' to the complex variable '$z$' and finally obtained that,

$$g(z) = g(0) \prod_{n=1}^{\infty} \left(1 - \frac{z}{z_n}\right), \tag{2.17}$$

where $f(0) \neq 0$, $z_n = R_n e^{i\theta_n}$, $R_n \leq R_{n+1}$ and $lim_{n\to\infty}\left(\frac{2WR_n}{n}\right) = 1$. In the formula 2.17 it has to be noted that the past and the future zeros have to be known.

Another problem they have considered is that, in which the zeros in the interval $[-\frac{T}{2},\ \frac{T}{2}]$, $T = \frac{1}{2W}$ occur at slightly less than the Nyquist rate and outside the interval the zeros occur at the Nyquist rate. Further, let there be number $N < WT$ and there be maxima of $2N$ zeros in $[\frac{-T}{2},\ \frac{T}{2}]$. These zeros are denoted by $z_n = t_n + iu_n$, $|t_n| < T/2$. Outside this interval these zeros occur at $t_n = \pm\left(\frac{n}{2W}\right)$, for $n = N{+}1,\ N{+}2,\ \ldots,$. Under these conditions Bond and Cahn [BC58] finally represented the function $g(t)$ in

terms of $g(0)$ and $z_n$'s. The expression for reconstruction is as follows -

$$g(t) = \sum_{n=-N}^{N} (-1)^n A_n \frac{sin(2\pi Wt - n\pi)}{2\pi Wt - n\pi}, \tag{2.18}$$

where $A_n$ is represented in terms of the $2N$ zeros inside the interval.

$$A_n = g(0) \frac{\prod_m \frac{1}{2Wz_m} \prod_m (2Wz_m - n)}{\prod_{m=1}^{N} -\left(\frac{1}{m}\right)^2 \prod_{\substack{m=-N \\ m \neq n}}^{N} (m-n)}. \tag{2.19}$$

Where $m$ is the index of zeros within the interval $[-\frac{T}{2}, \frac{T}{2}]$.

Bar-David[BD74] has considered the problem of representation of signals in terms of implicit samples, when the sampling instants are real variables (in contrast to the complex variables which are used in the previous case). He considered the case when the sampling instants $t_n$ are such that $g(t_n) = cos(2\pi t_n)$. The representation of the signal from the samples follows from the following theorem.

**Theorem 2.2.2** *Let $g(t)$ be a bounded band-limited function of bandwidth $W_0$, such that, the sampling expansion given by,*

$$g(z) = \lim_{n \to \infty} \sum_{-n}^{n} f\left(\frac{n}{2W}\right) \times \frac{sin(2\pi Wz - n\pi)}{2\pi Wz - n\pi} \tag{2.20}$$

*converges uniformly, for $W > W_0$, in any bounded region of $z$ plane. Let $C > |g(t)|$ and let*

$$f(z) = \{t : g(t) = C\ cos(2\pi Wt)\},\ n =, \ldots, -2, -1, 0, 1, 2, \ldots,.$$

*Then the following product also converges uniformly though conditionally, in the same region.*

$$\{t_n\} = [g(0) - C] \lim_{n \to \infty} \prod_{-n}^{n} \left(1 - \frac{z}{t_n}\right) + C\ cos(\pi Wz). \tag{2.21}$$

A sufficient condition for the convergence is that $t_{\pm k}$ should indicate the $k^{th}$ zero to the right (left) of the origin.

#### 2.2.2.5 Randomised Sampling:

In this type of sampling, the sampling instants are selected randomly. The sampling operation is mathematically defined as the product between $g(t)$ and $u(t)$. Where $u(t)$ is given by,

$$u(t) = \sum_{k=-\infty}^{\infty} \delta(t - t_k) \tag{2.22}$$

The sampling instants $t_k$'s can be selected in two ways. One possibility is to sample $t_k = t_{k-1} + \tau_k$, $k = 0, 1, 2, \ldots$, where $\tau_k$ is realisation of the random variable $\tau$. This type of sampling has been defined as additive random point process and was introduced by Sharpiro and Silverman [SS].

Another possibility for obtaining random samples is to take

$$t_k = kT + \tau_k.$$

Bilinskis and Mikelsons [BM92] have stated that the ratio $\frac{\sigma}{\mu}$, where $\sigma$ and $\mu$ are the standard deviation and mean of the probability distribution of the random variable $\tau_k$ respectively, plays a significant role in randomised sampling. This ratio can be varied to cover the complete range from deterministic to extremely randomised sampling.

Next we discuss the spectral analysis of randomly sampled signals. Let the signal to be randomly sampled be given by $g(t)$ and let the sampling be done using $u(t)$ given by 2.22. Let the estimated spectrum, when the signal is sampled at $2N$ instants, be,

$$\hat{G}(f) = \sum_{k=-N}^{N} g(t_k) e^{-j2\pi f t_k}.$$

The sampling instants are selected using the probability distribution function $\phi_k(t)$. The expected value of the estimated spectrum is given by,

$$E[\hat{G}(f)] = \sum_{k=-N}^{N} \int_{-\infty}^{\infty} g(t)\, e^{-j2\pi f t}\, \phi_k(t)\, dt$$

$$= \int_{-\infty}^{\infty} g(t)\, e^{-j2\pi ft} [\sum_{k=-N}^{N} \phi_k(t)]\, dt$$

If

$$\lim_{N\to\infty} [\sum_{k=-N}^{N} \phi_k(t)] = C, \tag{2.23}$$

then

$$\begin{aligned} \lim_{N\to\infty} E[\hat{G}(f)] &= C \int_{-\infty}^{\infty} g(t)\, e^{-j2\pi ft}\, dt, \\ &= C\, G(f). \end{aligned}$$

Hence we can conclude that the expected value of the estimated spectra of a randomly sampled signal, coincides with that of the spectra of the respective original signal, if condition 2.23 is satisfied.

This type of sampling is very promising in cases where there is no apriori information of the incoming signal. In such cases, the spectral estimation of an incoming signal can be done by sampling at randomly realised sampling instants in a large number of scans and the spectra can be estimated. The number of scans have to be increased till the estimate of the spectra stabilises. For a thorough study of randomised sampling we refer to [BM92].

### 2.2.3 Methods for Reconstructing Signals from Nonuniform Samples

#### 2.2.3.1 Lagrangian Interpolation:

An interpolating function, for nonuniform samples, which resembles the Lagrangian interpolation has been proposed by [Beu66],[Hig76]. Here the derivation of the inter-

polation is presented.

Let $\{e^{j\omega t_n}\}$ be a basis set in the frequency domain. The basis function in frequency domain is complete if any signal band-limited to $W$ can be represented in the frequency domain as,

$$G(f) = \sum_{-\infty}^{\infty} c_n e^{j\omega t_n}, \quad |f| \leq W. \tag{2.24}$$

The inverse Fourier transform of 2.24 is given by,

$$g(t) \;=\; \sum_{-\infty}^{\infty} c_n \; Sinc(2W(t - t_n)), \tag{2.25}$$

where $c_n$ is the inner product of $g(t)$ with another function $\psi_n(t)$, which is called biorthogonal of $Sinc(2W(t - t_n))$.

$$c_n = \int_{-\infty}^{\infty} g(t) \; \psi_n(t) \; dt, \tag{2.26}$$

and,

$$\int_{-\infty}^{\infty} \psi_k(t) Sinc(2W(t - t_n)) \; dt \;=\; \begin{cases} 1, & k = n \\ 0, & k \neq 0 \end{cases}.$$

In Equation 2.25 the $c_n$'s are not the samples of the signal at $t_n$'s, except for the case when $t_n = nT$. Equation 2.25 can be written in the sampling representation as

$$g(t) \;=\; \sum_{n=-\infty}^{\infty} g(t_n)\psi_n(t) \tag{2.27}$$

This equation can be readily verified as follows -

$$\begin{aligned} \sum_k |g(t_k)|^2 \;&=\; \sum_k \left| \int_{-\infty}^{\infty} g(t) \; Sinc(2W(t - t_k)) \; dt \right|^2, \text{ and by biorthogonality property} \\ &=\; \sum_k |c_k|^2. \end{aligned}$$

Hence if $\{e^{j\omega t_n}\}$ is complete, then the representation in Equation 2.27 is complete. An important problem is to find an explicit expression for $\psi_k(t)$. An expression for a

general complete set $\{t_n\}$ is not known. But under restrictions, an explicit expression can be found.

For the case when $|t_n - nT| \leq D \leq \frac{T}{4}$, $n = 0, \pm 1, \pm 2, \ldots$, $\{e^{j\omega t_n}\}$ is a basis for band-limited signals in the frequency domain and $\psi_n(t)$ can be shown to be the following Lagrangian function,

$$\psi_n(t) = \frac{H(t)}{H'(t_n)(t - t_n)} \tag{2.28}$$

$\psi_n(t_n) = 1$ and $\psi_n(t_k) \neq 0$, $k \neq n$. where,

$$H(t) = (t - t_0) \prod_{k=-\infty, k\neq 0}^{\infty} \left(1 - \frac{t}{t_k}\right) \tag{2.29}$$

The condition

$$|t_n - nT| < D < \frac{T}{4}, \; n = 0, \pm, \pm, \ldots \tag{2.30}$$

ensures the convergence of the expression 2.27. If the sampling set $\{t_n\}$ is finite, say $\{t_n : 0 \leq n \leq N\}$ then the classical Lagrangian interpolation formula is obtained. Hence Equation 2.28 can be considered as a generalised version of the Lagrangian interpolation.

If the condition given in inequality 2.30 is not satisfied but the rate of $\{t_n\}$ is higher than the Nyquist rate on the average and satisfies $|t_n - nT| < L < \infty$, $|t_n - t_m| > \delta > 0$, $m \neq n$, the interpolation Equations 2.27 and 2.28 are still valid but the but the product in 2.29 does not converge. However it can be shown that the following product converges pointwise and uniformly

$$H(t) = e^{at}(t - t_0) \prod_{k\neq 0} \left(1 - \frac{t}{t_k}\right) e^{t/t_k} \tag{2.31}$$

The omission of a finite number of samples does not alter the situation and the Equation 2.31 is still valid.

#### 2.2.3.2 Interpolation When the Samples of the Signal and the Differentials are Given:

For this case, an interpolation formula, using the Lagrangian formula, has been derived by Rawn[Raw89]. The following theorem states the interpolation formula -

**Theorem 2.2.3** *Let $g(t)$ be band-limited to $[-W, W]$, and the samples of $g(t)$ and its R-1 derivatives be known at $t_n$. Let $t_n$ be such that $|t_n - nRT| < \frac{T}{4R}$. Then*

$$g(t) = \sum_{n=-\infty}^{\infty} \left[ g(t_n) + \left(1 - \frac{t}{t_n}\right) g^1(t_n) + \ldots + \left(1 - \frac{t}{t_n}\right)^{R-1} g^{R-1}(t_n) \left[\psi_n(t)\right]^R \right]$$

*where,*

$$H(t) = (t - t_0) \prod_{k=-\infty, k\neq 0}^{\infty} \left(1 - \frac{t}{t_k}\right)$$

*and,*

$$g^k(t_n) = \frac{(-1)^k (t_n)^k}{k!} \frac{d^k}{dt^k} \left( \frac{g(t)}{[\psi_n(t)]^k} \right) \Bigg|_{t=t_n}, \quad 0 \leq k \leq R-1$$

Convergence of the series is uniform on $(-\infty, \infty)$. For the case when $t_n = \text{nTR}$, the interpolation reduces to uniform derivative sampling interpolation given by Linder and Abramson [LA60].

#### 2.2.3.3 An Iterative Method of Signal Recovery:

In this section an iterative method of signal reconstruction from nonuniform samples is discussed. This method is proposed by Wiley[Wil78] and uses a theorem by Sandberg.

**Theorem 2.2.4** *Let $Q$ be mapping of $\mathcal{K}$ in $\mathcal{K}$, where $K$ is a class of bandlimited square integrable signals, such that, for all $f, g \in \mathcal{K}$:*

$$Re\langle Qf - Qg,\ f - g\rangle \geq k_1 \|f - g\|^2 \tag{2.32}$$

$$\|PQf - PQg\| \leq k_2\|f - g\|, \tag{2.33}$$

*Where* $\langle , \rangle$ *denotes the inner product and* $\|f(t)\| = \left(\int_{-\infty}^{\infty} |f(t)|^2\, dt\right)^{1/2}$ *and where* $k_1$ *and* $k_2$ *are positive constants. Then for* $h \in \mathcal{K}$ *the equation* $h = PQf$ *has a unique solution* $(PQ)^{-1}h \in \mathcal{K}$ *given by* $(PQ)^{-1}h = \lim_{n\to\infty} f_n$ *where,*

$$f_{n+1} = \frac{k_1}{k_2}(h - PQf_n) + f_n \tag{2.34}$$

*and* $f_0$ *is an arbitrary element of* $\mathcal{K}$*. Furthermore for all* $h_1,\ h_2 \in \mathcal{K}$

$$\|(PQ)^{-1}h_1 - (PQ)^{-1}h_2\| \leq \frac{1}{k_1}\|(h_1 - h_2)\|.$$

Based on this theorem the sampling method is presented next. Let $s(t)$ be an interval average sampling function given by,

$$s(t) = \begin{cases} \frac{1}{\epsilon} & \frac{-\epsilon}{2} \leq t \leq \frac{\epsilon}{2} \\ 0 & otherwise \end{cases}$$

Let the non-equally spaced interval average sample sequence of a band-limited square integrable function $g(t)$ be

$$S(g(t)) \equiv \sum_{-\infty}^{\infty} \frac{s(t - t_n)}{\epsilon} \int_{t_n - \frac{\epsilon}{2}}^{t_n + \frac{\epsilon}{2}} g(t)\, dt \tag{2.35}$$

Let the sequence $t_n$ have the following properties -

$$|t_{n+1} - t_n| \geq d > 0 \tag{2.36}$$

$$\left|t_n - \frac{n}{2f_s}\right| < \frac{L}{2f_s} \tag{2.37}$$

Let $\epsilon < d$; in other words, the duration of the sampling pulse is to be less than minimum time between the sampling instants. Inequality 2.37 states that the spacing between two consecutive samples should be greater than a certain fixed positive quantity. Equation 2.37 requires that the separation between the sampling instants and the corresponding

uniform samples should be less than a fixed value. The sequence $t_n$ is said to have a uniform density of $2f_s$ according to a definition by Duffin and Schaffer [DS]. Further let $P$ be the band-limiting operator which transforms an arbitrary signal in $L^2(R)$ into a band-limited signal, in other words,

$$P(G(f)) = \begin{cases} G(f) & |f| < B \\ 0 & |f| \geq B \end{cases}$$

In [Wil78] it is shown that $P$ and $S()$ together satisfy theorem 2.2.4. Therefore the iterative scheme used in the theorem can be used to recover the signal from the samples. Let $f(t)$ be the original signal and $f(t_i)$, $i \in Z$ be the nonuniform samples. Let the LPF filtered version of the samples be $h(t)$. If $f_n(t)$ is the $n^{th}$ approximation of the signal $f(t)$, then

$$f_{n+1} = \frac{k_1}{k_2}(h - PQf_n) + f_n. \tag{2.38}$$

The scheme is shown in the Figure 2.3. In this figure -

P - low pass filter,

$S()$ -sampler, defined in the Equation 2.35,

$f_n(t)$ -$n^{th}$ approximation of the original signal,

h - the low passed version of the samples.

#### 2.2.3.4 A Nonlinear Method of Signal Recovery:

Before discussing the recovery problem, we present the spectral analysis of the nonuniform samples [Mar92].

Let $g(t)$ be the original signal and the pulse train, using which it is sampled, is denoted

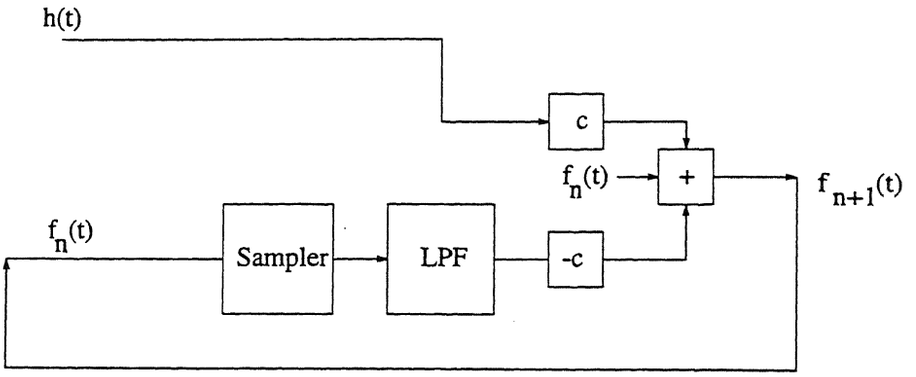


Figure 2.3: The scheme for the iterative method for signal recovery

by $g_p(t)$, and let

$$g_p(t) = \sum_k \delta(t - t_k) \tag{2.39}$$

Let $g_s(t)$ be the samples of the signal at instants $t_k$, $k \in Z$. Then,

$$g_s(t) = g(t)\, g_p(t)$$

and the theory of generalised function states that,

$$\delta(t - t_k) = |\dot{x}(t)|\, \delta([x(t)]), \tag{2.40}$$

provided that $x(t_k) = 0$, $\dot{x}(t_k) \neq 0$ and $g(t)$ has no zeros other than at $t_k$. One possible $x(t)$ can be written as,

$$x(t) = t - kT - \theta(t), \tag{2.41}$$

and $\theta(t)$ should satisfy the following condition,

$$t_k - kT - \theta(t_k) = 0.$$

Hence $\theta(t_k) = t_k - kT$ is the deviation of the samples from the uniform samples. From Equations 2.40 and 2.41 we have,

$$\delta(t - t_k) = |1 - \dot{\theta}(t)|\, \delta(t - kT - \theta(t)) \tag{2.42}$$

with the condition that $|\dot{\theta}(t)| \neq 1$. Marvasti and Lee [ML92] have given a sufficient condition so that this is valid. Substituting the value of $\delta(t - t_k)$ in 2.39, we have

$$g_p(t) = |1 - \dot{\theta}(t)| \sum_{k=-\infty}^{\infty} \delta(\phi(t) - kT)$$

where $\phi(t) = t - \theta(t)$. Since $\sum_{-\infty}^{\infty} \delta(\phi(t) - kT)$ is periodic with respect to $\phi(t)$ with a period $T$, its Fourier series expansion is given by,

$$\begin{aligned}\sum_{-\infty}^{\infty} \delta(\phi(t) - kT) &= \frac{|1 - \dot{\theta}(t)|}{T} \sum_{k} e^{jk\frac{2\pi}{T}\phi(t)} \\ &= \frac{|1 - \dot{\theta}(t)|}{T} \left[1 + 2\sum_{k=1}^{\infty} cos\left(\frac{2\pi kt}{T} - \frac{2\pi k\theta(t)}{T}\right)\right]\end{aligned}$$

It can be inferred from the above equation that $g_p(t)$ has a DC component of $\frac{|1-\dot{\theta}|}{T}$ plus a phase modulated signal, the phase modulation index given by $\frac{2\pi k}{T}$. Substituting for $g_p(t)$, $g_s(t)$ is given by,

$$g_s(t) = g(t)\frac{|1 - \dot{\theta}(t)|}{T} \left[1 + 2\sum_{k=1}^{\infty} cos\left(\frac{2\pi kt}{T} - \frac{2\pi k\phi(t)}{T}\right)\right]$$

If it is assumed that the bandwidth of $\theta(t)$ is less than $\frac{1}{2T}$, the modulation falls in the category of narrow band phase modulation. And the phase modulated part has a bandwidth of approximately twice the bandwidth of $\theta(t)$, which is less than $\frac{1}{T}$. Therefore low pass filtering $g_p(t)$ yields

$$\hat{g}_p(t) = \left(\frac{1-\dot{\theta}(t)}{T}\right)$$

for $1 > \dot{\theta}$. If the bandwidth of $\theta(t)$ is taken to be $W_\theta$, and if $\frac{1}{T} - W_\theta - W > W + W_\theta$, there is no overlap between the narrow band PM signal and $G(f) * (-\frac{\dot{\theta}}{T})$. Thus low

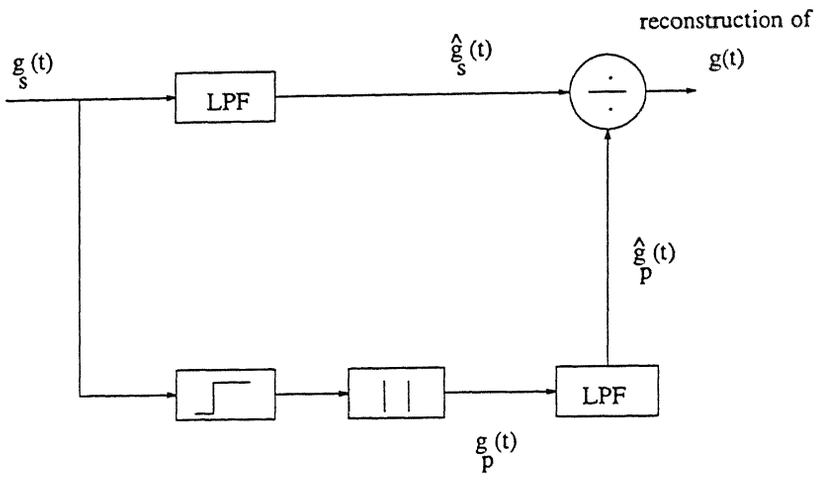


Figure 2.4: The scheme for the nonlinear method of signal recovery

pass filtering the nonuniform samples $g_s(t)$ gives

$$\hat{g}_s(t) = g(t)\left(\frac{1-\dot{\theta}(t)}{T}\right) \tag{2.43}$$

Therefor, the original signal can be recovered by dividing $\hat{g}_s(t)$ by $\hat{g}_p(t)$.

The recovery algorithm from the samples is shown in the Figure 2.4. The original samples are low pass filtered and $\hat{g}_s(t)$ is obtained. The samples are also used to obtain $g_p(t)$, the pulse train, by thresholding and finding the mod value (magnitude). Then low pass filtering $g_p(t)$, $\hat{g}_p(t)$ is found. Subsequently dividing $\hat{g}_s(t)$ by $\hat{g}_p(t)$ the reconstruction of $g(t)$ is obtained.

#### 2.2.3.5 Interpolation Using Generalised Sampling Theorem:

Before presenting the technique of interpolation, we discuss the Generalised sampling theorem [Kra59].

**Theorem 2.2.5** *Generalised Sampling Theorem: Let $x(t)$ be representable in the following form*

$$x(t) = \int_I \mathcal{K}(s,t)g(s)\,ds, \tag{2.44}$$

*where, $g(s)$, $\mathcal{K}(s,t) \in L^2(I)$. Let there exist $\{t_n\}$, such that, $\mathcal{K}(s,t_n)$ forms a Complete Orthonormal set on $L^2(I)$. Then the signal $x(t)$ is representable as*

$$x(t) = \lim_{N\to\infty} \sum_{|n|\leq N} x(t_n)S_n(t) \tag{2.45}$$

*where,*

$$S_n(t,t_n) = \frac{\int_I \mathcal{K}(x,t)\overline{\mathcal{K}(x,t_n)}\,dx}{\int_I |\mathcal{K}(x,t_n)|^2\,dx} \tag{2.46}$$

**Proof:** Since $\mathcal{K}(s,t_n)$ is a completely orthonormal set, therefore,

$$g(s) = \sum_{-\infty}^{\infty} c_n\,\overline{\mathcal{K}(s,t_n)} \tag{2.47}$$

where,

$$\begin{aligned} c_n(t) &= \frac{\int_I g(s)\mathcal{K}(x,t_n)\,dx}{\int_I |\mathcal{K}(x,t_n)|^2\,dx} \\ &= \frac{x(t_n)}{\int_I |\mathcal{K}(x,t_n)|^2\,dx} \end{aligned}$$

Multiplying Equation 2.47 on both sides by $\mathcal{K}(s,t)$ and integrating with respect to $s$ leads to,

$$x(t) = \sum_{n=-\infty}^{\infty} x(t_n)S_n(t,t_n) \tag{2.48}$$

If the set $\{t_n\}$ is available, then, $x(t)$ can be reconstructed using the Equation 2.48.

Example- Bessel's Interpolation- In this case $\mathcal{K}(s,t) = sJ_m(st)$, where $J_m$ are Bessel band-limited functions, band-limited to I=[0,W]. The interpolation function is given by

$$x(t) = \sum_{n=-\infty}^{\infty} x(t_n)\frac{J_m(t)}{(t_n - t)J_{m+1}(t_n)} \tag{2.49}$$

The proof can be found in [Mar92].

#### 2.2.3.6 Stability in Nonuniform Sampling:

In this discussion, the definition of stability and the condition for stable sampling expansion are reviewed. A few examples of stable sampling expansion are also presented.

A given class of signals $\{g(t)\}$ is said to possess a stable sampling expansion if there exists an admissible class of sampling sequences of real numbers $t_n, n \in I$, where I is an index set of integers fixed for each admissible class, such that the class of sequences of sample values $t_n$, $n \in I$ determines the class of signals in some sense (for example, a certain error norm tending to zero).

**Definition 2.2.1** *A sampling expansion is called stable if small corruptions in the amplitudes of the sample values leads to small changes in the reconstructed signal using the sample set [Lan67].*

Yao and Thomas [YT67] have defined the concept of stability with reference to band-limited signals only. Let $g(t)$ be the signal under investigation. Let the uncorrupted sequence of samples be $g(t_n)$ and the noise function be $f(t)$ which is band-limited to $[-B,\ B]$. Since the class of functions is a linear class, the corrupted sequence of samples is given by $g(t_n) + f(t_n), n \in I$. And the corresponding corrupted function is $(g(t) + f(t))$ which is band-limited to $[-B,\ B]$.

Next the condition for stable sampling expansion is presented. The class of functions band-limited to $[-B,\ B]$ is said to possess a stable sampling expansion with respect to a class of sampling sequences $t_n$, $n \in I$, if there exists a positive finite absolute constant $C$ ($C$ is independent of $g(t)$ and $t_n, n \in I$), such that, the condition

$$\int_{\infty}^{\infty} |g(t)|^2\, dt \ \leq\ C \sum_{n \in I} |g(t_n)|^2 \tag{2.50}$$

is valid for each sampling sequence and for each band-limited signal $g(t)$. The definition is apparently motivated by the fact that if the condition in Equation 2.50 is satisfied and additionally if the $L^2$ norm of the corrupting sequence given by $\sum_n |f(t_n)|^2$ is bounded, then the mean square reconstruction error is also bounded. This can be shown as follows -

$$\begin{aligned} \textit{mean square error} &= \int_{-\infty}^{\infty} |g(t) - (g(t) + f(t))|^2 \, dt && (2.51) \\ &= \int_{-\infty}^{\infty} |f(t)|^2 \, dt && (2.52) \\ &\leq C \sum_n |f(t_n)|^2 && (2.53) \\ &\leq C\,\delta, \; if \; \sum_n |f(t_n)|^2 < \delta < \infty. && (2.54) \end{aligned}$$

Before closing this subsection two examples of stable sampling expansion are presented.

Example-1 The class of signals band-limited to [-1/2, 1/2] possess a sampling expansion given by

$$g(t) = \sum_{-\infty}^{\infty} g(t_n)\psi_n(t)$$

with respect to each sampling sequence $t_n$ from the class

$$|t_n - n| \leq d < 1/4, \quad n \in I = \{0, \pm 1, \pm 2, \ldots.\} \tag{2.55}$$

In this expansion $\psi_n(t)$ is given by

$$\psi_n(t) = \frac{G(t)}{(t - t_n)G'(t_n)}$$

where,

$$G(t) = (t - t_0) \prod_{n=1}^{\infty} (1 - 1/t_n)(1 - t/t_{-n}).$$

This is a stable sampling expansion.

Example-2 The class of functions band-limited to $[-\frac{1}{2}+\frac{\epsilon}{2\pi}, \frac{1}{2} - \frac{\epsilon}{2\pi}]$ possess a sampling expansion given by

$$g(t) = \sum_{-\infty}^{\infty} g(t_n)\psi_n(t)$$

with respect to each sampling sequence $t_n$ from the class

$$|t_n - n| < L < \infty$$

$$\infty > |t_n - t_m| > 0, \quad n \neq m$$

Each composing function is given by

$$\psi_n(t) = \frac{G(t)}{(t - t_n)G'(t_n)}$$

where $G(t)$ is given by,

$$G(t) = Ae^{at}(t - t_0) \prod_{n=-\infty, n\neq 0}^{\infty} (1 - t/t_n)e^{t/t_n}$$

*or*

$$G(t) = Be^{bt}(t - t_0) \prod_{n=1}^{\infty} (1 - t/t_n)(t - t/t_{-n})$$

*with*

$$a = -\sum_{n=}^{\infty}(1/t_n + 1/t_{-n}) \text{ and } b = 0$$

This is also a stable sampling expansion. Further details can be found in Yao and Thomas[YT67].

### 2.2.4 Nonuniform Sampling of Time-Limited Signals

In the previous subsection we have considered the nonuniform sampling of signals on $R$. Here we will be discussing the nonuniform sampling of time-limited signals. In most

practical situations nonuniform sampling occurs as an undesirable effect and there is no choice but to deal with nonuniform data. A few examples are as follows [Mar92].

1) For applications in seismology and oceanography, when data is measured in a moving vehicle, then due to fluctuations in speed, random or uniform samples with jitter are inevitable.

2) Data tracked in digital flight control.

3) Data read from and recorded on a tape or disc with speed fluctuations.

4) Data loss due channel erasures and additive noise.

However, we review cases, wherein, nonuniform sampling has been deliberately introduced.

The basic problem that occurs in applying nonuniform sampling is as follows. Let $g(t)$ be a signal sampled in the interval $I$, at the points $t_i$, $i = 0, \ldots, N-1$. If $\hat{g}(t)$ is the reconstruction of the signal using a given interpolation procedure, then it is required to find the optimal $t_i$, $i = 0, \ldots, N-1$, such that the error between $g(t)$ and $\hat{g}(t)$ is minimised. This statement can be stated mathematically in the following way -

$$\begin{aligned} \epsilon_{opt} &= \min_{t_0,\ldots,t_N} \|g(t) - \hat{g}(t)\|^2 \\ (t_0, \ldots, t_{N-1})_{opt} &= \{(t_0, \ldots, t_{N-1}) \ : \ \|g(t) - \hat{g}(t)\|^2 = \epsilon_{opt}\} \end{aligned} \tag{2.56}$$

For example, this problem can be attempted with spline interpolation; in this case the error has to be minimised with respect to the knot locations. Attempts to solve the optimisation problem have been done [BdT88], [MGCH88]. Similarly, Shahein and Abbas [SA94] have attempted to compress ECG signals using cubic spline interpolation by placing the knots at nonuniform intervals. In spite of these attempts, how the local variations affect the sample locations has remained vague.

In this thesis, two aspects of the same problem have been formulated and algorithms

for solving the problems have been presented. In Chapter 4 of this thesis the optimal sampling problem is attempted and an algorithm is presented. For solving the problem, the time-scale localisation properties of the wavelet transform are utilised. In Chapter 5, the sample number distribution problem has been solved, leading to a multirate sampling strategy for time-limited signals. The problem considered is to distribute $N_0$ number of samples in $m$ partitions of the interval $I$ such that the mean square error between the original signal and the reconstructed signal is minimised. In each of the partitions the samples are placed uniformly. Certain constraints on the type of the interpolation used are also placed. Finally an algorithm for multirate sampling is presented. For solving the problem the notion of scale-limitedness with reference to wavelet transforms is used. The notion of scale-limitedness will be introduced in the Chapter 3.

# Chapter 3

# Signal Variation Characterisation Using Wavelet Transforms

In this chapter, a new signal variation measure, called scale-limitedness, is introduced with reference to wavelet transforms. A signal is called scale-limited if its wavelet transform is zero for all values of the scale below a certain value and for all shifts. The practical considerations due to which this concept has emerged have also been discussed. It has been shown through simulations, that signals with smaller scale-limits, have faster variation.

Scale-limitedness is similar to band-limitedness, but has some additional properties which makes it very useful. As an extension $\delta_0$-practical scale-limitedness has been defined. Finally, a few properties of scale-limited signals have been established. It is shown that all band-limited signals are scale-limited with respect to a class of wavelet families. Further, the existence of time-limited signals which are also scale-limited is established. Moreover, it is proved that, the larger the value of the scale-limit, the

smoother is the signal. The class $M^n$ is defined and it is shown that the Lagrangian interpolation for $n$ points is $\delta_0$-practically scale-limited with respect to a wavelet family whose mother wavelet is in $M^n$ space.

An application of the concept of scale-limitedness is also presented. The problem of sampling rate estimation of time-limited signals is introduced and an algorithm is presented which can be used for the sampling rate estimation. Initially, the signal for which the sampling rate has to be estimated, is sampled at an arbitrary high rate; then depending upon the required error performance and the scale-limit of the signal, the necessary number of samples are retained.

## 3.1 Introduction

The technique of applying transforms on signals, and studying them in both the original and in the transformed domains is well established in the area of signal processing. In conventional signal processing, Fourier transforms have been widely used. In recent years, however, the application of other transforms has increased. This is mainly due to the poor time-frequency localisation behaviour displayed by the Fourier transforms.

There are many applications in the field of engineering, wherein, important information is associated with the transients of the signal. In these cases it is often desirable to process these transients separately. These applications include: detection of characteristic points, edge detection, segmentation of images, etc. Consequently a need arose to develop transforms, which can characterise signals in time as well as in transform domains simultaneously. This was one of the reasons for studying wavelet transforms. There are certain other transforms which can be used for time-frequency analysis, for

example: short time Fourier transform and Wigner-Ville distribution [Coh89]. But flexibility in the choice of the kernel of the transform and existence of complete orthonormal bases for discrete wavelet transforms, are some of the reasons, due to which the use of wavelet transforms is increasing.

In wavelet transforms, the domain of the transformed signal is two dimensional; one dimension is shift and the other is called scale. The concept of scale is analogous to that of frequency in Fourier analysis. The class of band-limited signals consists of those signals whose Fourier transform vanishes outside an interval of finite length measure. The importance of scale parameter in the context of signal and image processing has already been emphasised [SS93], [SS94]. Bandlimitedness in Fourier transforms, has played a significant role in signal processing and system design. Consequently, for wavelet transform, it is logical to define the notion of Scale-limitedness and investigate its properties.

R. A. Gopinath et. al. [ea94], have defined essential Scale-limitedness for discrete wavelet transforms and also shown that band-limited signals are essentially Scale-limited. In this chapter, scale-limitedness is defined on the same lines as those of band-limitedness. When the magnitude of the scale value is closer to zero, the wavelet is sharper, so, the smallest scale value present in the signal plays the role of representing the fastest varying component; which is done by high frequencies in Fourier transforms. As the scale value is increased, the scaled version of the wavelet becomes slow varying. Moreover, at higher scales the amplitude of the term $\frac{1}{\sqrt{a}}\psi\left(\frac{t-b}{a}\right)$ keeps reducing. Consequently, the wavelet transform tends to zero at higher scales.

From the discussion it can be inferred that, for wavelet transforms, the higher limit of the scale parameter is, in general, infinity. Therefore, when specifying the scale-limits,

only the lower limit is stated, the higher limit is understood to be infinity. So the concept of scale-limit proceeds on the same lines as band-limitedness, but the higher limit for scale-limit being infinity, is not stated. For practical applications, $\delta_0$-practical scale-limitedness is defined, which reduces to essential scale-limitedness in the case of discrete wavelet transforms.

### 3.1.1 Wavelet Transforms

#### Definitions

Here we briefly review important definitions related to wavelet transforms, for details refer to [Dau92]. A function $\psi(t) \in L^2$ is called a wavelet if it satisfies the following condition,

$$C_\psi = \int |f|^{-1} |\Psi(f)|^2 \, df < \infty, \tag{3.1}$$

where,

$$\Psi(f) = \int_{-\infty}^{\infty} \psi(t) e^{-j2\pi ft} \, dt.$$

If $\Psi(f)$ is continuous, then the condition 3.1 is satisfied only when $\Psi(0) = 0$ or $\int \psi(t) \, dt = 0$. Using $\psi(t)$, a doubly indexed family of wavelets is generated by dilating and translating,

$$\psi^{a,b}(t) = |a|^{\frac{-1}{2}} \psi \left( \frac{t-b}{a} \right),$$

where $a, b \in R$, $a \neq 0$. We use positive as well as negative $a$ at this point, however, in all subsequent places the wavelet transform and its inverse is computed for positive $a$. The normalisation factor is chosen such that $||\psi^{a,b}|| = ||\psi||$.

The wavelet transform of $g(t) \in L^2(R)$ with respect to the family $\psi^{a,b}(t)$ is given by

$$W_{g,\psi}(a,b) = \langle\, g, \psi^{a,b}(t)\,\rangle, \tag{3.2}$$

$$= \int g(t)\, |a|^{-1/2} \overline{\psi\left(\frac{t-b}{a}\right)}\, dt. \tag{3.3}$$

We assume that $||\psi|| = 1$, so that $|W_{g,\psi}(a,b)| \leq ||g(t)||$, this follows from Cauchy-Schwarz inequality.

A function $g(t)$ can be recovered from its wavelet transform via the resolution of the following identity:

$$g(t) = C_\psi^{-1} \int_{a\in A} \int_{b\in B} \frac{dadb}{a^2}\, W_{g,\psi}(a,b)\, \psi^{a,b}(t), \tag{3.4}$$

where $W_{g,\psi}(a,b) \neq 0, a \in A \subset (0,\infty]$, $b \in B \subset R$. The energy of the signal $g(t)$ is given by,

$$\int_{-\infty}^{\infty} |g(t)|^2\, dt = C_\psi^{-1} \int_{a\in A} \int_{b\in B} \frac{dadb}{a^2}\, |W_{g,\psi}(a,b)|^2. \tag{3.5}$$

### 3.1.2 Practical Implementation of Wavelet Transforms: The Discrete Wavelet Transform

In Fourier transforms, the kernel of the transform is the function $e^{jx}$, in the case of wavelet transform the kernel is not unique. Any function which has finite energy and satisfies the admissibility condition (Equation 3.1) can be used as a wavelet. Obtaining such functions is a difficult task, but Mallat [Mal89] and Meyer[Mey91] have solved the problem partially by introducing the concept of Multiresolution analysis.

In Multiresolution analysis, the scale and the shift parameters are discretised and the wavelet transform is found only at discrete values. Typically, the scale parameter can be discretised to dyadic values, so that $a = 2^j$, $j \in Z$, $b = k2^j$, $j, k \in Z$.

Here only a brief outline of the concept is provided, a detailed discussion can be found in [Dau92]. In Multiresolution analysis, a sequence of successive approximation spaces denoted by $V_j$, $j \in Z$ is constructed, such that,

**P 1**

$$\ldots V_2 \subset V_1 \subset V_0 \subset V_{-1} \subset V_2 \ldots$$

**P 2**

$$\overline{\cup_{j \in Z} V_j} = L^2(R)$$

**P 3**

$$\cap_{j \in Z} V_j = \{0\}.$$

There is an additional constraint that, for $g \in L^2(R)$,

**P 4**

$$g \in V_j \leftrightarrow g(2^j) \in V_0$$

**P 5**

$$g \in V_0 \leftrightarrow g(. - k) \in V_0, \forall\, k \in Z.$$

This implies that all spaces should be scaled versions of $V_0$. To characterise the space $V_0$, an orthonormal basis is required for it. In Multiresolution analysis, this basis is of the following kind,

$$\phi(t - k), k \in Z.$$

So that,

**P 6**

$$< \phi(t-k), \phi(t-j) >= \delta_{jk}.$$

The basis of the space $V_j$ is denoted by $\{\phi_{j,k} : k \in Z\}$ and is given by,

$$\phi_{j,k} = 2^{-j/2}\, \phi(2^{-j}t - k) \tag{3.6}$$

Since, $V_0 \subset V_{-1}, \phi_{0,0}$ should be representable in terms of $\phi_{-1,n}$, $n \in Z$.

$$\phi_{0,0} = \sum_n h_n\, \phi_{-1,n}$$

$$\text{or, } \phi(t) = \sqrt{2}\sum_n h_n\, \phi(2t-n) \tag{3.7}$$

By shifting $t$ to $(t-k)$, it can shown that all the basis of $V_0$ are representable in terms of the basis of $V_{-1}$. Incidentally, Equation 3.7 also implies that,

$$\phi_{j,0} = \sum_n h_n\, \phi_{j-1,n}$$

By shifting $t$ by $t-k$, it is straight forward to show that all the bases of $V_j$ are representable in terms of bases of $V_{j-1}$. Therefore Equation 3.7 also implies that $V_j \subset V_{j-1}$. Hence to obtain property P 1, only Equation 3.7 has to be satisfied by the basis.

The basic result in Multiresolution analysis can be stated through the following theorem. This theorem establishes the existence of a wavelet basis $\psi_{j,k}$, $j \in Z$, $k \in Z$ for $L^2(R)$, where

$$\psi_{j,k} = 2^{-j/2}\, \psi(2^{-j}t - k) \tag{3.8}$$

for a given Multiresolution analysis setting, in which the properties P 1-P 6 are satisfied.

**Theorem 3.1.1** *If a ladder of subspaces $(V_j)_{j\in Z}$ in $L^2(R)$ satisfies the the properties P 1-P 6, then there exists an associated orthonormal wavelet basis,*

$$\{\psi_{j,k} \; ; \; j,k \in Z\} \text{ for } L^2(R), \text{ such that,}$$

$$P_{j-1} = P_j + \sum_k < .., \psi_{j,k} > \psi_{j,k} \tag{3.9}$$

*One possibility for the construction of the wavelet is,*

$$\psi(t) = \sum_n (-1)^{n-1} h_{-n-1} \phi(2t - n) \tag{3.10}$$

The convergence of the series is in $L^2$-sense.

The space spanned by $\psi_{j,k}$ is denoted by $W_j$. Hence,

$$V_{j-1} = V_j \bigoplus W_j$$

For further analysis the notation of approximate and detail signals is introduced.

$< g(t), \phi_{j,k} >, k \in Z$, is called the approximate signal in the $j^{th}$ space and is denoted by $A_j^k g$. $< g(t), \psi_{j,k} >, k \in Z$, is called the detail signal in the $j^{th}$ space and is denoted by $D_j^k g$.

For the purpose of practical implementation of the algorithm, the samples of the signal are taken equal to the approximate signal in the space $V_0$. Once this assumption is made, successive approximate signals in spaces $V_1, V_2, V_3, \ldots$ can be found and also the detail signal in the spaces $W_j, j = 1, 2, 3, \ldots$ can be found. This assumption is made on the following grounds. The scaling function $\phi(t)$ is a low-pass filter. The approximate signal in $V_0$ is given by,

$$\begin{aligned} A_0^k \, g &= \int_{-\infty}^{\infty} \phi(t-k) g(t) dt \\ &= \int_{-\infty}^{\infty} G(f) \overline{\phi(f) e^{-j2\pi fk}} df \end{aligned}$$

If, $G(f) \neq 0, f \in [-B, B]$ and $\psi(f) = 1, f \in [-B, B]$. Then,

$$\begin{aligned} A_0^k\, g &= \int_{-B}^{B} G(f) e^{j2\pi fk} df \\ &= g(k) \end{aligned}$$

Hence the approximate signal for $j = 0$ is $g(k), k \in Z$. Next it is shown that the $j^{th}$ approximation can be found if the $(j-1)^{th}$ approximation is known. It is also shown that the $j^{th}$ detail signal can be found if the $(j-1)^{th}$ approximate signal is known.

$$A_j^k\, g = \int_{-\infty}^{\infty} g(t) \frac{1}{\sqrt{2^j}} \phi\left(\frac{t - k2^j}{2^j}\right) dt$$

From Equation 3.7 it can be shown that,

$$\phi_{j,k} = \sum_m h_{m-2k}\, \phi_{j-1,m}, \tag{3.11}$$

$$\text{therefore, } < g(t), \phi_{j,k} > = \sum_m \overline{h_{m-2k}} < g(t), \phi_{j-1,m} >, \tag{3.12}$$

$$\text{or, } A_j^k\, g = \sum_m \overline{h_{m-2k}}\, A_{j-1}^m g \tag{3.13}$$

Hence the approximate signal at the $(j)^{th}$ level can be obtained by convolving the approximate signal at $(j-1)^{th}$ level by the filter $\overline{h_{-n}}$ and then subsampling by 2.

Similarly starting from Equation 3.10 with $l_n = (-1)^{n-1} h_{-n-1}$, the following relation can be shown,

$$\psi_{j,k} = \sum_m \overline{l_{m-2k}}\, \phi_{j-1,m}, \tag{3.14}$$

$$\text{therefore, } < g(t), \psi_{j,k} > = \sum_m \overline{l_{m-2k}} < g(t), \phi_{j-1,m} >, \tag{3.15}$$

$$\text{or, } D_j^k g > = \sum_m \overline{l_{m-2k}}\, A_{j-1}^m g \tag{3.16}$$

Hence from the approximate signal at the $(j-1)^{th}$ level the detail signal at the $j^{th}$ can be found. The detail signal, denoted by $D_j^k g$, is the wavelet transform $W_{g,\psi}(a, b)$ for $a = 2^j$, $b = k2^j$. The final algorithm is shown in Figure 3.1.

In section 3.2, scale-limitedness is defined and its various extensions are given. In section 3.3, the connection between scale-limitedness and the vanishing moment property is discussed. The theorems related to scale-limitedness are presented in section 3.4. In section 3.5, an algorithm for sampling rate estimation is presented, which uses the concept of scale-limitedness. Finally the conclusions are presented in section 3.6.

## 3.2 Scale-limitedness

The practical considerations which have led to the emergence of this concept are outlined below. The wavelets at low scales have faster variation; this is illustrated in the Figure 3.2; where $\frac{1}{\sqrt{a}}\psi\left(\frac{t}{a}\right)$ is plotted for a=0.25, 1, 4 respectively, where $\psi(t) = (\pi t)^{-1}(sin(2\pi t) - sin(\pi t))$. In wavelet decomposition, low scale wavelets capture the relatively fast varying portions of the signal. To elaborate this further, let us go into the definition of the wavelet transform. The wavelet transform is an inner product between $g(t)$ and $\frac{1}{\sqrt{a}}\psi\left(\frac{t-b}{a}\right)$. The parameter $b$ shifts the wavelet $\psi\left(\frac{t}{a}\right)$ by $b$ units; as a result of this, $W_{g,\psi}(a,b)$ gives the behaviour of the signal at $t = b$.

The admissibility condition ensures that $\int \psi(t)\, dt = 0$, i.e., the mean of the wavelet is always zero. If the signal $g(t)$ is constant on a set of finite length measure around the point $t = b$, then there exists a certain $a_0$, such that, $W_{g,\psi}(a,b) = 0$ for $a < a_0$, when compactly supported wavelets are used, however, for the case of noncompactly supported wavelets, the wavelet transform will have a relatively small value. In general, due to the admissibility condition, the value of the wavelet transform is low in those regions, wherein, the signal is relatively slow varying as compared to the wavelet. This point is further clarified, when the relation between scale-limitedness and vanishing moment property of the wavelet is discussed. Moreover, if $g(t)$ is slow varying for

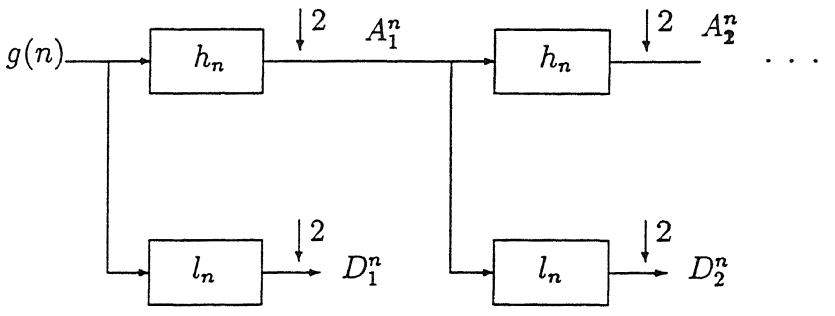


Figure 3.1: Implementation of Multiresolution analysis

$t \in D \subset R$, then there exists $a_0$ such that, for $a < a_0$ and $b \in D$, $W_{g,\psi}(a,b)$ will have negligible contribution in reconstructing $g(t)$ from $W_{g,\psi}(a,b)$, $a \in R^+, b \in R$.

In the following a few examples are presented, which illustrate that the wavelet transform of a signal $g(t)$ will have relatively large value for shift parameter taking values in a subset of the real line, if the signal has relatively fast variation for time parameters in the same subset. We take 240 samples of the signal, then the multiresolution analysis is used to find the wavelet transform of the signal. In all the examples we have taken 240 samples for computing wavelet transforms. The number of samples taken equal to $2^k$ for some positive $k$. In our case we compute wavelet transform upto scale 16 only, which means that at the last level the approximate signal in the decomposition has 15 samples. This has been done to reduce the required storage space. Decomposition upto level scale equal to 16 is sufficient to prove the correctness of the theory. In Figure 3.3, a test signal $g(t)$ is plotted, which has fast variation in the interval [100,200]. In Figure 3.4, taking the signal in Figure 3.1 as $g(t)$, $W_{g,\psi}(2,b)$ has been plotted. The wavelet transform of the same signal for scales 4, 8, 16 respectively have been plotted in Figures 3.5, 3.6, 3.7. This wavelet transform is computed using Daubechies $8^\psi$ compactly supported wavelet [Dau92] and Mallet's algorithm [Mal89]. The length of the filter $h_n$ corresponding to this wavelet is 16. It can be observed that the curve $W_{g,\psi}(2,b)$ has

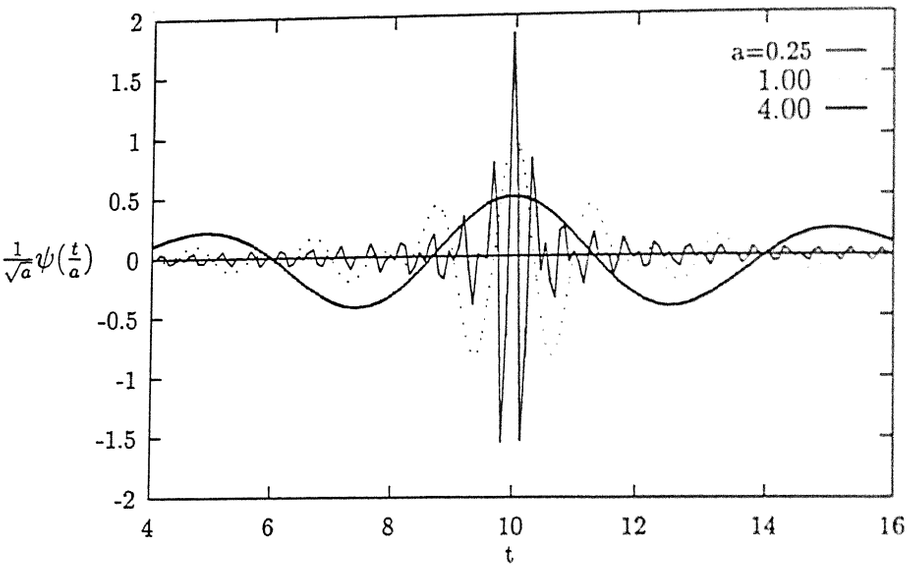


Figure 3.2: $\frac{1}{a^{1/2}}\psi\left(\frac{t}{a}\right)$, for a=0.25, 1, 4.

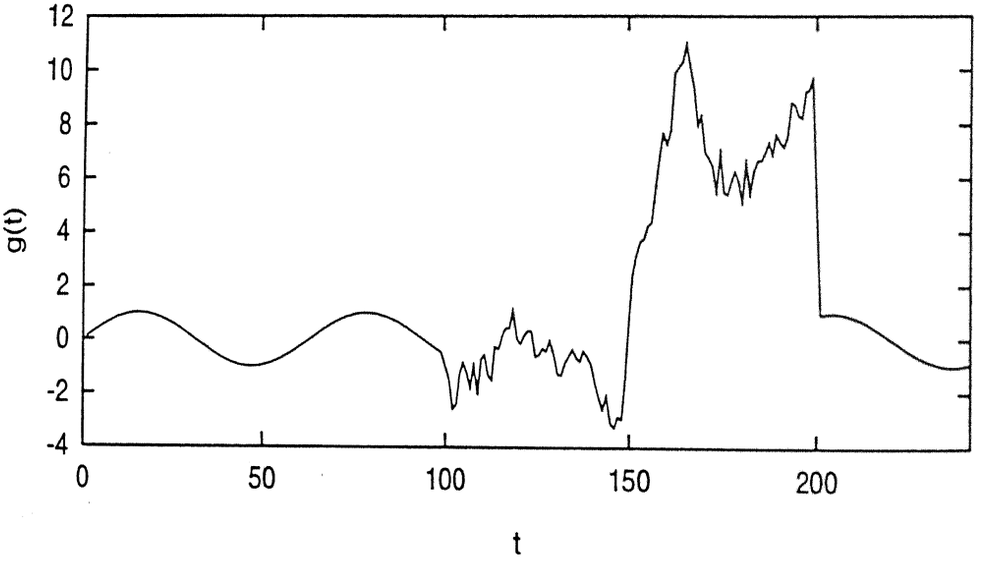


Figure 3.3: The test signal.

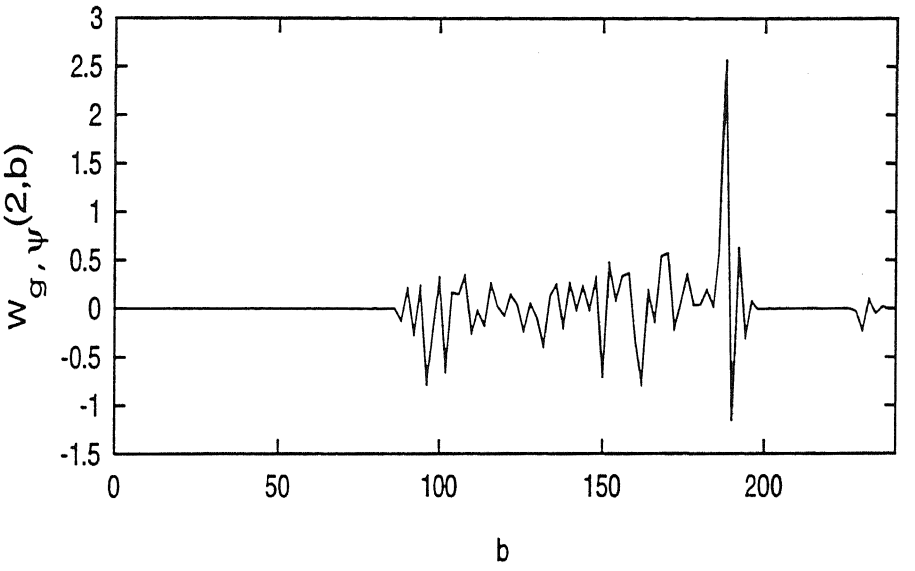


Figure 3.4: The wavelet transform of the test signal shown in Figure 3.3 for scale value equal to 2.

significant values in the interval [85,185], which is same as [100,200] translated by 15 time units. This shift has occurred due to the asymmetry of the mother wavelet. From this example, it can be inferred that at low scales, the wavelet transform is enhanced in a region where the signal variations are fast in time domain. To some extent, this feature can be observed in Figure 3.3. However, at higher scales this feature gets less prominent.

A similar behaviour can be observed in the next two examples. In Figure 3.8 the test signal shown has significant variations on the sets given by [0, 30] and [130, 180]. The wavelet transform of the signal for scales 2, 4, 8, 16 respectively has been plotted in Figures 3.9, 3.10, 3.11, 3.12. In this case as well, at scale value equal to 2, the wavelet transform has significant values in the sets which are left shifted with respect to [0,

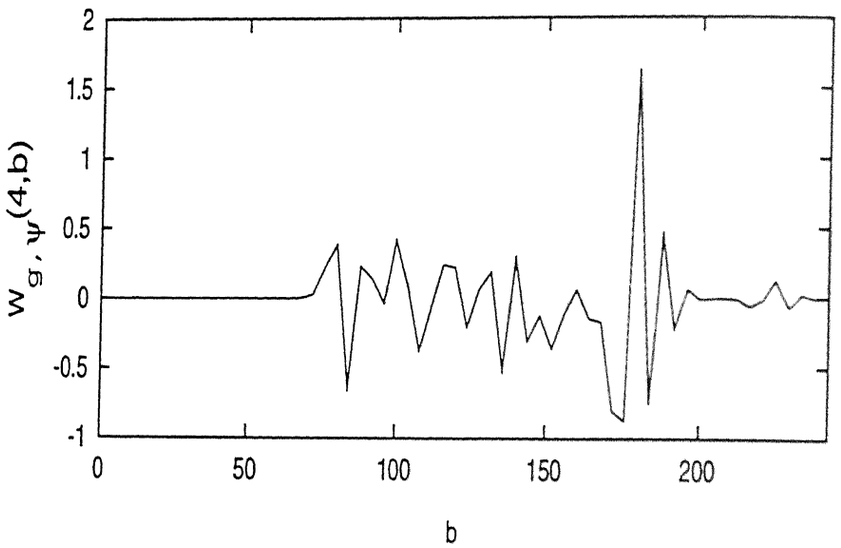


Figure 3.5: The wavelet transform of the test signal shown in Figure 3.3 for scale value equal to 4.

30] and [130, 180]. However at higher scales, the phenomenon of wavelet transform enhancement for scale parameter taking values in sets where the signal is varying fast becomes less prominent. This can be observed from the plots in Figures 3.8, 3.9, 3.10.

In Figure 3.13, the test signal analysed in the third example has been presented. this signal has many regions of fast variation. In this example as well, at low scales, the wavelet transform has significant values in the region which is left shifted from the region in which the signal has fast variation. Gradually at higher scales this behaviour gets less prominent. The fact, that the wavelet coefficients can be used to find the points of time at which significant changes occur, has been observed in [DJ94]. By eliminating fast varying components, it is possible to construct signals which are scale-limited. For any wavelet $\psi(t)$ and a given $a_0$, a class of signals g(t) can be constructed

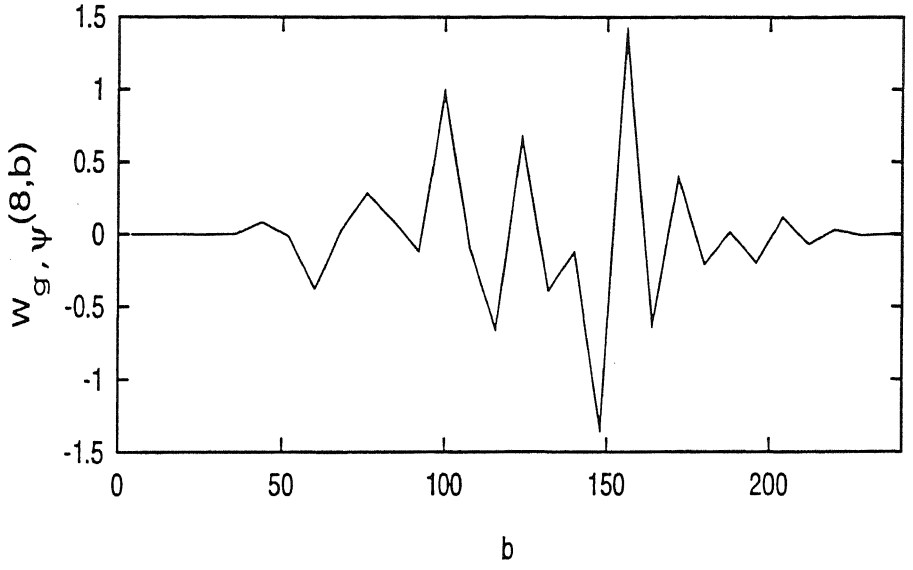


Figure 3.6: The wavelet transform of the test signal shown in the Figure 3.3 for scale value equal to 8.

for which $W_{g,\psi}(a,b) = 0$, for $a < a_0$ and all $b$. The class of scale-limited signals, scale-limited to $a_0$, consists of signals which do not have faster variation than that indicated by $\psi\left(\frac{t-b}{a}\right)$.

### 3.2.1 Definitions

**Definition 3.2.1** *Scale-limitedness: A signal $g(t) \in L^2(R)$ is said to be scale-limited to $a_l$ with respect to a wavelet family $\psi\left(\frac{t-b}{a}\right)$, $a \in R^+, b \in R$, if $W_{g,\psi}(a,b) = 0$, for $a < a_l$, $a_l > 0$, $\forall b$.*

The class of scale-limited signals for which $a \in (a_l, \infty)$, consists of signals which do not have faster components than those indicated by the wavelet $\psi\left(\frac{t-b}{a_l}\right)$.

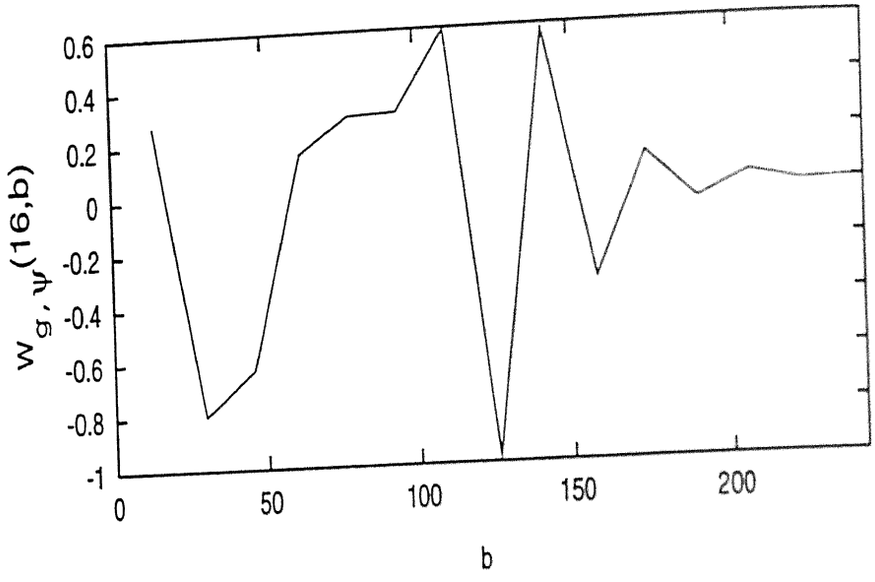


Figure 3.7: The wavelet transform of the test signal shown in the Figure 3.3 for scale value equal to 16.

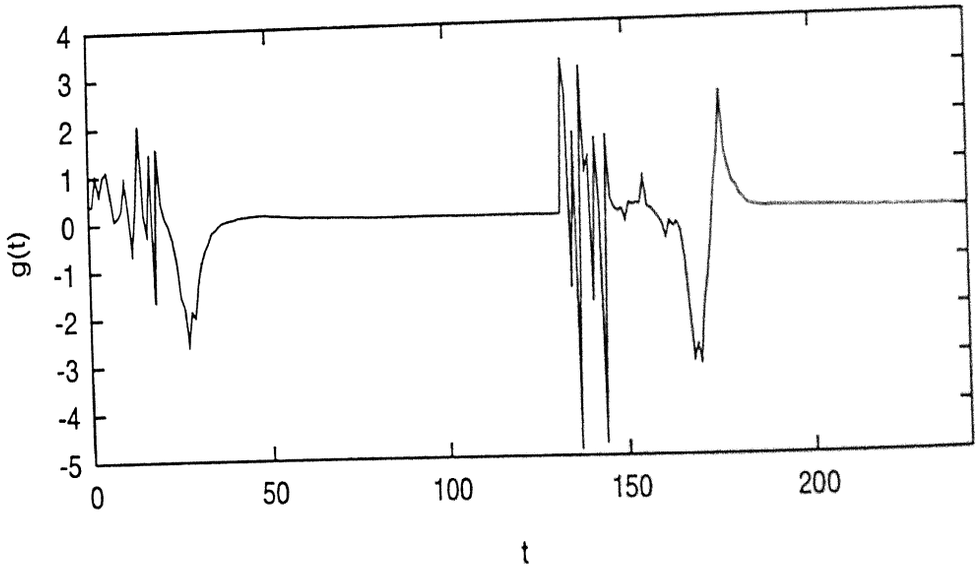


Figure 3.8: The test signal.

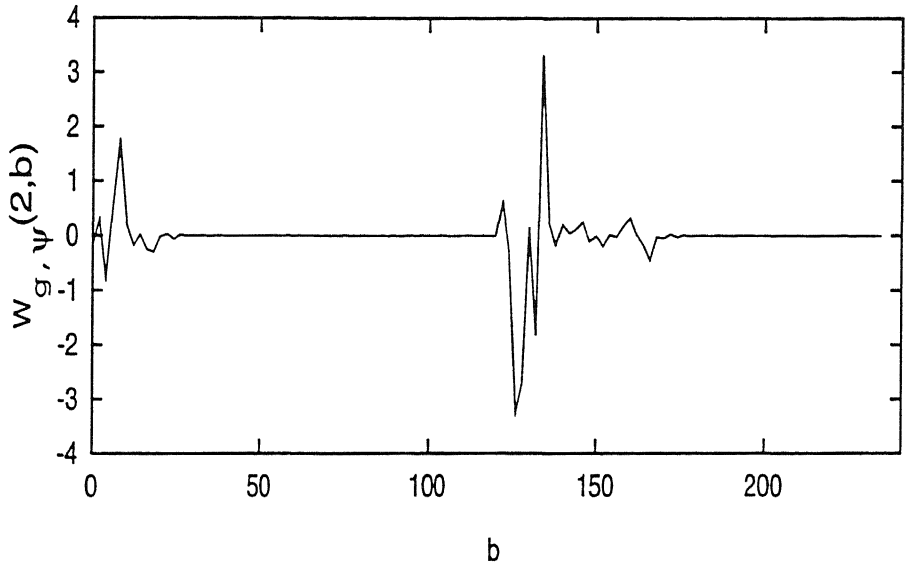


Figure 3.9: The wavelet transform of the test signal shown in the Figure 3.8 for scale value equal to 2.

| Signal | Scale-limits | Dyadic scale-limits |
|---|---|---|
| 4(a) | 8.2092 | 8 |
| 5(a) | 4.0870 | 4 |
| 6(a) | 2.6250 | 2 |

Table 3.1: Scale-limits and dyadic scale-limits of the signals shown in figures 3.18, 3.20, 3.22, for $\delta_0 = 0.05$

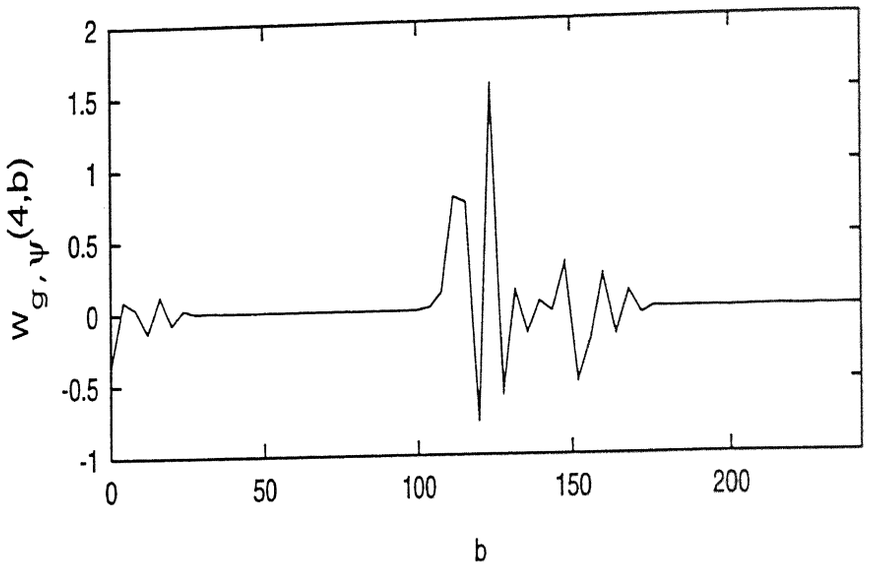


Figure 3.10: The wavelet transform of the test signal shown in the Figure 3.8 for scale value equal to 4.

**Definition 3.2.2** *$\delta_0$-Practical Scale Limitedness: A signal $g(t) \in L^2$ is called $\delta_0$-practically scale-limited to $a_l$ if*

$$a_l = sup\{a_l' : \frac{C_\psi^{-1} \int_0^{a_l'} \int_{-\infty}^{\infty} \frac{dadb}{a^2} |W_{g,\psi}(a,b)|^2}{E} < \delta_0\}. \tag{3.17}$$

*where,*
$E = \int_{-\infty}^{\infty} dt\, |g(t)|^2 = C_\psi^{-1} \int_0^{\infty} \int_{-\infty}^{\infty} \frac{dadb}{a^2} |W_{g,\psi}(a,b)|^2$, *for a predefined* $\delta_0$, $0 < \delta_0 < 1$.

Through the notion of $\delta_0$-practical scale-limitedness, all those signals are classified, for which the fraction of the energy below a scale value is less than a predefined quantity.

Next, a few examples are presented in which three signals and their scale-limits are found. In these examples, the signals and their energy distribution with respect to the various scales, has been presented. Here the energy distribution with respect to various

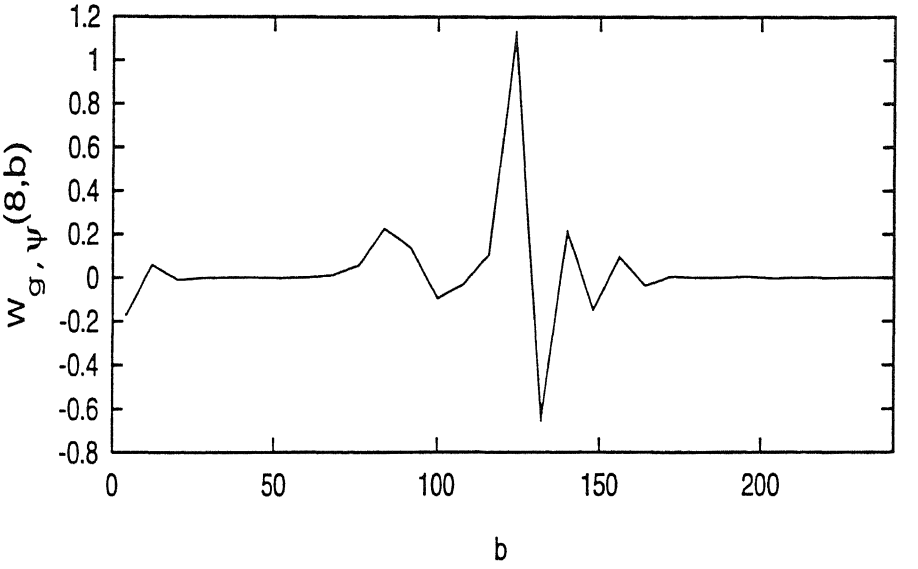


Figure 3.11: The wavelet transform of the test signal shown in the Figure 3.8 for scale value equal to 8.

scales is characterised by $\delta(a_l')$, which is equal to the energy content in the signal below the scale $a_l'$. The quantity $\delta(a_l')$ is given by the following -

$$\delta(a_l') = \frac{C_\psi^{-1} \int_0^{a_l'} \int_{-\infty}^{\infty} \frac{dadb}{a^2} |W_{g,\psi}(a,b)|^2}{E}. \tag{3.18}$$

Since the Multiresolution algorithm is used to find the wavelet transform, the value of $\delta(a_l')$ is found only for $a_l' = 2,\ 4,\ 8,\ 16$. The value of $\delta(a_l')$ is given by -

$$\delta(a_l') = \frac{E - \sum_k |\langle g(t), \phi_{j,k} \rangle|^2}{E},\ a_l' = 2^j,\ j = 1,\ 2,\ 3,\ 4. \tag{3.19}$$

The energy of the signal is approximated by -

$$E = \sum_k |g(t_k)|^2 \tag{3.20}$$

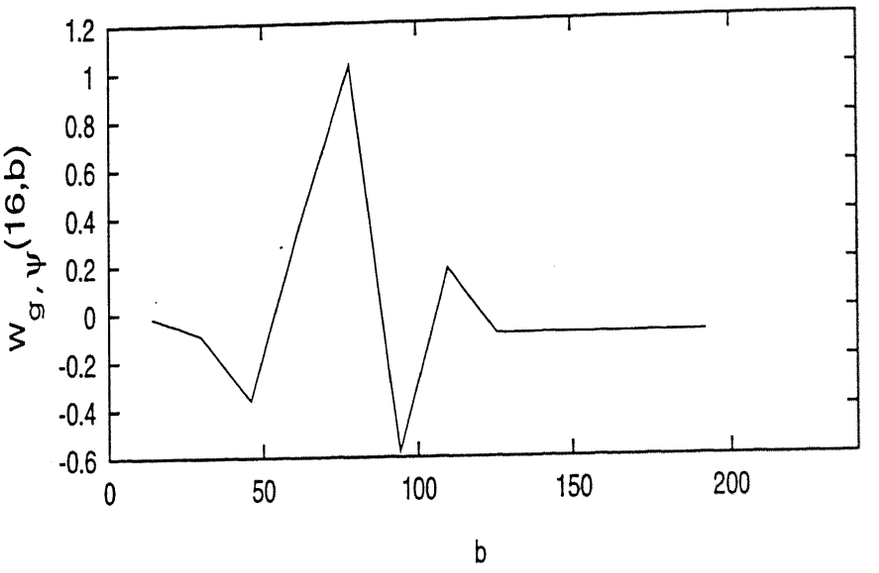


Figure 3.12: The wavelet transform of the test signal shown in the Figure 3.8 for scale value equal to 16.

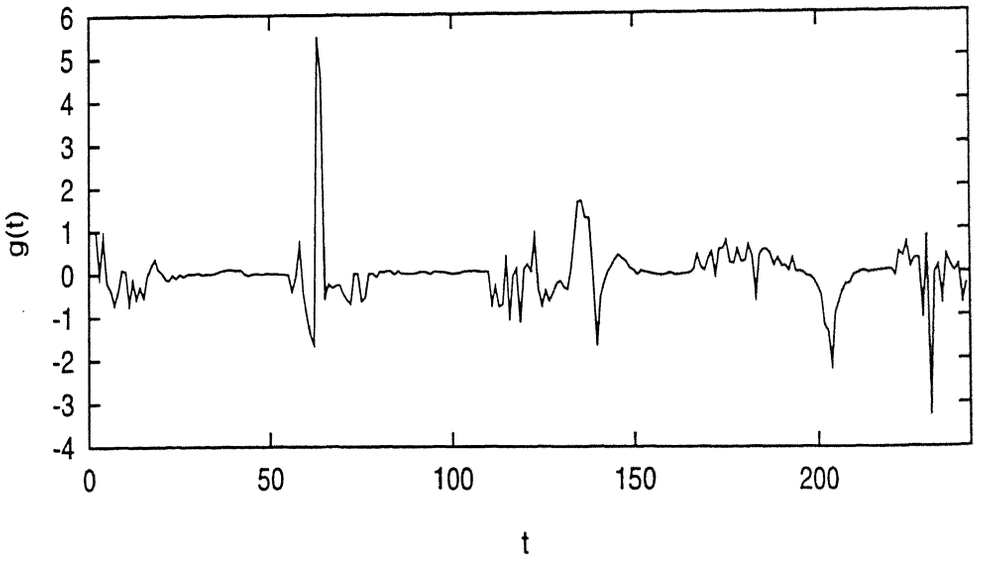


Figure 3.13: The test signal.

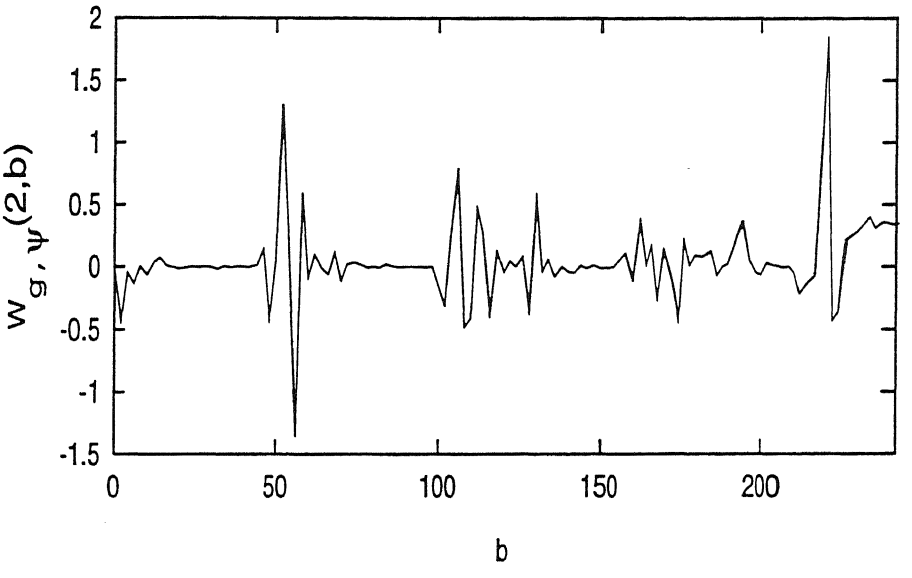


Figure 3.14: The wavelet transform of the test signal shown in the Figure 3.13 for scale equal to 2.

Hence $\delta(a'_l)$ is given by-

$$\delta(a'_l) = \frac{\sum_k |g(t_k)|^2 - \sum_k |\langle g(t), \phi_{j,k}\rangle|^2}{\sum_k |g(t_k)|^2}, \; a'_l = 2^j, \; j = 1, \; 2, \; 3, \; 4. \qquad (3.21)$$

Using the plots of $\delta(a'_l)$ versus $a'_l$, the scale-limits of the three signals have been evaluated.

**Computation of the Scale-limits:** Since the available Multiresolution algorithms provide the wavelet transform for dyadic scale values, therefore the intermediate scale-limit values are obtained using linear interpolation. For finding the scale-limit for $\delta_0 = 0.05$, these are the steps:

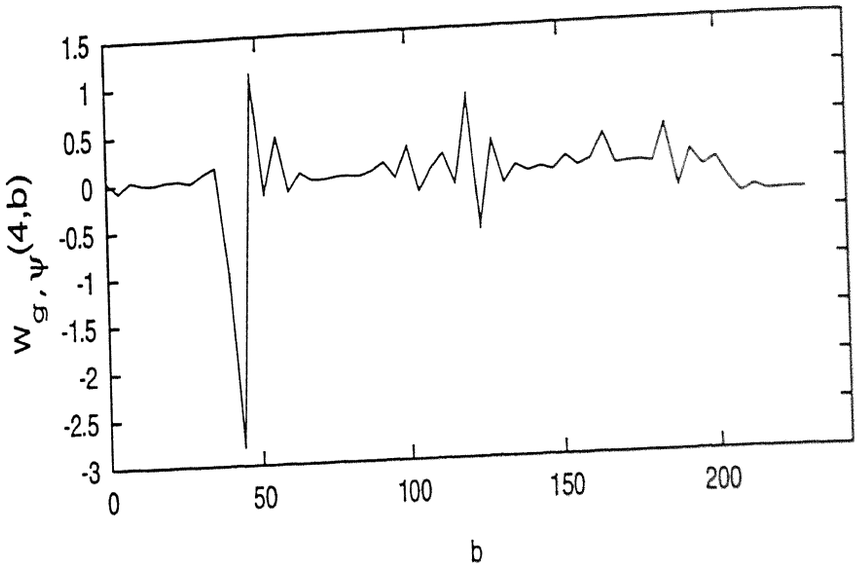


Figure 3.15: The wavelet transform of the test signal shown in the Figure 3.13 for scale value equal to 4.

- Find $j = j_0$ such that:

$$\delta(2^{j_0}) < 0.05 < \delta(2^{j_0+1})$$

- Then use the interpolation formula for finding the scale-limit:

$$a_l = 2^{j_0} + \frac{(2^{j_0+1} - 2^{j_0})}{(\delta(2^{j_0+1}) - \delta(2^{j_0}))}(0.05 - \delta(2^{j_0}))$$

In Figure 3.18, the signal to be scale analysed is shown; in Figure 3.19 the fraction of the energy below $a_l'$ is plotted with respect to $a_l'$. From the curve, the scale-limit of the signal curve shown in Figure 3.18 is 7.8934. Scale-limits of the signals shown in Figures 3.18, 3.20 and 3.22 are tabulated in Table 3.1. It can be inferred from the examples that signals having faster variation have smaller scale-limits. Therefore, scale-limit can be used as a measure of variation of the signals. In the same table

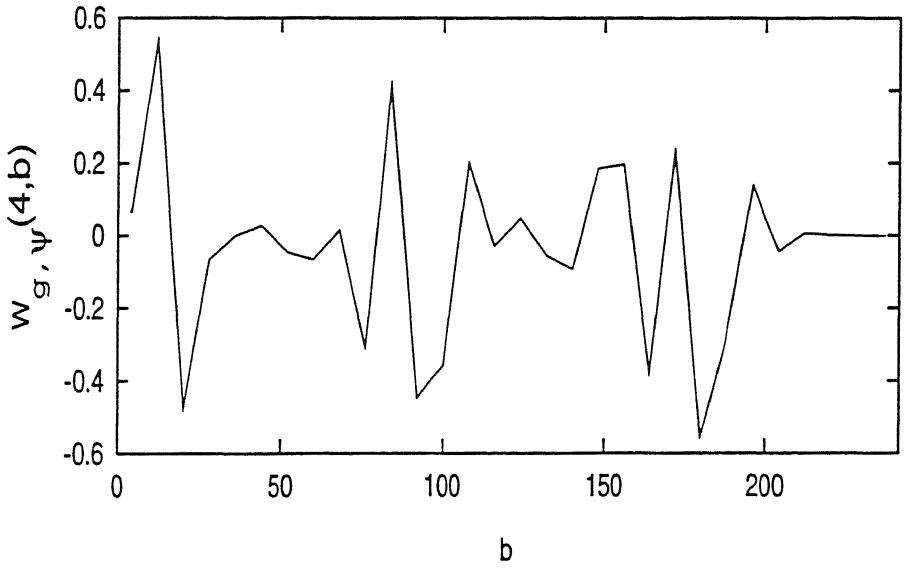


Figure 3.16: The wavelet transform of the test signal shown in the Figure 3.13 for scale value equal to 8.

scale-limits are also tabulated for the case, when the permissible values of the scale-limit are $2^j$, $j \in Z$. These scale-limits are called dyadic scale-limits. It is important to note, that if a signal is scale-limited with respect to a wavelet family, then it will be scale-limited with respect to another wavelet family if both the families generate the same multiresolution analysis.

In reference [ea94], the scale-limitedness is defined such that the signals have only dyadic scale-limits. By allowing scale-limits to have real values it is possible to characterise variation in a much more effective way. Because an addition of small amount of energy at smaller scales may not alter the dyadic scale-limit, however, the $\delta_0$-practical scale-limit defined here would get changed.

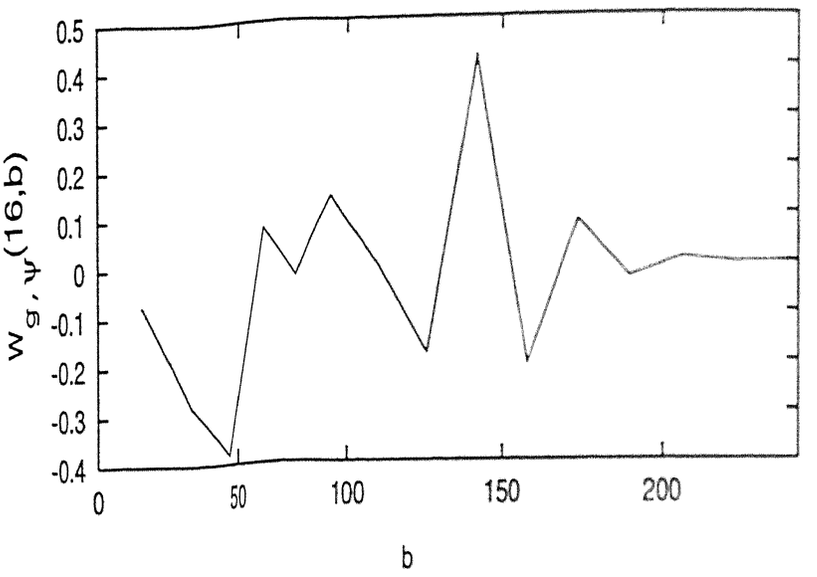


Figure 3.17: The wavelet transform of the test signal shown in the Figure 3.13 for the scale value equal to 16.

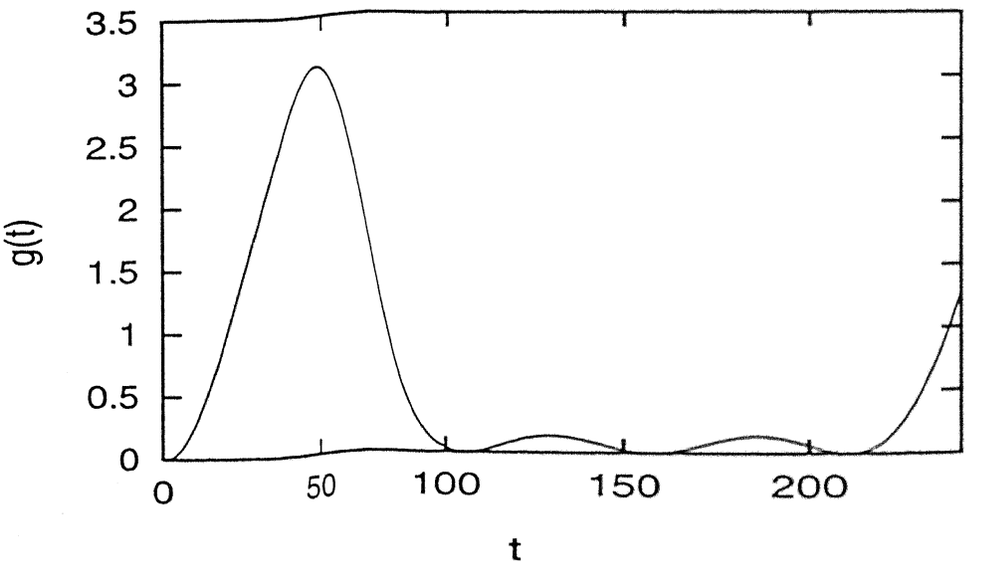


Figure 3.18: The test signal

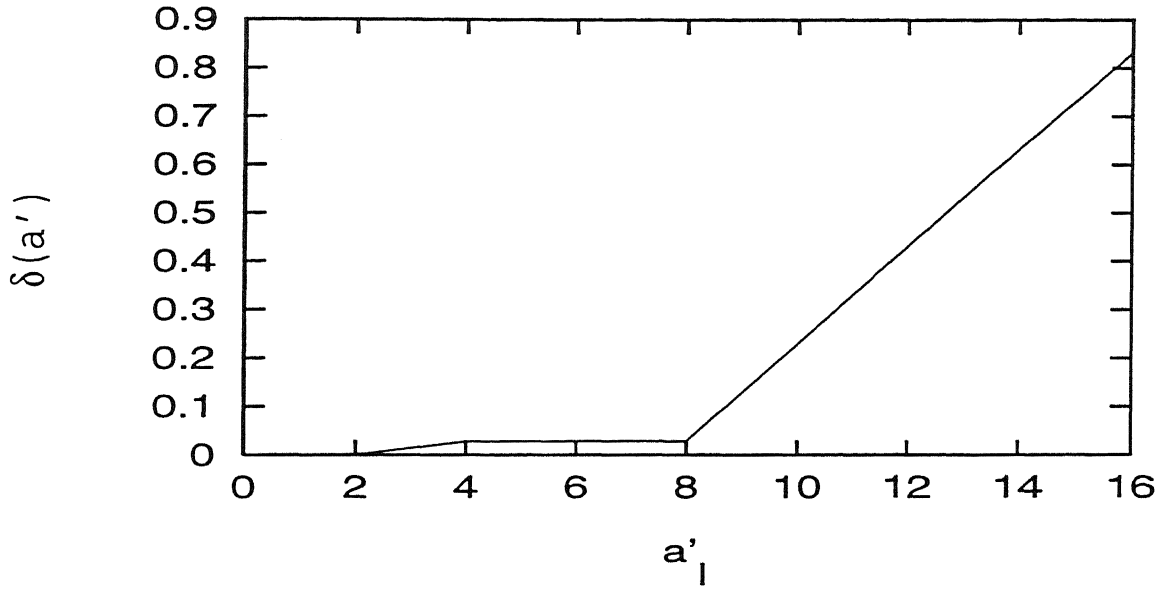


Figure 3.19: $\delta(a'_l)$ vs $a'_l$, for the test signal shown in Figure 3.18

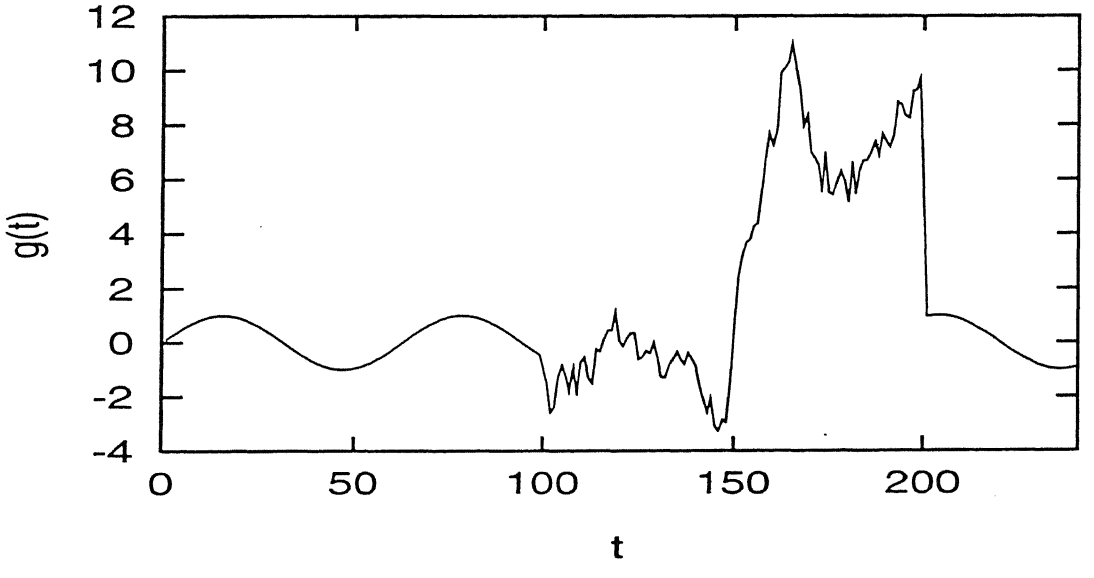


Figure 3.20: The test signal

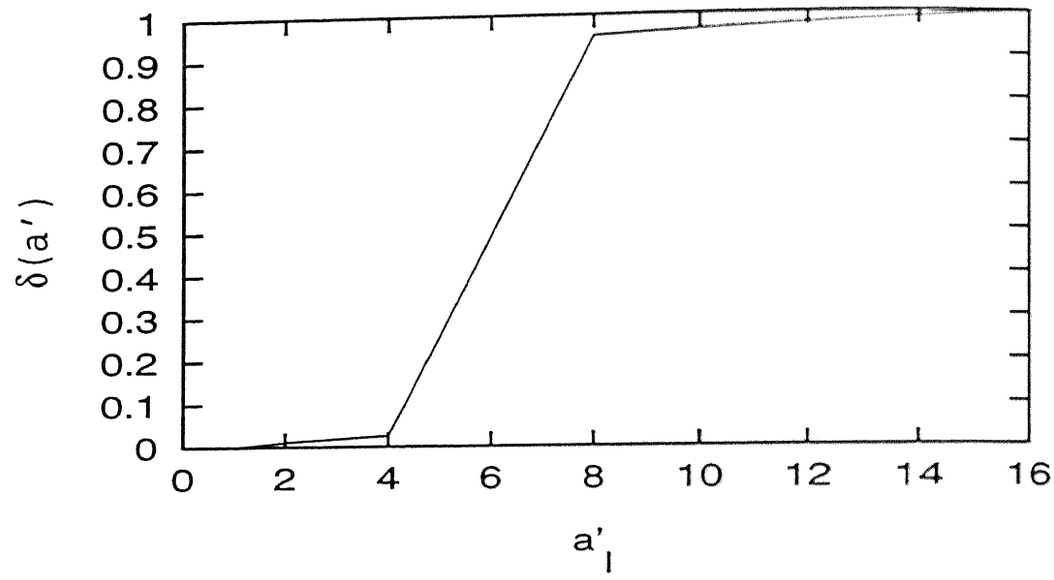


Figure 3.21: $\delta(a'_l)$ vs $a'_l$, for the test signal shown in Figure 3.20

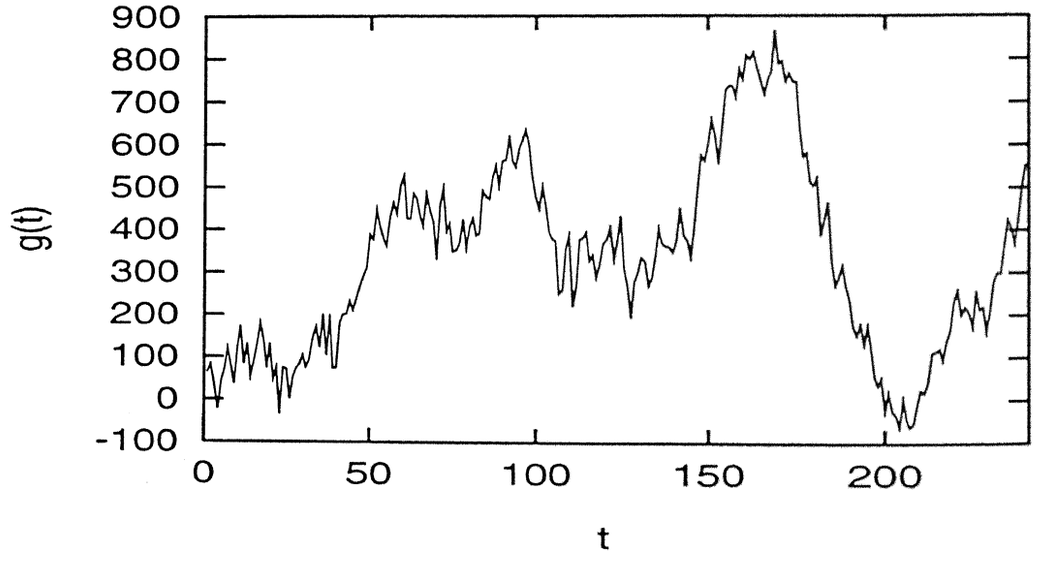


Figure 3.22: The test signal

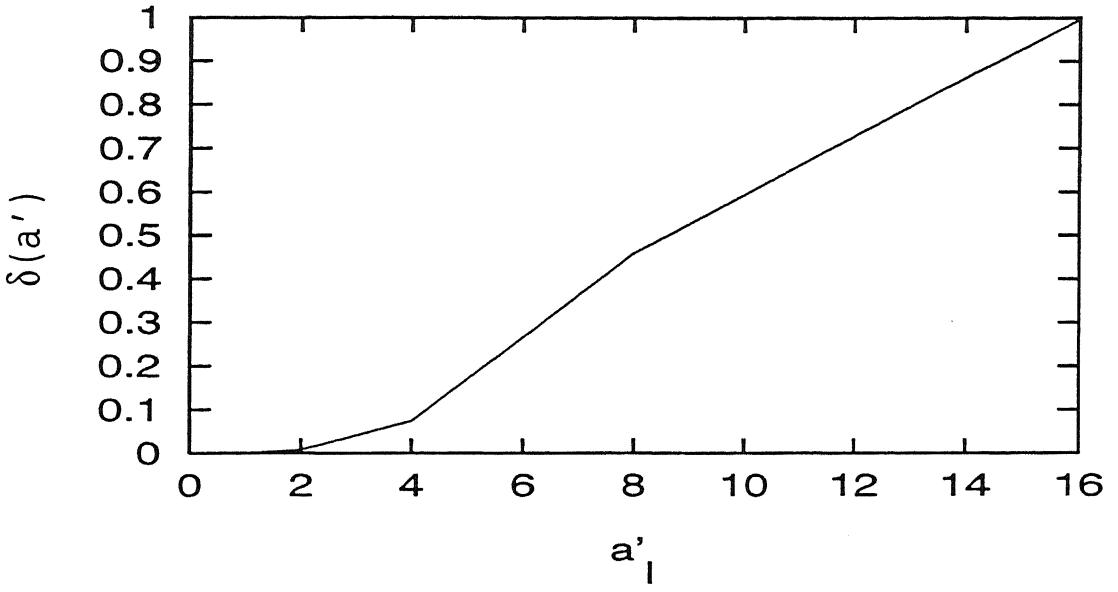


Figure 3.23: $\delta(a_l')$ vs $a_l'$, for the test signal shown in Figure 3.22

## 3.3 Higher Order Vanishing Moments and Scale-limitedness

Here it will be shown, that the property, that signals with faster variations have smaller scale-limits, is due to higher order vanishing moment property of the wavelets. Essentially, for faster varying signals to have smaller scale-limits, faster signals should have their wavelet transform enhanced at lower scales. This is ensured by the higher order vanishing moment property of the wavelets. Before discussing this in further detail, two notions, namely - space of $M^n$ and effective support are introduced.

**Definition 3.3.1** *Space of $M^n$: A function $\psi(x) \in L^2(R)$ is said to be in $M^n$, if $\int \psi(x)x^l dx = 0, l = 0, ..., n$.*

We call $M^n$ as the $n$ vanishing moment space. This in turn implies that for $\psi(x) \in M^n$, $\int \psi(\frac{x}{a}) x^l dx = 0, a > 0, l = 0, ...n$. Let us define the notion of effective support of a wavelet; this notion is applicable to the class of square integrable functions.

**Definition 3.3.2** *Effective Support: The wavelet $\psi(t)$ is said to have a support of $R_\epsilon \subset R$ if,*

$$R_\epsilon = inf\{R^i{}_\epsilon : \frac{\int_{t \in R^i{}_\epsilon} dt|\psi(t)|^2}{E} = \epsilon\}, 0 < \epsilon < 1.$$

Let us separately write the equation in the definition as follows,

$$\frac{\int_{t \in R^i{}_\epsilon} dt|\psi(t)|^2}{E} = \epsilon \tag{3.22}$$

The existence of such $R^i_\epsilon$ 's follows from the square integrability of the wavelet.

**Lemma 3.3.1** *There exist $R^i_\epsilon$ 's such that the Equation 3.22 is satisfied for a piecewise square integrable function $\psi(t)$ and for $0 < \epsilon < 1$.*

PROOF: Let us define a function $F_\psi(x)$,

$$F_\psi(x) = \frac{\int_{-\infty}^{x} |\psi(t)|^2 \, dt}{E}.$$

Since $F_\psi(x)$ is a cumulative energy distribution function, therefore, it is non decreasing. So for any $\epsilon < 1$, where E is the energy of the function $\psi$, it is possible to find uncountably many $(x_1, x_2)$ such that $(F_\psi(x_2) - F_\psi(x_1)) = \epsilon$. This establishes the existence of $R^i_\epsilon$'s for every given $0 < \epsilon < 1$.

$R^i_\epsilon$ can also be constructed as $\cup_j (x_{1j}, x_{2j})$, the disjoint sets $(x_{1j}, x_{2j})$ selected such that $\sum_j (F(x_{2j}) - F(x_{1j})) = \epsilon$. For compactly supported wavelets, we take $\epsilon = 1$, so

that $R_\epsilon$ equal to the support of the wavelet. For non-compactly supported wavelets $\epsilon$ close but not equal to one. So that, a large fraction of the Wavelet energy falls in the effective support. At low scales the effective support of the Wavelet $\psi(\frac{t}{a})$ reduces. It is straight forward to show that if $\psi(\frac{t}{a_1})$ has an effective support of $R_1$ and $\psi(\frac{t}{a_2})$ has an effective support of $R_2$ and $a_1 > a_2$ then $L(R_2) < L(R_1)$. At low scales inside the $\epsilon$-effective support($\epsilon$ close to 1) if the signal is given a polynomial representation then a slow varying signal gets represented by lower order polynomials. Suppose the wavelet is in the $M^n$ space, signals represented by polynomials of order less than $n^{th}$ order will have zero wavelet transform, if the wavelet support and the support of the signal overlap. In general, slower signals will have low wavelet transform at low scales. The wavelet transform of a signal satisfies the following bound -

$$|W_{g,\psi}(a,b)|^2 \leq min_{l \leq n} \int_0^A |g(t) - \hat{g}(t)|^2 \, dt$$

Where $\hat{g}(t)$ is an $l^{th}$ order Lagrangian approximation of the signal $\hat{g}(t)$. This can be proved by writing, $g(t) = \hat{g}(t) + (g(t) - \hat{g}(t))$, then taking the wavelet transform and noting that, the wavelet transform of $\hat{g}(t)$ is zero because it is a polynomial of order less than or equal to $n$. Then Cauchy-Schwarz inequality can be applied to prove the result. Hence, within the support of the wavelet the closer a signal is to any polynomial upto order $n$ the smaller will its wavelet transform be. Therefore, slower signals (which are approximated with very low error upto order $n$) will have larger $\delta_0$-practical scale-limits.

## 3.4 Properties of Scale-limitedness

In the first theorem, it is shown that the class of band-limited signals are scale-limited with respect to wavelets which satisfy a certain condition.

**Theorem 3.4.1** *A signal band-limited to [-B,B] is scale-limited to* $\frac{f_l}{B}$ *with respect to a wavelet family* $\psi\left(\frac{t-b}{a}\right), a \in R^+, b \in R$ *for which* $\hat{\psi}(f) = 0, |f| < f_l$.

PROOF: The wavelet transform of the signal $g(t)$ with respect to the family $\psi^{a,b}(t)$ is given by

$$\begin{aligned} W_{g,\psi}(a,b) &= \langle g, \psi^{a,b}(t) \rangle, \\ &= \int dt\ g(t)\ |a|^{-1/2}\ \overline{\psi\left(\frac{t-b}{a}\right)}, \\ &= \int_{-B}^{+B} df\ G(f)\ |a|^{-1/2}\ \overline{\psi(af)}\ \exp^{-j2\pi fb}, \text{ by } Parseval's\ theorem. \end{aligned}$$

If,

$$G(f) = 0, f \notin (-B, +B),$$

$$\psi(f) = 0, f \in (-f_l, f_l),$$

then the smallest value of 'a' for which $W_{g,\psi}(a,b) \neq 0$ is $a = \frac{f_l}{B}$, hence for $a < \frac{f_l}{B}$, $W_{g,\psi}(a,b) = 0$.
Hence proved.

The next theorem states that there exist time-limited signals which are scale-limited. This is fairly straight forward because the wavelets considered are compact, but there is no parallel to this result in Fourier transforms. Because there is no time-limited signal which is band-limited.

**Theorem 3.4.2** *With respect to every compact support wavelet family there exists a class of time-limited signals which are scale-limited as well.*

PROOF: Let $\psi(t)$ be compact on $(-c_1, c_2)$, $c_1,\ c_2 > 0$. Let us consider the class of signals generated by, taking $|W_{g,\psi}(a,b)| < \infty$, and,

$$\begin{aligned} W_{g\psi}(a,b) &= 0, a \notin [a_l,\ a_u], \\ W_{g\psi}(a,b) &= 0, b \notin [b_l,\ b_u]. \end{aligned}$$

The class of signals generated is given by,

$$g(t) = C_\psi^{-1} \int_{a_l}^{a_u} \int_{b_l}^{b_u} \frac{dadb}{a^2}\, W_{g,\psi}(a,b)\, \psi\left(\frac{t-b}{a}\right),$$

It is important to note, that, for $a \notin [a_l,\ a_u]$ and $b \notin [b_l\ b{-}u]$ $\psi\left(\frac{t-b}{a}\right) = 0$, $for\ t < b_l - c_1\ a_u, t > b_u + a_u\ c_2$. Hence the class of signals $g(t)$ so generated is time-limited to $b_l - c_1\ a_u < t < b_u + a_u\ c_2$. So the class of signals is shift, scale and time-limited. Hence proved.

The next theorem states that the modulus value of the $n^{th}$ derivative of a scale-limited signal is upper bounded by $\frac{C'}{a_l^n}$.

**Theorem 3.4.3** *For the class of n times differentiable scale-limited, time-limited signals, the $n^{th}$ derivative satisfies the following inequality,*

$$\left|\frac{d^n}{dt^n} g(t)\right| \leq \frac{C'}{a_l^n}, \tag{3.23}$$

*where,*

$$C' = \frac{1}{nC_\psi}(c_2 + c_1)\ |\psi^n(t)|_{max}\ ||g||,$$

*provided that the wavelet has compact support of $(-c_1, c_2)$, $c_1,\ c_2 > 0$ and its $n^{th}$ differential exists.*

PROOF: If $\psi(t)$ has a support of $(-c_1, c_2)$, $c_1$, $c_2 > 0$ then $v(\frac{t}{a})$ has a support of $(ac_1, ac_2)$.

$$
\begin{aligned}
g(t) &= C_\psi^{-1} \int_{a \in A} \int_{b \in B} \frac{dadb}{a^2} W_{g,v}(a,b)\, v^{a,b}, \\
Then,\ \frac{d^n}{dt^n} g(t) &= C_\psi^{-1} \int_{a \in A} \int_{b \in B} \frac{dadb}{a^2} W_{g,v}(a,b)\, \frac{d^n}{dt^n} v\left(\frac{t-b}{a}\right), \\
and,\ |\frac{d^n}{dt^n} g(t)| &\leq C_\psi^{-1} \int_{a \in A} \int_{b \in B} \frac{dadb}{a^2} |W_{g,v}(a,b)| |\frac{d^n}{dt^n} v\left(\frac{t-b}{a}\right)| \\
or,\ |\frac{d^n}{dt^n} g(t)| &\leq |\psi^n(t)|_{max}\, C_\psi^{-1} \int_{a_l}^{\infty} \int_{t-c_2 a}^{t+c_1 a} \frac{dadb}{a^{n+2}} |W_{g,v}(a,b)|.
\end{aligned}
$$

$b \in (t - c_2 a, t + c_1 a)$, *because* $\psi(\frac{t-b}{a}) \neq 0$ *only for*, $-c_1 < \frac{t-b}{a} < c_2$

*or* $t - c_2 a < b < t + c_1 a$.

$$
\begin{aligned}
|\frac{d^n}{dt^n} g(t)| &\leq |\psi^n(t)|_{max} |W_{g,\psi}(a,b)|_{max} C_\psi^{-1} \int_{a_l}^{\infty} \int_{t-c_2 a}^{t+c_1 a} \frac{dadb}{a^{n+2}}, \\
or,\ |\frac{d^n}{dt^n} g(t)| &\leq \frac{|\psi^n(t)|_{max}\, |W_{g,\psi}(a,b)|_{max}\, C_\psi^{-1}(c_2 + c_1)}{n\, a_l^n}, \\
or,\ |\frac{d^n}{dt^n} g(t)| &\leq \frac{C'}{a_l^n}.
\end{aligned}
$$

where, $C' = \frac{1}{nC_\psi}(c_2 + c_1)||g(t)|||\psi^n(t)|_{max}$.

Hence proved.

**Corollary 3.4.1** *For the class of differentiable scale-limited, time-limited signals the derivative satisfies the following inequality,*

$$
|\frac{d}{dt} g(t)| \leq \frac{C'}{a_l}, \tag{3.24}
$$

*where,*

$$
C' = C_\psi^{-1}(c_2 + c_1)\, |\psi'(t)|_{max}\, ||g||,
$$

*provided that the wavelet has compact support of* $(-c_1, c_2)$, $c_1$, $c_2 > 0$. *If the first differential of the wavelet exists.*

The next theorem states that under certain conditions the Lagrangian interpolating function is $\delta_0$-practically scale-limited on a finite interval. Let $g(t), t \in [0, A]$ be the original signal and $g(t_i)$, $i = 1, .., n$ be the samples of the signal in the interval [0, $A$]. Let $\hat{g}(t)$ be the approximation of the signal obtained by using the $n$ samples using Lagrangian interpolation. Then,

$$\hat{g}(t) = \sum_{i=1}^{n} g(t_i)\Pi_{j,\ j\neq i}\frac{t-t_j}{t_i-t_j},\ t \in [0,\ A],\ 0 \text{ otherwise;} \tag{3.25}$$

$\hat{g}(t)$ can always be written in the following form

$$\hat{g}(t) = a_0 + a_1\, t + a_2\, t^2 + ... + a_{n-1}t^{n-1},\ t \in [0,\ A],\ 0 \text{ otherwise.} \tag{3.26}$$

Let $\psi(t)$ be a compact wavelet with support $[-w_1,\ w_2]$. Also let $\psi(t)$ be in $(n-1)$ vanishing moment space. Then we have the following theorem-

**Theorem 3.4.4** *The time-limited interpolating function* $\hat{g}(t)$ *given by 3.26 is* $\delta_0$*-practically scale-limited to* $a_l$ *for*

$$\delta_0 = \frac{\int_{a=0}^{a_l}\int_{b=-a_l w_2}^{a_l w_1}\frac{1}{a^2}|W_{\hat{g},\psi}(a,b)|^2\ da\ db}{E} + \frac{\int_{a=0}^{a_l}\int_{b=A-a_l w_2}^{A+a_l w_1}\frac{1}{a^2}|W_{\hat{g},\psi}(a,b)|^2\ da\ db}{E}, \tag{3.27}$$

*provided that* $\psi(t)$ *is in* $M^{n-1}$ *space and also compact with support* $[-w_1,\ w_2]$.

PROOF: For $a_l$ to be $\delta_0$-practical scale-limit, $\delta_0$ should be equal to the fractional energy for $a \in [0,\ a_l]$ and for all 'b'. For $a \in [0,\ a_l]$ and $b \notin [-a_1\ w_2,\ A + a_l\ w_1]$ the wavelet transform is zero, because there is no overlap between $\hat{g}(t)$ and $\psi\left(\frac{t-b}{a}\right)$. The wavelet transform is given by,

$$W_{\hat{g},\ \psi}(a,\ b) = \int_0^A \frac{1}{\sqrt{a}}\,\hat{g}(t)\,\psi\left(\frac{t-b}{a}\right)\,dt$$

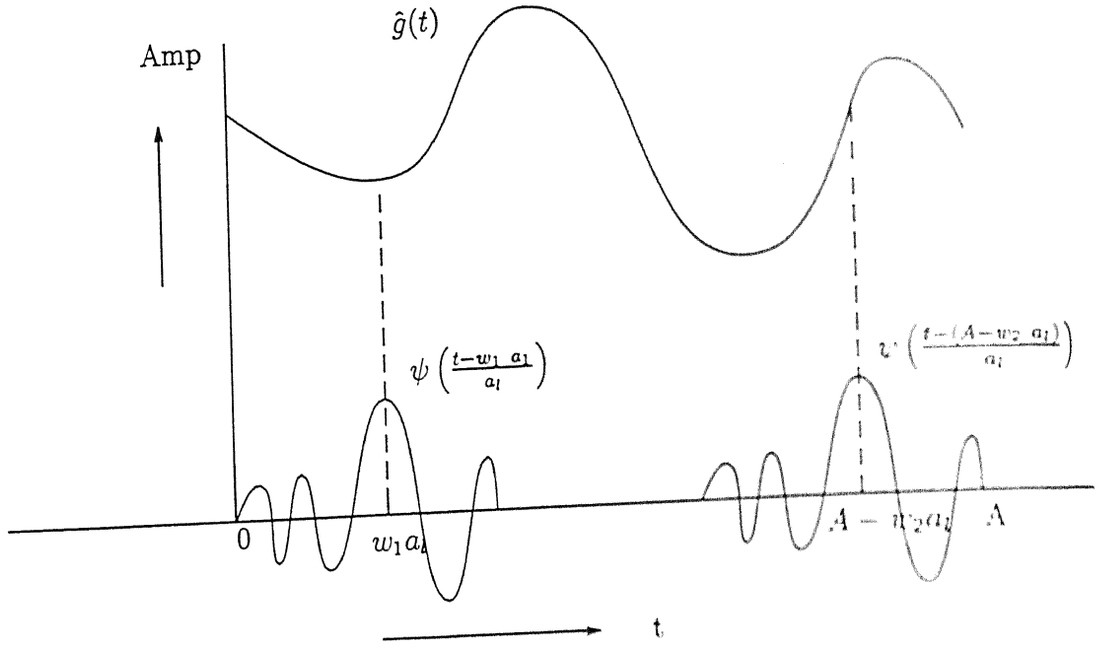


Figure 3.24: $\hat{g}(t)$ and $\psi\left(\frac{t-b}{a}\right)$ for b=$a_l\ w_1$, $A - w_2\ a_l$.

Refer to figure 3.24, since $\hat{g}(t)$ is given by Equation 3.26 and $\psi(t)$ is in $(n-1)$ vanishing moment space, $W_{\hat{g},\,\psi}(a,b) = 0$, for $a \in [0,\ a_l]$ and $b \in\ [a_l\ w_1,\ A - a_l\ w_2]$. Therefore for $a \in [0,\ a_l]$, the region of 'b' in which $W_{g,\psi} \neq 0$, is $[-a_l\ w_2,\ a_l\ w_1] \cup [A - a_l\ w_2,\ A + a_l\ w_1]$. The fractional energy for this region is given by Equation 3.27. Hence if $\delta_0$ is selected equal to the value given by 3.27, then $\hat{g}(t)$ will be $\delta_0$-practically scale-limited to $a_l$. Hence proved.

**Theorem 3.4.5** *Any function $g(t) \in V_j$ is scale-limited to $2^j$.*

Proof: Since $g(t) \in V_j$, therefore $g(t) \in \oplus_{k=j-1}^{\infty} W_k$. Therefore g(t) has the following representation.

$$g(t) \;=\; \sum_{k=j-1}^{\infty} \sum_{n=-\infty}^{\infty} \langle g(t), \frac{1}{\sqrt{2^k}} \psi\left(\frac{t-n2^k}{2^k}\right) \rangle \frac{1}{\sqrt{2^k}} \psi\left(\frac{t-n2^k}{2^k}\right)$$

Let us compute the wavelet transform of the function $g(t)$ with respect to the wavelets given by, $\frac{1}{2^m}\psi\left(\frac{t-l2^m}{2^m}\right)$ for $l \in Z$ and $m = 0, 1, ..., j-1, j$.

For $l \in Z$ and $m = 0, 1, ..., j-1, j$,

$$W_{g,\psi}(2^m, l2^m) = \langle g(t), \frac{1}{\sqrt{2^m}}\psi\left(\frac{t-l2^m}{2^m}\right)\rangle.$$

$$= \sum_{k=j-1}^{\infty}\sum_{n=-\infty}^{\infty}\langle g(t), \frac{1}{\sqrt{2^k}}\psi\left(\frac{t-n2^k}{2^k}\right)\rangle\langle\frac{1}{\sqrt{2^k}}\psi\left(\frac{t-n2^k}{2^k}\right), \frac{1}{\sqrt{2^m}}\psi\left(\frac{t-l2^m}{2^m}\right)\rangle$$

Since the Multiresolution analysis forms an orthonormal wavelet family,

$$\langle\frac{1}{\sqrt{2^k}}\psi\left(\frac{t-n2^k}{2^k}\right), \frac{1}{\sqrt{2^m}}\psi\left(\frac{t-l2^m}{2^m}\right)\rangle = \delta_{n,l}\,\delta_{k,m}.$$

Therefore, for $l \in Z$ and $m = 0, 1, ..., j-1, j$,

$$W_{g,\psi}(2^m, l2^m) = 0.$$

Any function in $V_j$ is scale-limited to $2^j$.

Hence proved.

This result follows from the definition of $V_j$, however the obvious result has been proved in an elegant way.

## 3.5 Sampling Rate Estimation using the Concept of Scale-limitedness

In this section, an algorithm for estimating the required sampling rate for a signal, given the required error performance, is proposed. An expansion in terms of the samples is

also presented. The concept of scale-limitedness with reference to wavelet transforms, which has already been introduced, is used as the measure of variation. The proposed algorithm proceeds by sampling the signal initially at a high rate, then recursively subsampling depending upon the required error performance.

In conventional signal processing, the Shannon sampling theorem is applied and signals are sampled uniformly. The sampling rate is taken to be $2B$, if the bandwidth of the signal is $B$. A detailed account of Shannon's theorem and its various extensions can be found in [Jer77], [Mar93]. In practice, this presents two problems due to the time limited nature of practical signals.

- An apriori estimate of the bandwidth must be known.
- Only a finite number of samples are available; therefore the resulting approximation of the signal in terms of the samples is subject to truncation error [Beu76].

In the absence of any information of the bandwidth of a signal, it becomes very difficult to estimate the sampling rate required. Here an attempt is made to solve the problem using wavelet transforms. The problem attempted here is as follows- *Given any finite duration signal, whose samples are available at arbitrary high rate, what is the sampling rate required for representing the initial set of samples with a specified error bound* $\epsilon$.

The problem of representing a discrete signal in terms of samples of the wavelet transform domain is extensively studied. The wavelet transform of a signal is the inner product between the signal and shifted, scaled versions of a function called the mother wavelet. In practice, only the samples of the signal to be analysed are known. The approximation of the signal can be found by passing the sequence through a bank of filters[Mal89]. Algorithms based on this concept provide a method of represent-

ing a discrete sequence in terms of the wavelet transform values at scales $2^j$ and the corresponding shifts $2^j\ k$. Using the approximation sequence at any stage and the transforms(detail signals) at the previous stages, the original sample sequence can be reconstructed. All this has been discussed in detail in the earlier sections.

In [Mal91],[MZ92], [MH92] the original sample sequence is represented in terms of the maxima of the wavelet transform at scales $2^j$ for a range of consecutive integers $j$ and the final low pass approximation. This algorithm is based on Mallat's conjecture that the wavelet transform maxima and the final low pass version are sufficient for complete representation of the signal. Meyer [Mey91] has given counter examples to show that this conjecture is not correct, but practically it leads to a sufficiently accurate representation of the original sample sequence.

In [Ber92] the completeness problem of a non-uniform sampling of wavelet transform of a periodic signal discrete time signal is studied. In this case the sampling was done at the extrema of the transform. In [AHT95] the completeness of an arbitrary sampling of a discrete time wavelet transform of a periodic signal is dealt with.

Instead of representing a signal in terms of the samples of the wavelet transform and approximate signal, here the wavelet transform decomposition is used to estimate the sampling rate required in the time domain. The motive behind developing a sampling rate estimator is that, it is much more useful to store samples of a signal rather than samples of any transformed version.

The strategy evolved here is to initially sample the given signal at a very high rate, then subsample by a fraction of 2, repeating the process till the reconstruction error remains within the permissible limit. Simulation results for speech and simulated signals are presented. Here it is shown that for a given number of samples the error bound is

inversely proportional to the scale limit.

### 3.5.1 Theory behind the Sampling and Reconstruction Algorithm

The sampling problem attempted here, is posed as a problem of minimisation of the fractional mean square reconstruction error between the original signal and the reconstructed signal using the samples. The problem attempted here is as follows - *Given a signal* $g(t), t \in [0, A]$, *where* $A$ *is a positive finite number, what is the minimum sampling rate required such that the fractional mean square reconstruction error remains bounded by a predefined quantity* $\epsilon$.

Next we present a theorem which gives a bound on the fractional mean square reconstruction error in terms of the samples used for reconstruction. Although the theorem developed here is for continuous signals, the algorithm is adapted for the case when initially the samples are available at an arbitrary rate and the required number of samples have to be picked out of the initial set, such that the fractional mean square reconstruction error between the initial sample set and the reconstructed sample set is minimised.

Before stating the algorithm, the main result is presented. Let $g(t)$, $t \in [0, A]$ be the original signal and it is sampled at $N$ points, $t_i, i = 0, 1, ..., N-1$, where $t_i \in [0, A]$. Let the energy of the signal be $E$. The main result is as follows-

**Theorem 3.5.1** *The fractional mean square reconstruction error satisfies the following inequality,*

Or,

$$\delta_0 \leq \int_0^A |g(t) - \hat{g}(t)|^2 \, dt \leq \frac{C}{a_l \, n^\alpha} + \delta_0$$

Hence proved.

Let us denote the fractional mean square error in the transformed domain by $E_{rr}(a, n)$, in general 'b' takes values on $B(a)$ therefore,

$$E_{rr}(a, n) = \int_{b \in B(a)} |W_{g,\psi}(a, b) - W_{\hat{g},\psi}(a, b)|^2 \, db.$$

The basis of the assumption 3.29 is that as the number of samples increases, the original and the reconstructed signals come close, which in turn implies that the transformed signals of the original and the reconstructed signals come close. Therefore, any monotonically decreasing function can be used to bound the error, the specific form given in inequality 3.29 is assumed because it is computationally easy to deal with.

The strategy of sampling adopted is, that initially the signal is sampled at an arbitrary high rate, then, the required number of samples are retained such that the fractional mean square reconstruction remains less than the required value. Let the initial number of samples be $N_0$ and number of samples finally retained be $N$. Before discussing the application of theorem 3.5.1, the following simplifications are made:

(1) Only dyadic scale-limits are considered, so $a_l = 2^j$ $j \geq 0$. Therefore in place of $\delta_0$, $\delta_{d,2^j}$ are substituted in the inequality, where $\delta_{d,2^j}$ is the fraction of energy below $2^j$..

(2) $n = \frac{N_0}{2^k}$, $k \geq 0$.

(3) Given any $n$, the reconstruction is done according to the following equation:

$$\hat{g}(t) = \sum_{m=1}^{\frac{N_0}{2^k}} g(m\,2^k)\,\frac{1}{\sqrt{(2^k)}}\,\phi\left(\frac{t-m\,2^k}{2^k}\right).$$

The condition (2) ensures that the rate of sampling obtained is a $2^{-k}$th multiple of the initial rate of sampling, where $k$ is an integer. The reason for taking such rates is that it is easy to combine signals sampled at such rate for transmission as well as for storage purposes.

The condition (3) ensures that $\hat{g}(t)$ is scale-limited to $2^k$. For applying the inequality, for $a_l = 2^j$ the reconstructed signal $\hat{g}(t)$ should be scale-limited to $2^j$. For $n = \frac{N_0}{2^k}$ this is ensured by taking $2^k > 2^j$ or $n < \frac{N}{2^j}$.

Under these simplifications, the final form of theorem 3.5.1 is,

$$\delta_{d,2^j} \leq \frac{\int_0^A |g(t)-\hat{g}(t)|^2\,dt}{\int_0^A |g(t)|^2\,dt} \leq \delta_{d,2^j} + \frac{C}{n^\alpha a_l} \quad n \leq \left(\frac{N_0}{2^j}\right) \tag{3.30}$$

For any specified $\epsilon$, the strategy adopted for sampling is as follows: First the values of $\delta_{d,2^j}$ are found, upto the $j$ value, such that, $\delta_{d,2^j} < \epsilon$. Let $j_0$ be the largest integer of $j$ such that $\delta_{d,2^j} < \epsilon$. Next the value of reconstruction error is calculated for $n = \frac{N_0}{2^{j_0}}$; if it is less than $\epsilon$, then values of $j$ higher than $j_0$ are tested till the error becomes larger than $\epsilon$. This provides us with the lowest sampling rate possible for a specified error $\epsilon$. If the reconstruction error is more than $\epsilon$ for $n = 2^j$, then lower values of $j$ are tried till the lowest possible sampling rate is obtained.

Before discussing the algorithm, a few practical considerations are discussed. Theoretically the fractional mean square error is given by the following integral -

$$fractional\ mean\ square\ error = \frac{\int_0^A |g(t)-\hat{g}(t)|^2\,dt}{\int_0^A |g(t)|^2\,dt},$$

however, we make the following approximation.

$$\int_0^A |g(t) - \hat{g}(t)|^2 \, dt \;=\; \frac{\sum_{k=1}^{N_0-1}[g(k\frac{A}{N_0}) \;-\; \hat{g}(k\frac{A}{N_0})]^2}{\sum_{k=1}^{N_0-1}[g(k\frac{A}{N_0})]^2} \tag{3.31}$$

Any other method of area calculation can be used.

Secondly to quantify the reduction in the sampling rate a performance measure, denoted by $r(\epsilon)$, is defined.

$$r(\epsilon) \;=\; \frac{Minimum\ number\ of\ samples\ for\ a\ reconstruction\ error\ less\ than\ \epsilon}{Initial\ number\ of\ samples}$$

### 3.5.2 Algorithm for Sampling Rate Estimation

The problem that has been attempted here is to obtain the sampling rate of a time-limited signal such that the fractional mean square reconstruction error remains bounded by $\epsilon$. Practically, the problem is, given $N_0$ samples of a signal it is required to find the smallest number $N$, such that, the fractional mean square reconstruction error between the original sample set and the reconstructed sample set using $N$ samples is less than $\epsilon$.

The algorithm presented here utilises the theorem presented in the previous section. In developing the algorithm we utilise the result that the fractional mean square error when the signal is reconstructed using $\frac{N_0}{2^j}$ where $N_0$ is number of samples in the initial set, is lower bounded by $\delta_{d,2^j}$.

First the values of $\delta_{d,2^j}$ for $j = 1,\ 2,\ 3,\ 4$ are found. Then the largest value of $j$ is found such that $\delta_{d,2^j} \;\leq\; \epsilon$; we denote this value by $j_0$. Next we find the fractional mean square error for $N = \frac{N_0}{2^{j_0}}$, where $N_0$ are the initial number of samples.

If this fractional mean square error is less than $\epsilon$, then the optimum number of samples are either $N$ or less than $N$. Next we find the fractional mean square error for the number of samples equal to $\frac{N}{2^k}$ for $k > j_0$, until $k = j_{opt}$ is found such that the fractional mean square error for $\frac{N_0}{2^{j_{opt}+1}}$ is greater than $\epsilon$, but the fractional mean square error for $\frac{N_0}{2^{j_{opt}}}$ samples is less than $\epsilon$. If the fractional mean square error for $j = j_0$ is greater than $\epsilon$, then the fractional mean square error for successively lower values of $j$ is computed. And this process is stopped when $j = j_{opt}$ is found, such that the fractional mean square error when the reconstruction is done using $\frac{N_0}{2^j_{opt}}$ is less than $\epsilon$.

If there exists no $j$ such that the fractional mean square error using $\frac{N_0}{2^j}$ samples is less than or equal to $\epsilon$, then all the samples have to be retained and using the algorithm no compression is possible.

For a given performance specification that the error should not exceed $\epsilon$, the possible reduction in the sampling rate can be found using the following algorithm.

BEGIN

**Step 3.1** *Sample the given signal at the highest possible rate and store in g[i], i=0, ...,* $N_0 - 1$.

**Step 3.2** *Find* $\delta_{d,2^j}$*'s for all* $j \geq 1$ *and* $\delta_{d,2^j} < \epsilon$.

**Step 3.3** *If no* $\delta_{d,2^j}$ *exists such that* $j \geq 1$ *and* $\delta_{d,2^j} \leq \epsilon$. *Then all the samples have to be kept and the algorithm be stopped.* Because under this condition this algorithm will not give any sampling rate reduction.

**Step 3.4** *If there exists* $j_0 \geq 1$, *such that,* $\delta_{d,2^j} \leq \epsilon$ *for* $j \leq j_0$, *then find the fractional mean square error, given by* $\frac{||g(t)-\tilde{g}(t)||^2}{\int_0^A |g(t)|^2 \, dt}$, *for* $a_l = 2^{j_0}$ *and* $n = \frac{N_0}{2^{j_0}}$. *If this error is less*

*than $\epsilon$, then check the fractional mean square error with $n = \frac{N_0}{2^j}$ for successively higher values of $j$ starting from $j_0 + 1$. And select the minimum expected sampling rate.*

**Step 3.5** *In step 4, if the reconstruction error is greater than $\epsilon$, then check the reconstruction error for successively lower values of $j$ and stop the iteration when the minimum possible sampling rate is obtained.*

END

In step 4 the largest $\delta_{d,2^j}$ is selected so that the search for the optimum sampling rate starts from theoretically minimum possible value. It is important to note, that in practice the $\hat{g}(t)$ may not be strictly *scale – limited* to $2^j$ since at the edges the functions $\phi(t)$ get windowed.

### 3.5.3 Simulation Results

In the simulation results that are presented in this section, two sets of signals are taken and using the algorithm, the sampling rate reduction is found. Further, the values the values of the $C$ and $\alpha$ parameters for the respective sets are found using the the first three signals of each set and these parameters are used to predict the fractional mean square error for the fourth signal of each set. The sets of signals used for two examples are presented in the Table-3.2.

Two classes of signals have been analysed using the proposed algorithm. First the set of simulated signals are analysed and the possible reduction in the sampling rate is found for a predefined value of $\epsilon$. The second class considered is of vowel sounds sampled at $10k samples/sec$. In both the cases, three signals are used to find the parameters $C$

| | Example 1 | Example 2 |
|---|---|---|
| 1 | $sin(exp(-0.2t)t)$ | utterance ooo |
| 2 | $cos(0.1t)\ sin(exp(-0.2t)t)$ | utterance uuu |
| 3 | $sin(sin(exp(-0.2t)t)0.1t)$ | utterance eee |
| 4 | $t^{3/2}\ exp(-0.05\ t)$ | utterance aww |

Table 3.2: The sets of signals used for sampling rate estimation

and $\alpha$. These values are used to predict the error for a test signal. Even in the absence of any error specification, the bounds are useful to get a rough estimate of the error.

For both the cases the value of $\epsilon$ is taken to 0.2. The tables have been given after the figures, wherein the actual values of errors are presented.

#### 3.5.3.1 Case 1: Simulated Signals

For a class of simulated signals, the value of $r(\epsilon)$ for $\epsilon = 0.2$ is tabulated in Table 3.2. In the same table the fractional error is also presented. The original and the reconstructed signals are shown in Figures 3.25, 3.26, 3.27, 3.28. The simulated signals have been used to find $C$ and $\alpha$; these values have been used to predict the error bound of the signal $g_4(t)$. For finding $C$ and $\alpha$, the value of $\frac{\|W_{g,\psi}(a,b)-W_{\hat{g},\psi}(a,b)\|^2}{\int_0^A |g(t)|^2\ dt}$ (the norm calculated with respect to $b$), which is denoted by $E_{rr}(a,n)$, has been plotted with respect to $n$, with varying values of $a$, in Figures 3.29, 3.30, 3.31. In Figure 3.32 the values of all the $E_{rr}(a,n)$ are plotted. By fixing the value of $\alpha$ equal to 2 and varying the value of $C$, the value of $C$ such that the curve $\frac{C}{n^\alpha}$ closely upper bounds the curves $E_{rr}(a,n)$ is given by 2000. For these values of $C$ and $\alpha$, the predicted error bound for $n = 60$, for $g_4(t)$ is given by 0.286997, whereas the actual error from Table-3.3 is 0.176366.

#### 3.5.3.2 Case 2: Speech Signals

In the case of speech signals the algorithm is tested on the vowel utterances and the values of $r(\epsilon)$ are presented in Table 3. The signals are sampled at a rate of $10k$ *samples/second.* The original and the reconstructed signals are shown in the Figures 3.33, 3.34, 3.35, 3.36. The utterances ooo, uuu, eee are used to find the values of $C$ and $\alpha$. For finding $C$ and $\alpha$, the value of $E_{rr}(a, n)$ has been plotted with respect to $n$, with varying values of $a$, in Figures 3.37 , 3.38, 3.39, 3.40. Using the same procedure in the case of simulated signals, for $\alpha = 2$ the value of $C$ has been found to be 10500. For these values of $C$ and $\alpha$ the predicted error bound for $n = 120$ for $\epsilon = 0.2$ is given by 0.451500, whereas the actual error from Table-3.4 is 0.173133.

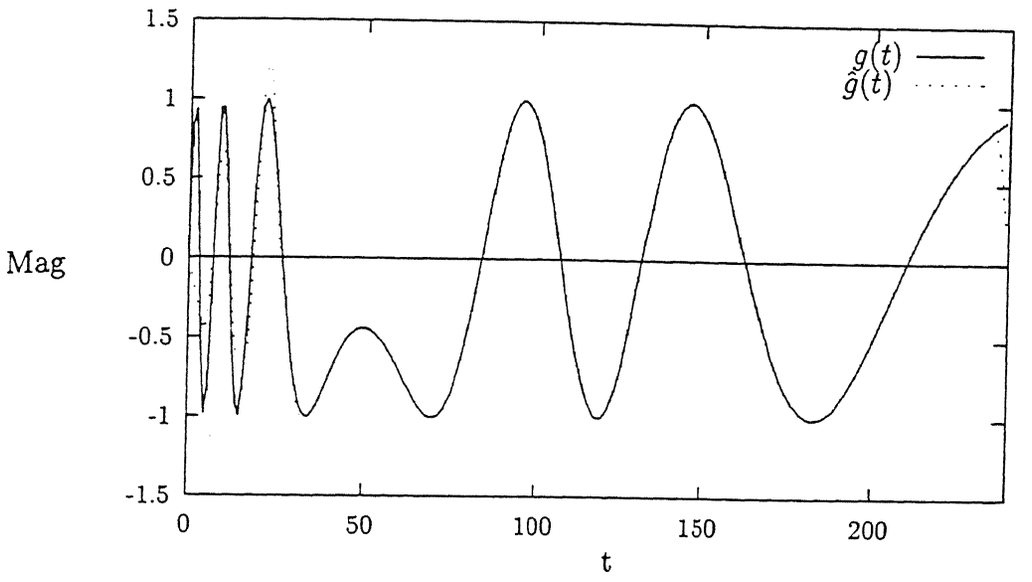


Figure 3.25: The simulated signal $g(t) = g_1(t) = sin(exp(-\ 0.2t)t)$ and the reconstructed signal using the proposed scale-limited reconstruction algorithm.

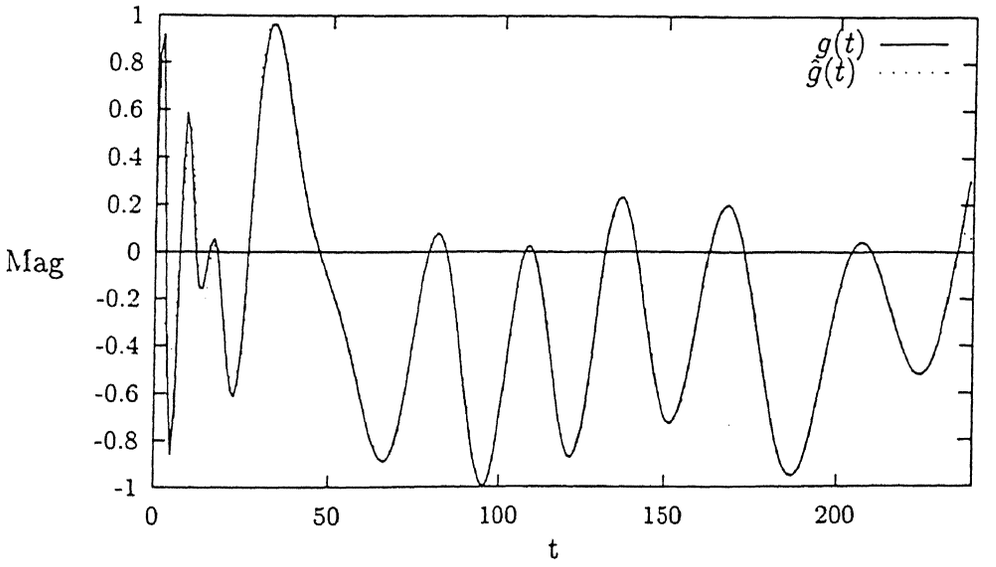


Figure 3.26: The simulated signal $g(t) = g_2(t) = cos(0.1t)\ sin(exp(-\ 0.2t)t)$ and the reconstructed signal using the proposed scale-limited reconstruction algorithm.

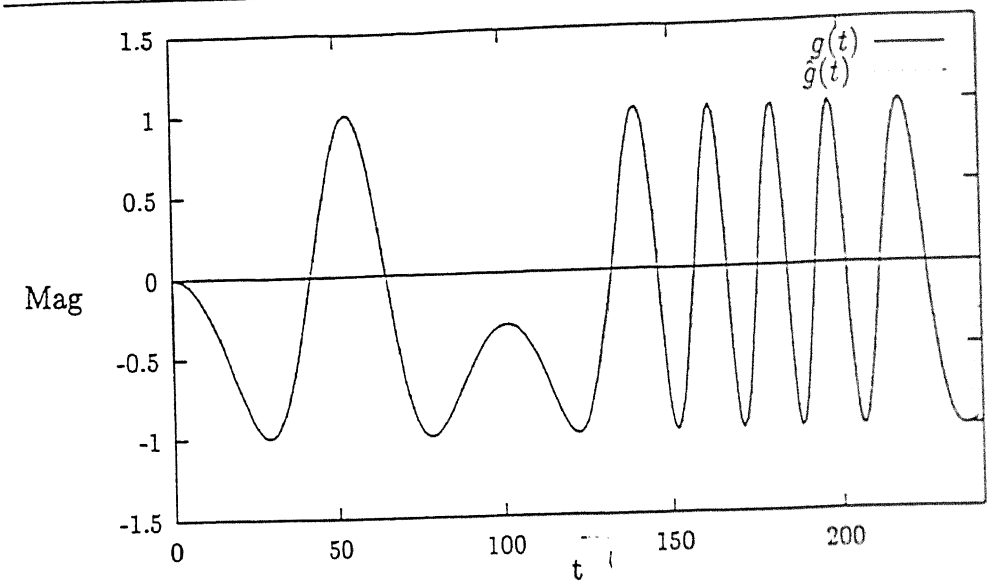


Figure 3.27: The simulated signal $g(t) = g_3(t) = sin(sin(exp(-\ 0.2t)t)\ 0.1t)$ and the reconstructed signal using the proposed scale-limited reconstruction algorithm.

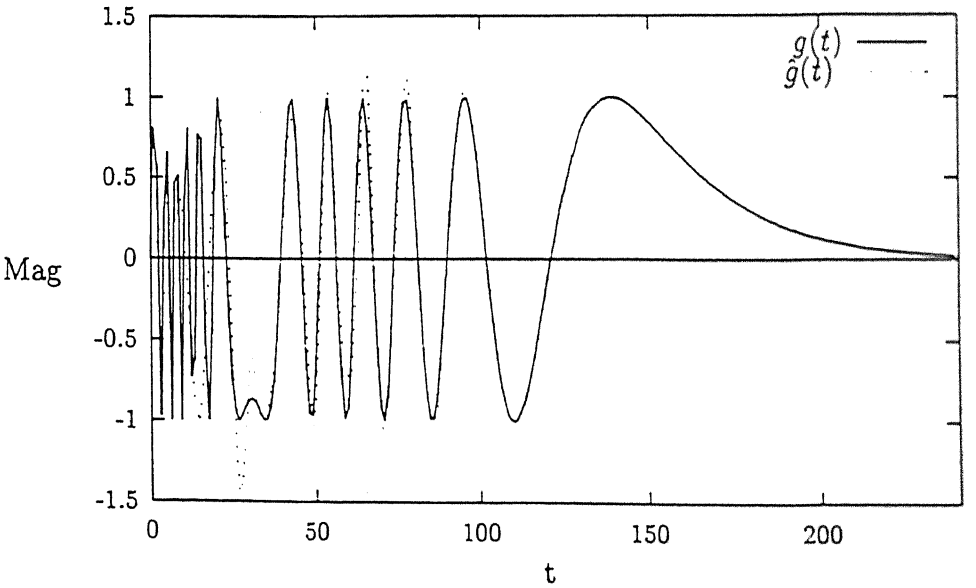


Figure 3.28: The simulated signal $g(t) = g_4(t) = t^{3/2}\ exp(-0.05\ t)$ and the reconstructed signal using the proposed scale-limited reconstruction algorithm.

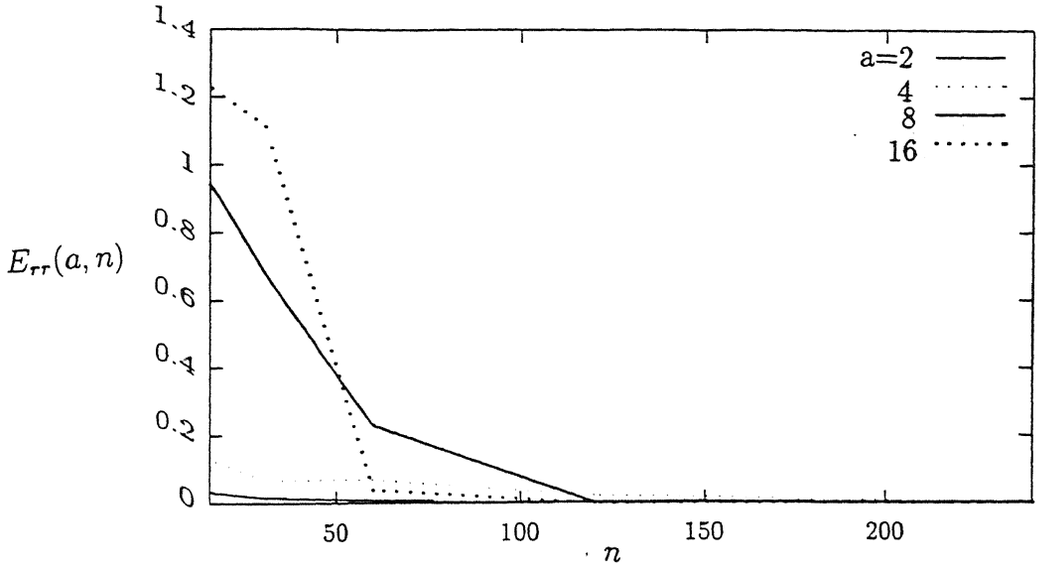


Figure 3.29: $E_{rr}(a,n)$ vs $n$ for the signal $g_1(t)$, where, $E_{rr}(a,n)$ is the error between the original and the reconstructed signal and $n$ is the number of samples used for signal reconstruction.

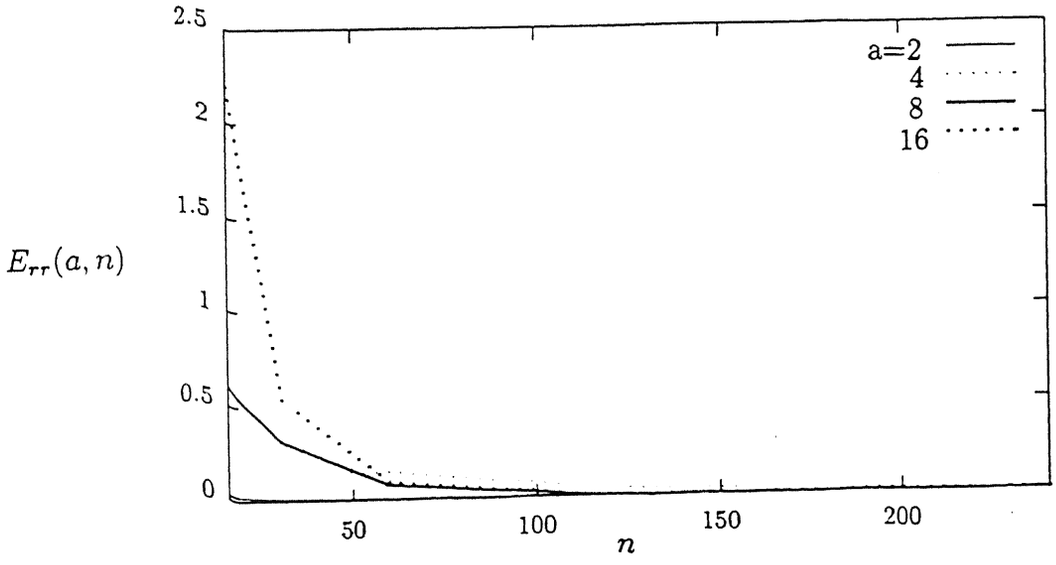


Figure 3.30: $E_{rr}(a,n)$ vs $n$ for the signal $g_2(t)$, where, $E_{rr}(a,n)$ is the error between the original and the reconstructed signal and $n$ is the number of samples used for signal reconstruction.

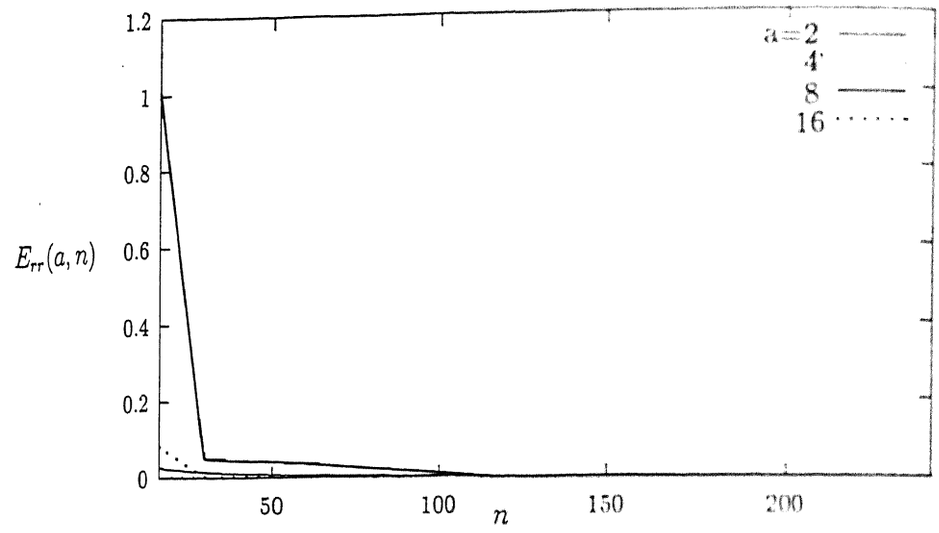


Figure 3.31: $E_{rr}(a,n)$ vs $n$ for the signal $g_3(t)$, where, $E_{rr}(a,n)$ is the error between the original and the reconstructed signal and $n$ is the number of samples used for signal reconstruction.

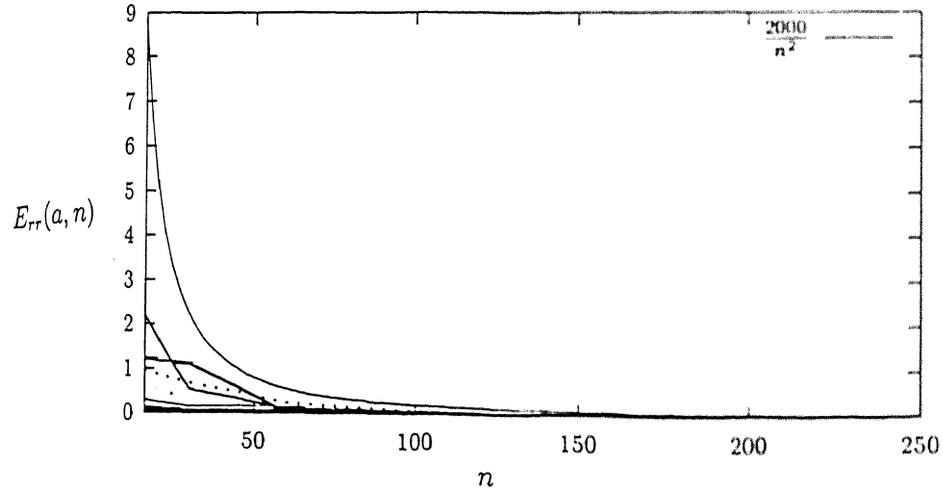


Figure 3.32: $E_{rr}(a,n)$ vs $n$ for the signals $g_1(t)$, $g_2(t)$, $g_3(t)$ *and* $\frac{2000}{n^2}$, where, $E_{rr}(a,n)$ is the error between the original and the reconstructed signal and $n$ is the number of samples used for signal reconstruction.

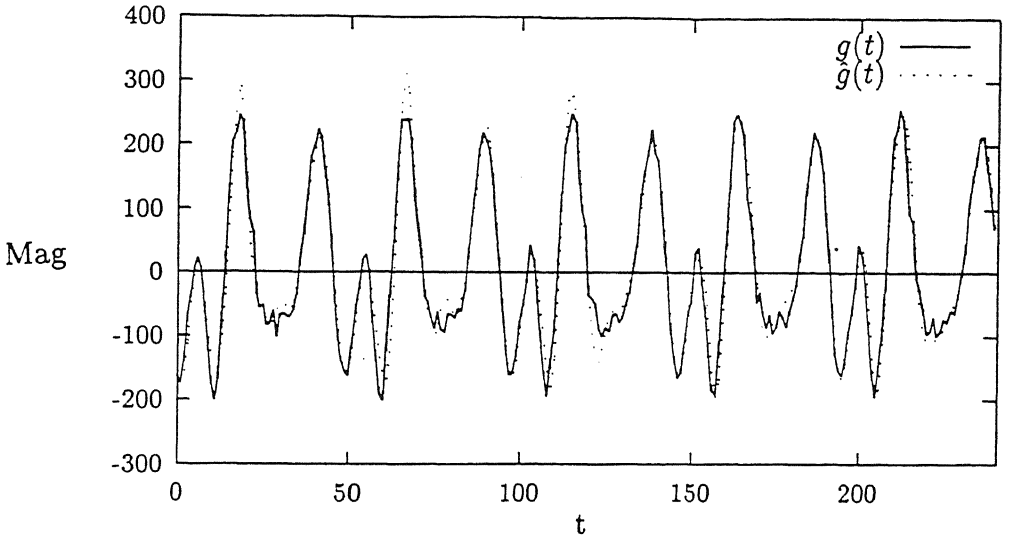


Figure 3.33: The speech utterance 'ooo' and the reconstructed signal using the proposed scale-limited reconstruction algorithm.

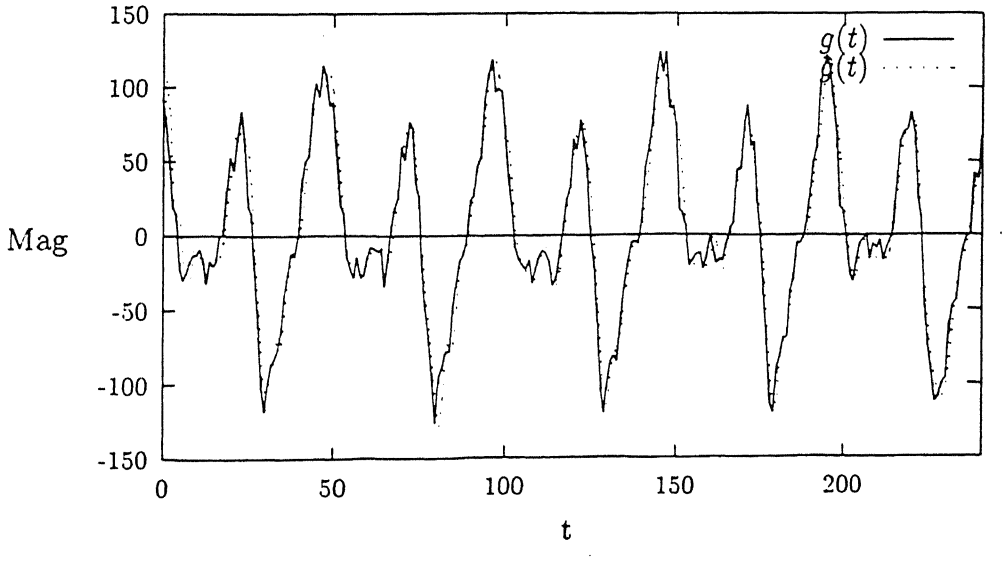


Figure 3.34: The speech utterance 'uuu' and the reconstructed signal using the proposed scale-limited reconstruction algorithm.

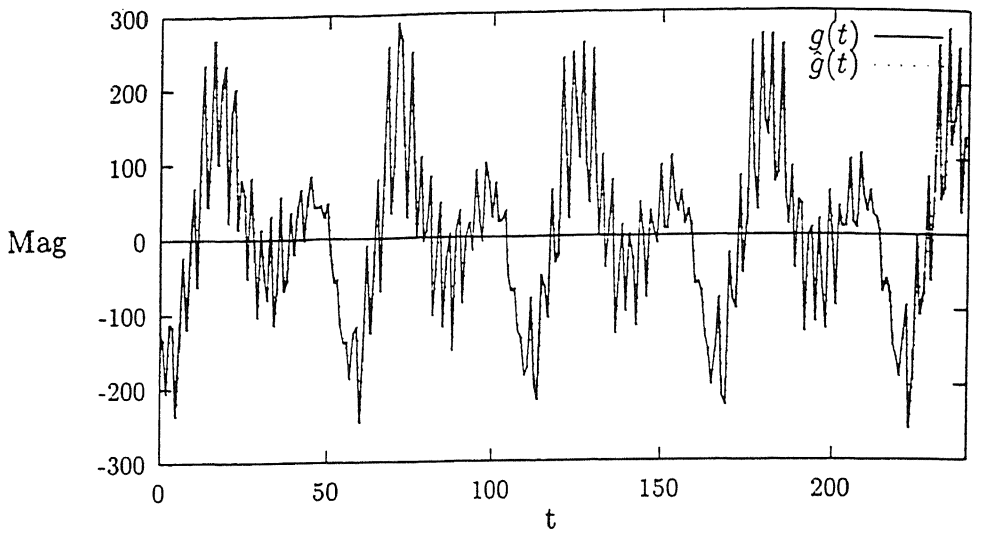


Figure 3.35: The speech utterance 'eee' and the reconstructed signal using the proposed scale-limited reconstruction algorithm.

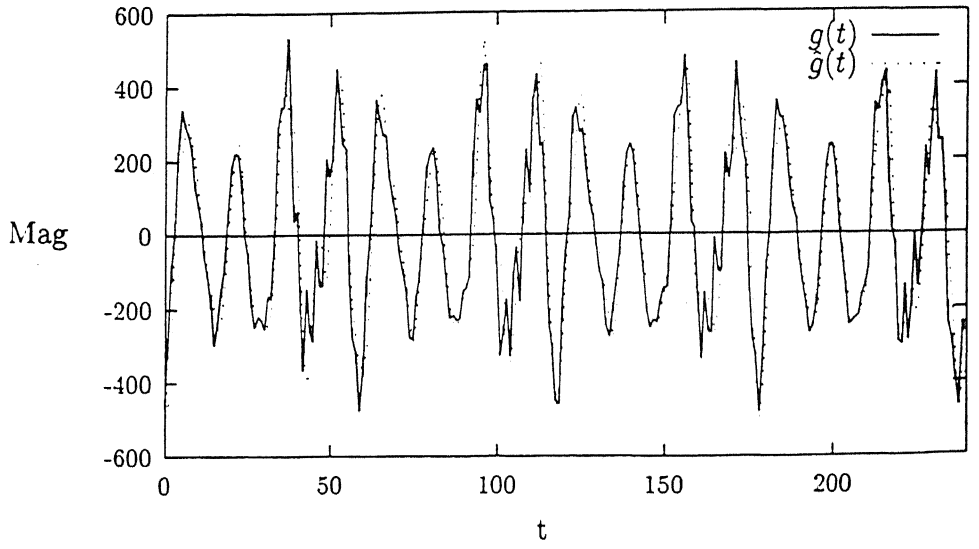


Figure 3.36: The speech utterance 'aww' and the reconstructed signal using the proposed scale-limited reconstruction algorithm.

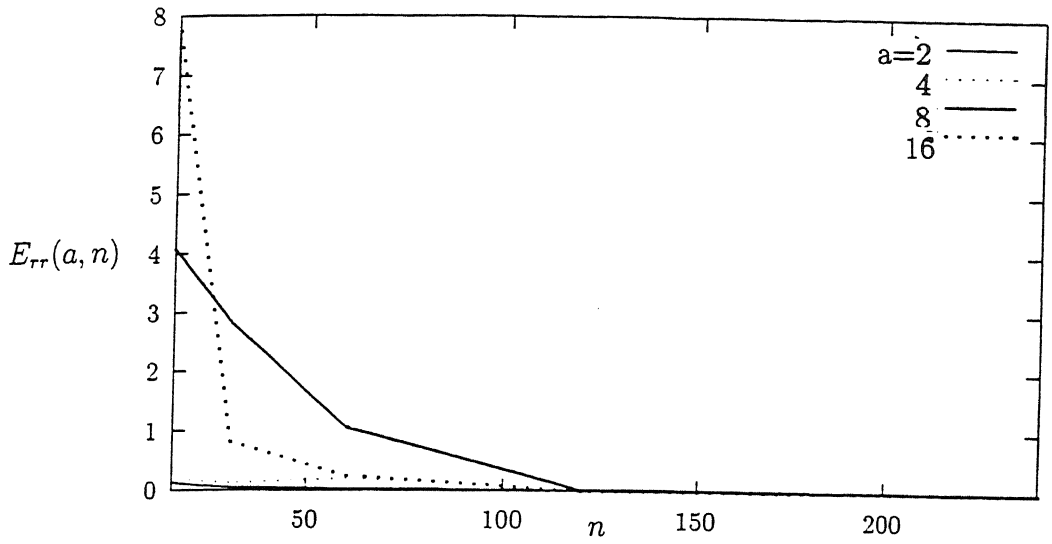


Figure 3.37: $E_{rr}(a,n)$ vs $n$ for the utterance 'ooo', where, $E_{rr}(a,n)$ is the error between the original and the reconstructed signal and $n$ is the number of samples used for signal reconstruction.

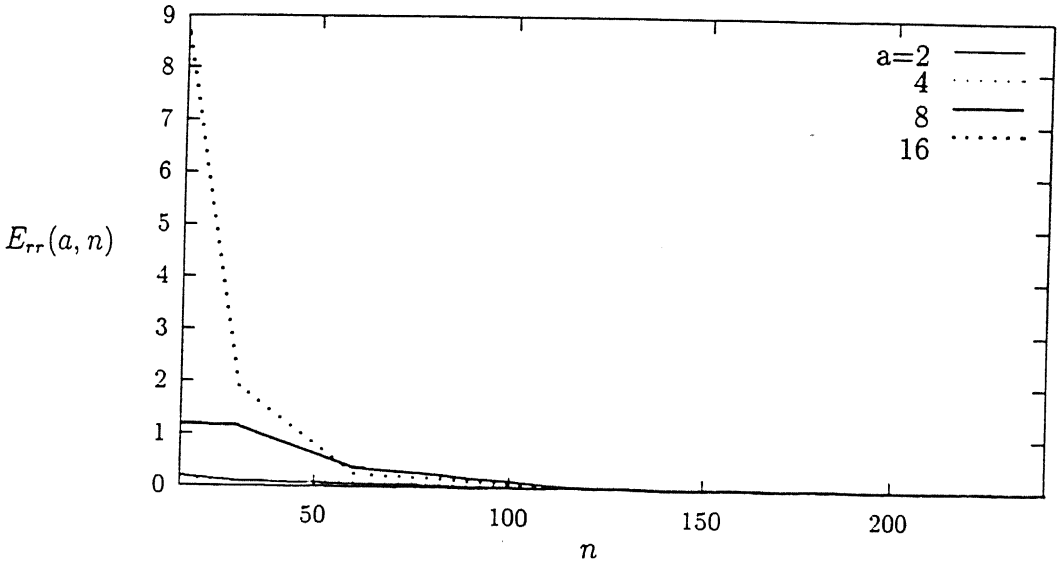


Figure 3.38: $E_{rr}(a,n)$ vs $n$ for the utterance 'uuu' , where, $E_{rr}(a,n)$ is the error between the original and the reconstructed signal and $n$ is the number of samples used for signal reconstruction.

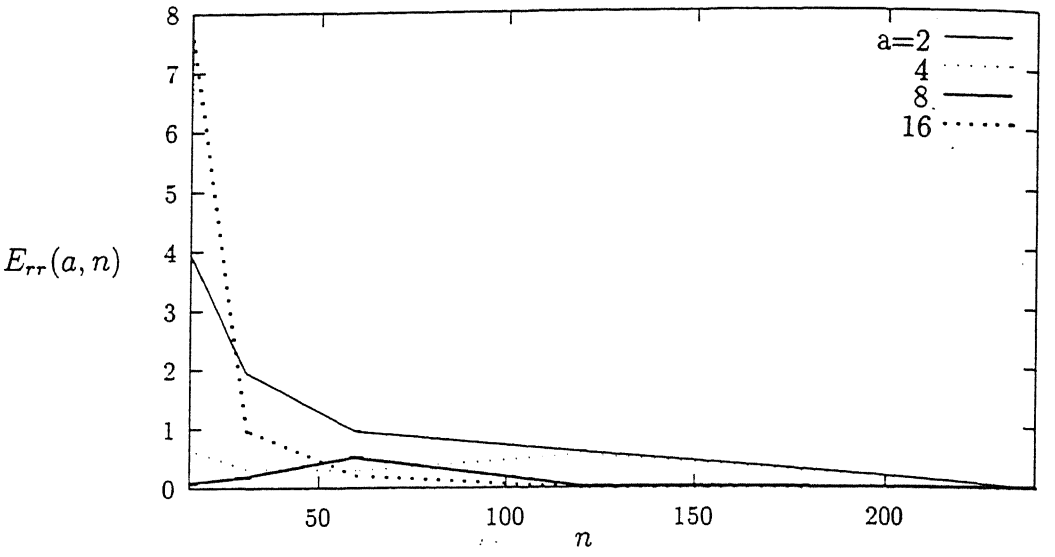


Figure 3.39: $E_{rr}(a,n)$ vs $n$ for the utterance 'eee', where, $E_{rr}(a,n)$ is the error between the original and the reconstructed signal and $n$ is the number of samples used for signal reconstruction.

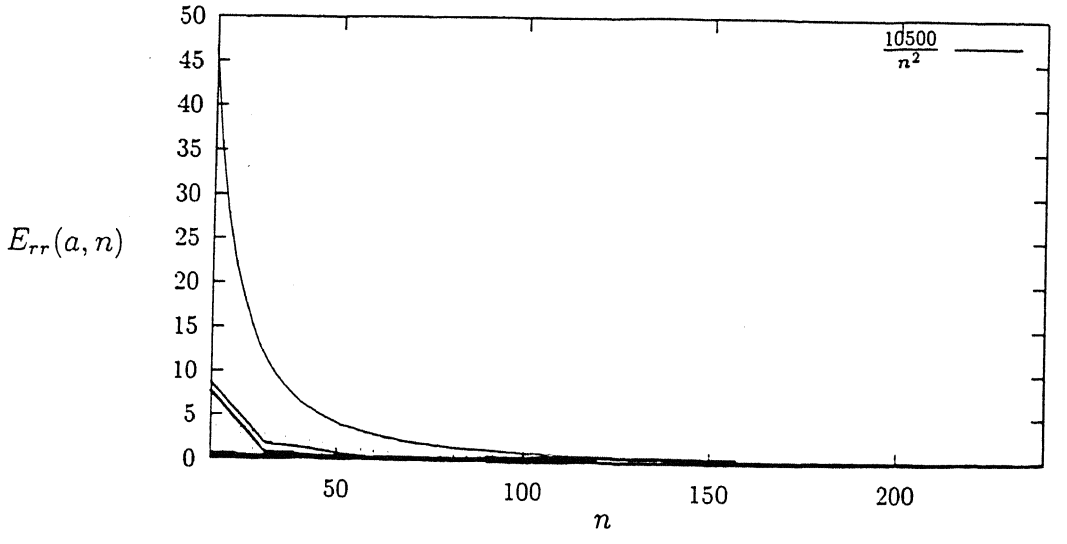


Figure 3.40: $E_{rr}(a,n)$ vs $n$ for the utterances 'ooo', 'uuu', 'eee', and the function $\frac{10500}{n^2}$, where, $E_{rr}(a,n)$ is the error between the original and the reconstructed signal and $n$ is the number of samples used for signal reconstruction.

| signal | r($\epsilon$),$\epsilon$=0.2 | Actual error | $\delta(2)$ | $\delta(4)$ | $\delta(8)$ | $\delta(16)$ |
|---|---|---|---|---|---|---|
| $g_1(t)$ | 0.25 | 0.056265 | 0.014273 | 0.112611 | 0.369805 | 0.941584 |
| $g_2(t)$ | 0.25 | 0.075113 | 0.027899 | 0.099544 | 0.325605 | 0.915409 |
| $g_3(t)$ | 0.25 | 0.010434 | 0.001740 | 0.137147 | 0.343022 | 0.950383 |
| $g_4(t)$ | 0.25 | 0.176366 | 0.109399 | 0.148108 | 0.414172 | 0.989439 |

Table 3.3: The value of compression(r($\epsilon$ )) for the signals $g_1(t)$, $g_2(t)$, $g_3(t)$, $g_4(t)$, for $\epsilon$ =0.2.

| signal | r($\epsilon$), $\epsilon$ =0.2 | Actual error | $\delta(2)$ | $\delta(4)$ | $\delta(8)$ | $\delta(16)$ |
|---|---|---|---|---|---|---|
| ooo | 0.25 | 0.057822 | 0.019652 | 0.105810 | 0.606019 | 0.971977 |
| uuu | 0.25 | 0.060928 | 0.024830 | 0.155246 | 0.388315 | 0.963102 |
| eee | 1.00 | 0.000000 | 0.269291 | 0.431910 | 0.590559 | 0.990329 |
| aww | 0.5 | 0.173133 | 0.086965 | 0.225765 | 0.800895 | 0.992502 |

Table 3.4: The value of compression(r($\epsilon$ )) for the signals 'ooo', 'uuu', 'eee', 'aww', for $\epsilon$ =0.2.

## 3.6 Conclusions

The purpose of this chapter is to introduce a new concept, which can be used to characterise variations in signals. This concept is proposed with reference to wavelet transforms and is termed as scale-limitedness. A few examples are given, in which, the signals and their computed scale-limits are presented. The relation between higher order vanishing moment property and scale-limitedness is also analysed. Further, a few theorems related to scale-limitedness are also presented. Finally, a sampling strategy is proposed which gives the minimum possible sampling rate for a given error performance.

The chapter starts with the review of wavelet transforms and first the definition of continuous wavelet transform is presented. Next, the practical implementation of the wavelet transform using the concept of multiresolution analysis is discussed. In multiresolution analysis, the scale and the shift parameters are discretised and the wavelet transform is only found on a discrete set.

The significance of scale and shift parameters, which are associated with wavelet transforms, is discussed next. It has been illustrated using an example that at lower scales the wavelet becomes sharper. This property has an important role in the definition of the proposed signal variation measure.

The wavelet transform of a signal $g(t)$, denoted by $W_{g,\psi}(a,\ b)$, is the inner product between the signal and the function $\frac{1}{\sqrt{a}}\psi\left(\frac{t-b}{a}\right)$. The shift parameter, denoted by 'b', shifts the wavelet to $t = b$ and therefore, the wavelet transform gives the behaviour of the signal at $t = b$. At lower scales the wavelet transform gives the fast varying component present in the signal. Therefore, the wavelet transform is enhanced at

lower scales, in regions, wherein, the signal is varying fast. This has been illustrated by plotting the wavelet transforms of signals shown in Figures 3.3, 3.8, 3.11.

By eliminating fast varying components, it is possible to construct signals which are scale-limited. Further, signals which do not have components faster than those indicated by a wavelet at a given scale, are scale-limited.

A signal is called scale-limited, if its wavelet transform is zero for all scales below a certain scale value and for all shifts. Another definition, termed as $\delta_0$-practical scale-limitedness is also introduced. A signal is called $\delta_0$-practically scale-limited to $a_l$, if $a_l$ is the largest scale value below which the fraction of the energy, for all shifts, is less than $\delta_0$. Next three examples are presented, in which the signals are plotted and their scale-limits are computed. It can be inferred from these examples that, the signals which are faster varying have smaller scale-limits.

To compute scale-limits, the fraction of the energy, for scales less than 2, 4, 8 and 16 are plotted with respect to the scale value. Next, for the fixed $\delta_0$, which is 0.05 in our examples, the largest value of scale is found be which the fraction of the energy is less than $\delta_0$. This gives the $\delta_0$-practical scale-limit of the signal.

Next the relation between the higher order vanishing moment property and scale-limitedness is discussed. It can be inferred that, signals which are faster varying have smaller scale-limits because of the vanishing moment property of the wavelet.

A few theorems have been stated and proved next. It has been shown that, a signal which is band-limited is also scale-limited. Moreover, it has been proved that there exist time-limited signals which are scale-limited. Further it is shown that, signals which have smaller scale-limits have their differentials more loosely bounded. Next

it is shown that the Lagrangian interpolating function is $\delta_0$-practically scale-limited. Finally it is shown that, signals which are in $V_j$ are scale-limited with a scale-limit of $2^j$.

As an application of scale-limitedness, a sampling rate estimation method for signals is proposed. For estimating the sampling rate, a theorem is proved, which states that signals with smaller scale-limits should be sampled at a relatively faster rate for the same error bound. This method proceeds by first over sampling the signal, then finding the scale-limit using the multiresolution analysis. And finally, given a bound on the error, reduction in the number of samples is found such that the error remains less than the bound. The method gives a sampling rate reduction of a multiple of $2^j$, where '$j$' is an integer greater than zero.

Finally, these are the conclusions of this chapter-

- Signals which are faster varying, have a relatively smaller scale-limits.
- Scale-limited signals satisfy the following properties-
  - Signals which are band-limited are also scale-limited.
  - There exist time-limited signals which are scale-limited as well.
  - Signals having smaller scale-limits have looser bounds on their differentials.
  - The Lagrangian interpolating function is $\delta_0$-practically scale-limited.
  - Signals which are in $V_j$ have a scale-limit of $2^j$.
- It has been shown that, for the same error performance, the signals with smaller scale-limits should be sampled at a higher rate.

# Chapter 4

# Optimal Sample Placement Using Wavelet Transforms

In this chapter, the problem of sample placement is introduced and an algorithm for nonuniform sampling is presented. The sample placement problem deals with the optimal placement of the samples in the interval of the signal so that the fractional mean square error between the original signal and the reconstructed signal is minimised. The interpolation is done using functions which are local, in other words they have most of their energy concentrated in a small region. For calculating the error between the original and the reconstructed signals, the fractional mean square error is used. The fractional mean square error is the ratio of the mean square error and the energy of the original signal. Simulation results have been presented, in which, the original and the reconstructed signals have been plotted. The mean square error verses the number of samples has also been tabulated.

## 4.1 Problem Statement

The problem formulated in this chapter is referred as sample placement problem.

Given $g(t), t \in [0, A]$, what is the $N$ tuple $(t_0, t_1, ..., t_{N-1})_{opt}$ such that $\frac{\int_0^A |g(t) - \hat{g}(t)|^2 \, dt}{E_g}$ is minimised, where $\hat{g}(t)$ is the reconstruction of $g(t)$ using the samples $g(t_i)$, $t_i \in [0, A]$, $\forall i$ and $E_g$ is the energy of the signal. In other words, the optimisation problem can be written as,

$$\min_{t_0, \, ..., \, t_{N-1}} \frac{\int_0^A |g(t) - \hat{g}(t)|^2 \, dt}{E_g} \tag{4.1}$$

where, $E_g = \int_0^A |g(t)|^2 \, dt$.

Certain conditions on the type of interpolation to be used, are also assumed, which are given below.

$$(a) \quad \hat{g}(t) = \sum_k g(t_k) \, h_k \, (t - t_k, t_{k-1}, t_{k+1}). \tag{4.2}$$

$$(b) \quad \hat{g}(t_k) = g(t_k). \tag{4.3}$$

$$\tag{4.4}$$

This condition is achieved by setting,

$$h_k(0, t_{k-1}, t_{k+1}) = 1, \; h_k(t_j - t_k, t_{k-1}, t_{k+1}) = 0, \text{ for } j \neq k. \tag{4.5}$$

The condition (a) gives a representation of the interpolated signal in terms of the samples and certain functions which are window functions. Here, those functions which decay down in time are called window functions. Mathematically stated, these functions tend to zero as $|t| \to \infty$. The condition (b) on the interpolation ensures that, at

the sampling instant, the value of the interpolated signal is same as the value of the of the original signal.

For the purpose of simulation the following form of $h_k(t, t_{k-1}, t_{k+1})$ is assumed,

$$h_k(t - t_k, t_{k-1}, t_k) = \begin{cases} e^{\frac{(t-t_k)^2}{\alpha_k(t_k, t_{k+1})}}, & t_k \leq t \\ e^{\frac{(t-t_k)^2}{\beta_k(t_k, t_{k-1})}}, & t \leq t_k \end{cases} \tag{4.6}$$

The parameter $\alpha_k$ is such that $|h_k(t_{k+1} - t_k, t_{k-1}, t_{k+1})| = \epsilon$.
The parameter $\beta_k$ is such that $|h_k(t_{k-1} - t_k, t_{k-1}, t_{k+1})| = \epsilon$.
Here $\epsilon$ is arbitraryly small. In our simulations, the value of $\epsilon$ is taken to be 0.1. For the form of $h_k(t)$ given in 4.6, the condition given in (b) gets satisfied, with a negligible error. The problem formulated can be solved by exhaustive search, but then the search space of each of the variable is [0, $A$]. However, we introduce a novel, algorithm which reduces the computational complexity of the problem and at the same time gives a suboptimal solution.

## 4.2 A Suboptimal Solution

In the practical implementation, the signal is sampled at an arbitrary high rate and a large number of samples are obtained. Let the number of samples be $N_0$. Then the problem of $N$ sample placement reduces to picking $N$ samples out of $N_0$ samples such that the error between the reconstructed samples at the initial $N_0$ points and the actual function values at those points is minimised. Here an algorithm is provided to pick these $N$ number of points. The optimal sample placement for varying values of $N$ are found and the original and the reconstructed signals are plotted; the fractional mean square reconstruction error is also computed.

### 4.2.1 Strategy Adapted

For solving the problem, specific properties of wavelet transform description of the signal are utilised. These properties are developed as theorems. The basic concept utilised in developing the algorithm is to sample the signal initially at those points in the time domain at which the wavelet transform has maxima. The subsequent samples are picked at the neighbourhood of these sampling instants. After presenting the theorems, the reason and the conceptual basis for adapting this strategy is discussed.

Next we develop certain theorems relating to the mean square error between the original signal and the reconstructed signal using $N$ number of samples.

Let the wavelet transform of $h_k(t, t_{k-1}, t_{k+1})$ be denoted by $W_{g,h_k}(a, b)$.

**Lemma 4.2.1** *If the wavelet transform of $h_k(t, t_{k-1}, t_{k+1})$ is denoted by $W_{h_k,\psi}(a, b)$ then the wavelet transform of $h_k(t - t_k, t_{k-1}, t_{k+1})$ is given by, $W_{h_k,\psi}(a, b - t_k)$.*

**Proof:** The wavelet transform of $h_k(t - t_k, t_{k-1}, t_{k+1})$ is given by

$$= \int_{-\infty}^{\infty} h_k(t - t_k, t_{k-1}, t_{k+1})\ \psi\left(\frac{t-b}{a}\right)\ dt$$

Let $t - t_k = z$, then the wavelet transform becomes,

$$= \int_{-\infty}^{\infty} h_k(z, t_{k-1}, t_{k+1})\ \psi\left(\frac{z-(b-t_k)}{a}\right)\ dz$$
$$= W_{h_k,\psi}(a, b - t_k).$$

Hence proved.

It can be inferred from the Lemma that a shift in time domain leads to the same amount of shift in the wavelet transformed domain. Using the Lemma we prove the following theorem.

**Theorem 4.2.1** *If*

$$g(t) = \sum_k g(t_k)\ h_k(t - t_k, t_{k-1}, t_{k+1}) \tag{4.7}$$

*Then,*

$$W_{g,\psi}(a,b) = \sum_k g(t_k) W_{h_k,\psi}(a, b - t_k) \tag{4.8}$$

*for all* $a \in S \subseteq R$, $b \in L \subseteq R$. *where* $S$ *and* $L$ *are the domains of 'a' and 'b' respectively.*

**Proof:** Taking the wavelet transform of both sides of the Equation 4.7, we obtain the following,

$$\begin{aligned}
LHS &= W_{g,\psi}(a,b) \\
RHS &= \int_{-\infty}^{\infty} \sum_k \left(g(t_k)\ h_k(t - t_k, t_{k-1}, t_{k+1})\right) \psi\left(\frac{t-b}{a}\right) dt \\
&= \sum_k g(t_k) \int_{-\infty}^{\infty} h_k(t - t_k, t_{k-1}, t_{k+1}) \psi\left(\frac{t-b}{a}\right) dt \\
&= \sum_k g(t_k) W_{h_k,\psi}(a, b - t_k), \text{ using Lemma 4.1}
\end{aligned}$$

Hence proved.

This proof is valid for $a \in S \subseteq R$, $b \in L \subseteq R$. The significance of this result is that if any signal has a representation of the kind given in 4.7, then at each scale, the wavelet transform also has a representation which in terms of shifted versions of certain functions. For developing the final algorithm the inequality versions of the theorems are put to use.

**Theorem 4.2.2** *If*

$$W_{g,\psi}(a,b) = \sum_k g(t_k) W_{h_k,\psi}(a, b - t_k) \tag{4.9}$$

*For some $a \in S \subseteq R$, $b \in L \subseteq R$, then*

$$g(t) = \sum_k g(t_k)\ h_k(t - t_k, t_{k-1}, t_{k+1}), \tag{4.10}$$

*provided the following two conditions are satisfied, viz,*
*(a) The bandwidth of the wavelet $\psi(t)$ is greater than or equal to that of the signal $g(t)$.*
*(b) Within the bandwidth, the Fourier transform of $\psi(t)$ is zero only on a set of measure zero.*

**Proof:** Let $F_t[.]$ denote the Fourier transform operator, given by,

$$F_t[g(t)] = \int_{\infty}^{\infty} g(t)\ exp(-j2\pi\ f\ t)\ dt$$

Let $\Psi(f) = F_t[\psi(t)]$, our strategy is to take the Fourier transform of both sides of the Equation 4.9 and equate, this leads us to the 4.10. Let 4.9 is true for some $a = a^* \in S$.

$$F_b[W_{g,\psi}(a^*, b)] = -\sqrt{a^*}G(f)\Psi(-a^*f),$$

Similarly,

$$F_b[W_{h_k,\psi}(a^*, b)] = -\sqrt{a^*}\ \Psi\ (-a^*f)\ H_k(f, t_{k-1}, t_{k+1}),$$
$$\text{where,} H_k(f, t_{k-1}, t_{k+1}) = F_t[h_k(t, t_{k-1}, t_{k+1})]$$

Therefore taking the Fourier transform of the LHS and RHS of Equation 4.9 and cancellation of the term $\psi_f(-a^*f)$ leads to,

$$G(f) = \sum_k g(t_k)\ h_k(f, t_{k-1}, t_{k+1}), \tag{4.11}$$

provided that the bandwidth of the signal $\psi(t)$ is greater than or equal to that of $g(t)$. Secondly, within the bandwidth of the $\psi$ $(t)$, the magnitude of $\hat{\psi}(f)$ is zero only on a set of measure zero.

Hence proved.

**Corollary 4.2.1** *If*

$$W_{g,\psi}(a,b) = \sum_k g(t_k) W_{h_k,\psi}(a, b - t_k)$$

*For all* $a \in S \subseteq R$, $b \in L \subseteq R$, *then*

$$g(t) = \sum_k g(t_k)\ h_k(t - t_k, t_{k-1}, t_{k+1}).$$

*If the following two conditions are satisfied,*
*(a) The bandwidth of the wavelet* $\psi(t)$ *is greater than or equal to that of the signal* $g(t)$.
*(b) Within the bandwidth, the Fourier transform of* $\psi(t)$ *is zero only on a set of measure zero.*

The proof of this is contained in the proof of the theorem presented above. In fact the only difference between the theorem and the corollary is that the corollary considers the equality in 4.9 to be valid for all 'a' values , whereas in case of the theorem this equality is taken only for some 'a'.

Next we present the inequality versions of the same theorems.

**Theorem 4.2.3** *If,*

$$\frac{1}{E_g} \int_0^A |g(t) - \sum_k g(t_k) h_k(t - t_k, t_{k-1}, t_{k+1})|^2\ dt \leq \epsilon_{rr}$$

*Then,*

$$\frac{1}{E_g} \int_{b \in L(a)} |W_{g,\psi}(a^*, b) - \sum_k g(t_k) W_{h_k,\psi}(a^*, b - t_k)\ |^2\ db \leq M^2\ \epsilon_{rr}$$

*for all* $a^* \in S$, $b \in L(a)$. *Also the following condition is assumed-* $|\sqrt{a^*}\psi(a^* f)| \leq M$, $\forall a^* \in S$.

**Proof:** Using Parseval's theorem-

$$\frac{1}{E_g}\int_{b\in L(a)} |W_{g,\psi}(a^*,b) \;-\; \sum_k g(t_k)W_{h_k,\psi}(a^*,b-t_k)|^2 db$$

$$= \frac{1}{E_g}\int_{-\infty}^{\infty} |G(f) - \sum_k g(t_k)h_k(f,t_{k-1},t_{k+1})\; e^{j2\pi f t_k}|^2\; |\sqrt{(a^*)}\psi(a^*f)|^2\; df$$

Assuming that-

$$|\sqrt{a^*}\psi(a^*f)| \;\leq\; M,\; \forall a \in S. \tag{4.12}$$

$$\begin{aligned}
&= \frac{1}{E_g}\int_{-\infty}^{\infty} |G(f) - \sum_k g(t_k)h_k(f,t_{k-1},t_{k+1})\; e^{j2\pi f t_k}|^2\; |\sqrt{(a^*)}\psi(a^*f)|^2\; df \\
&\leq \frac{M^2}{E_g}\int_0^A |G(f) - \sum_k g(t_k)h_k(f,t_{k-1},t_{k+1})\; e^{j2\pi f t_k}|^2\; df \\
&\leq \frac{M^2}{E_g}\,\epsilon_{rr}, \qquad \text{Again by Parseval's theorem.}
\end{aligned}$$

Hence Proved.

For the type of interpolation given in 4.2, this theorem proves that, if the error in the transform domain is bounded at all scales with the additional condition that 4.12 is satisfied then the mean square error in the time domain has a bound which is proportional to the bound on the error in the wavelet transform domain.

Finally we state the following theorem.

**Theorem 4.2.4** *If,*

$$\frac{1}{E_g}\int_{b\in L(a)} |W_{g,\psi}(a,b) \;-\; \sum_k g(t_k)W_{h_k,\psi}(a,b-t_k)\;|^2\; db \leq \epsilon(a) \tag{4.13}$$

*for all* $a \in S$, $b \in L(a)$. *Then,*

$$\frac{1}{E_g}\int_0^A |g(t) - \sum_k g(t_k)h_k(t-t_k, t_{k-1}, t_{k+1})|^2 \, dt \leq \int_{a_0}^{\infty} \frac{\epsilon(a)}{a^2} \, da \qquad (4.14)$$

Proof:

$$\frac{1}{E_g}\int_0^A |g(t) - \sum_k g(t_k)h_k(t-t_k, t_{k-1}, t_{k+1})|^2 \, dt \;=$$

$$\frac{1}{E_g}\int_{a_0}^{\infty} \frac{1}{a^2}\int_{b\in L(a)} |W_{g,\psi}(a,b) - \sum_k g(t_k)W_{h_k,\psi}(a, b-t_k)|^2 \, db$$

Using the inequality 4.13, we obtain,

$$\frac{1}{E_g}\int_0^A |g(t) - \sum_k g(t_k)h_k(t-t_k, t_{k-1}, t_{k+1}) \, dt \leq \int_{a=a_0}^{\infty} \frac{\epsilon(a)}{a^2} da$$

Hence proved.

This result leads to the an algorithm for sample placement. All the theorems indicate that if the error becomes small in the time domain then the error in the transform domain at all scales also becomes small and vice versa. The final theorem provides us with an algorithm for sample placement.

The algorithm for sampling has to be developed on the basic objective that, the samples should be placed in such a fashion that the mean square reconstruction error is minimised. From the Equation 4.14, it can be inferred that the strategy of sample placement should be such that the mean square error in the transform domain should be made small at the different scales, in order to keep the error bound on the reconstruction error be small. Further, at lower scales the error in the transform domain should be relatively lower. The reason is that in the error bound in the Equation 4.14

is integral of a term which is inversely proportional to $a^2$. At lower scales the argument of the integral blows up therefore the error $\epsilon(a)$ at lower scales should be made smaller to make the overall error small. Further, the functions $W_{g,\psi}(a,b)$ functions are local, the reason for this is as follows. If the support of $\psi\left(\frac{t-b}{a}\right)$ is $[-s_1,\ s_2]$ and since the support of $h_k(t-t_k,\ t_{k-1},\ t_{k+1})$ is $[t_{k-1},\ t_{k+1}]$, the support of $W_{h_k,\psi}(a,b)$ is $[t_{k-1}-s_2,\ t_{k+1}+s_1]$. Therefore, in order to make the mean square error in the transform small at any particular $a$ the $t_k$'s should be selected in regions wherein the $|W_{g,\psi}(a,b)|$ is significant.

The problem of sampling that we have formulated requires the placement of fixed number of samples in the domain of the signal. Due to the considerations discussed above, we adopt the following strategy of sampling. The initial samples are placed at the points in time at which the wavelet transform has maximum at the different scales in the '$b$' domain. In other words, the initial samples are taken at $t = t_k$'s if $|W_{g\psi}(a_i,b)|$ has maxima for $b = t_k$ for each of the $a_i$. Moreover, more samples are taken using the information at lower scales. Further, if all the maxima are exhausted and still same more samples can be taken then they are taken at the neighbourhood of the maxima. The strategy adopted for placing the samples around the maxima is as follows. First the samples are placed closest to the left of the maxima, subsequently the samples are placed to the right of the maxima, ensuring that no two samples are repeated. The steps described are repeated until all the samples are exhausted. The detailed algorithm is discussed in a subsequent section.

### 4.2.2 Practical Considerations

Here we discuss the practical implementation of the concept developed in the previous subsection. The basic concept proposed is to sample the signal at those instants in the time domain at which the wavelet transform has significant values in the transformed domain.

Let us consider the problem of placing $N$ samples at $t = t_k$, $k = 0$, ..., $N - 1$. if the wavelet transform $|W_{g,\psi}(a, b)|$ has maxima at all scales at $b = t_i$, i=0, ...N. As already discussed in the chapter 3, using Multiresolution algorithm a signal can be decomposed into $W_{g,\psi}(a, b)$, for $a = 2^j$ and $b = k\ 2^j$, where $j = 1,\ 2,\ 3,\ 4,\ ....$ Here we decompose only upto $j = 4$.

For applying the Multiresolution algorithm, the samples of the initial signal are required, therefore the signal is sampled an arbitrary high rate. Next the wavelet transform is computed by passing the sampled signal through the bank of filters described in the Chapter 3. The wavelet with respect to which the wavelet transform is computed is $\psi^8$. Once the wavelet transform is computed, the peaks of the wavelet transform are picked. If for $0 < k2^j < A$, $|W_{g,\psi}(2^j, k2^j)| \geq |W_{g,\psi}(2^j, (k-1)2^j)|$ and $|W_{g,\psi}(2^j, k2^j)| \geq |W_{g,\psi}(2^j, (k+1)2^j)|$, then $k2^j$ is a maximum at scale $2^j$, therefore we sample at $t = k2^j$. If all the maxima are exhausted and some more samples have to be placed then they are placed at the neighbourhood of $t = b'$, if the maximum at some scale had occurred at some $b = b'$. The algorithm is presented in the next subsection.

### 4.2.3 Algorithm

Before presenting the algorithm we discuss certain practical issues. If $N$ is the number of samples to be distributed in the domain of the signal, then it is required to decide, how many samples have to be placed using the information of the different scales. Initially, our policy is to place a maximum of $\frac{N}{16}$ samples using the transform information at scale equal to 16, similarly $\frac{N}{8}$, $\frac{N}{4}$, $\frac{N}{2}$ are the number of samples distributed using the transform information at scales 8, 4, 2, respectively. The reason for making this choice is that, the error bound in the inequality 4.14, is inversely proportional to $a^2$, therefore error at smaller scales in the transformed domain blows the error bound in the time domain. Hence to keep the error bound small, the appropriate choice for sample distribution is to place relatively more samples using information at smaller scales. Further, we place the sample at a certain value in time domain if the wavelet transform has a maximum, at some scale, at the same value in b-domain.

If the number of samples allocated to any scale is more than the number of peaks in the $|W_{g,\psi}(a,b)|$ then, there is a surplus of samples. The strategy for placing these samples also has to be decided. Our policy is to allocate the surplus samples of all scales to lowest possible scale, then if there is a surplus left then these samples are allocated to successively higher scales. Finally if the maxima of the $|W_{g,\psi}(a,b)|$ at all scales are exhausted and still some more samples of the signal can be taken then these samples are placed in the neighbourhood of $b$-values at which the maxima have occurred. These samples are placed in successive scans. In the first scan the samples are placed in the left of the peaks, in the second scan the samples are to the right of the peaks in the modulus of the wavelet transform. This sequence of the scans is repeated until all the samples are taken, taking into care that the samples are not repeated. The final

algorithm is as follows-

Set $\Delta = 0$.

**Step 1:** Read the input signal $g[n]$ and compute the wavelet transform $W_{g,\psi}(2^j, k2^j)$, for j=1, 2, 3, 4.

**Step 2:** Find the local maxima in $|W_{g,\psi}(2^j, k2^j)|$ at each scale. Note down the $b$-co-ordinates at which the maxima occur.

**Step 3:** Find the number of samples allocated to each scale. If $N$ is the number of samples that have to be placed, then,
Number of samples allocated to scale 16 $= \frac{N}{16}$,
Number of samples allocated to scale 8 $= \frac{N}{8}$,
Number of samples allocated to scale 4 $= \frac{N}{4}$,
Number of samples allocated to scale 2 $= \frac{7N}{16}$.
$N$ is chosen to be a multiple of 16.

**Step 4:** Calculate the surplus at all scales. This surplus is denoted by $S_0$.

$$S_0 =$$

$$\begin{aligned}
&\mathrm{P_{os}}(\text{Number of samples allocated to Scale 2} - \text{Number of local maxima in } |\mathrm{W_{g,\psi}}(2, 2k)|) \\
+\ &\mathrm{P_{os}}(\text{Number of samples allocated to Scale 4} - \text{Number of local maxima in } |\mathrm{W_{g,\psi}}(4, 4k)|) \\
+\ &\mathrm{P_{os}}(\text{Number of samples allocated to Scale 8} - \text{Number of local maxima in } |\mathrm{W_{g,\psi}}(8, 8k)|) \\
+\ &\mathrm{P_{os}}(\text{Number of samples allocated to Scale 16} - \text{Number of local maxima in } |\mathrm{W_{g,\psi}}(16, 16k)|),
\end{aligned}$$

where,

$$P_{os}(x) \begin{cases} x & x \geq 0 \\ 0, & Otherwise \end{cases}$$

**Step 5:** If ($S_0 = 0$) then goto Step 15, else Number of samples allocated to scale 2 = Number of samples allocated to scale 2 + $S_0$.

$Surplus_1$ = Number of samples allocated to scale 2 - Number of local maxima in $|W_{g,\psi}(2, 2k)|$

$S_1 = P_{os}(Surplus_1)$

if ($Surplus_1$) > 0 then

( Number of samples allocated to scale 2 = Number of local maxima in $|W_{g,\psi}(2, 2k)|$)

If $S_1 = 0$ then goto Step 15.

Number of samples allocated to scale 4 =Number of samples allocated to scale 4 + $S_1$.

$Surplus_2$ = Number of samples allocated to scale 4 - Number of local maxima in $|W_{g,\psi}(4, 4k)|$

$S_2 = P_{os}(Surplus_2)$

if ($Surplus_2$) > 0 then ( Number of samples allocated to scale 4 = Number of local maxima in $|W_{g,\psi}(4, 4k)|$)

If $S_2 = 0$ then goto Step 15.

Number of samples allocated to scale 8 = Number of samples allocated to scale 8 + $S_2$.

$Surplus_3$ = Number of samples allocated to scale 8 - Number of local maxima in $|W_{g,\psi}(8, 8k)|$

$S_3 = P_{os}(Surplus_3)$

if ($Surplus_3$) > 0 then ( Number of samples allocated to scale 16 = Number of local maxima in $|W_{g,\psi}(16, 16k)|$), else goto Step 15.

**Step 6:** If ($Surplus_3$) > 0 then $Surplus = S_3$.

**Step 7:** $\Delta = \Delta + 1$

**Step 8:** $i = 1$, Let $N'$ be the number of samples picked upto this step.

**Step 9:** Let the points at which the samples, previously allocated, be picked at $b_i$. Check if $b_i - \Delta$ is same as any of the picked samples, if not, then, pick a sample at $b_i - \Delta$. $Surplus = Surplus - 1$. The overall surplus of samples is denoted by $Surplus$. If $Surplus = 0$ goto Step 15.

**Step 10:** $i = i + 1$, if $i < N'$ goto 9

**Step 11:** i=1, Let $N''$ be the number of samples picked upto this step. And let $b_i$ be the location of these samples.

**Step 12:** Check if $b_i + \Delta$ is same as any of the picked samples, if not, then, pick a sample at $b_i + \Delta$. $Surplus = Surplus - 1$. If $Surplus = 0$ goto Step 15.

**Step 13:** $i = i + 1$, if $i < N'$ goto 12

**Step 14:** If $Surplus > 0$ then goto Step 7.

**Step 15:** Pick the samples at the alloted number of points at each scale at the maxima of $|W_{g,\psi}(a,b)|$ and in the neighbourhood of these samples (if the algorithm passes through 7-15). Print all the picked samples in a file.

**Step 16:** These samples are used to reconstruct the original set of samples, these set of samples is denoted by $\hat{g}[n]$.

**Step 17:** Find the mean square error which is approximated by step wise approxima-

tion. Error = $\sum_{i=0}^{N_0-1}(g[i]-\hat{g}[i])^2$

**Step18:** Stop.

This algorithm is applied for $N_0 = 240$, and various values of $N$. The values of $N$ used are $N = 160, 176, 192, 208, 224, 240$. The simulation results are discussed in detail in the next section.

## 4.3 Simulation Results

The purpose of this section is to demonstrate the use of the presented algorithm for sampling a signal and for its reconstruction. Here we will discuss the sampling and reconstruction of four different signals. The number of samples considered for each of the signals are 160, 176, 192, 208, 224, 240. In each of the examples first we present the table of the reconstruction error, then the plots of the original signal and the reconstructed signal for various number of samples are presented and discussed.

**Example 4.1** The signal sampled in this example has been shown in Figure 4.1. In Table 4.1, the fractional mean square error for various numbers of samples is presented. The various numbers of samples for which the fractional errors have been tabulated are 160, 176, 192, 208, 224, 240. For each of the numbers the reconstructed signal and the fractional mean square error are obtained. To find the mean square error, the signal is reconstructed at the initial set of samples. Then, using the original sample set and the reconstructed set the fractional mean square error is found. It can be observed from the table, that, the fractional mean square error reduces as the number of samples increases.

| Figure label | Number of samples | fractional mean square error |
|---|---|---|
| Figure 5.2 | 160 | 0.245425 |
| Figure 5.3 | 176 | 0.226022 |
| Figure 5.4 | 192 | 0.144026 |
| Figure 5.5 | 208 | 0.127318 |
| Figure 5.6 | 224 | 0.006546 |
| | 240 | 0.000000 |

Table 4.1: Error-N for the original shown in Figure 4.1.

In Figure 4.2, the original signal and the reconstructed signal are plotted for the case when the signal, shown in Figure 4.1, is reconstructed using 160 samples. In Figure 4.3, the original signal and the reconstructed signal are plotted for the case when the signal,shown in Figure 4.1 is reconstructed using 176 samples. In Figure 4.4, the original signal and the reconstructed signal are plotted for the case when the signal, shown in Figure 4.1, is reconstructed using 192 samples. In Figure 4.5, the original signal and the reconstructed signal are plotted for the case when the signal, shown in Figure 4.1, is reconstructed using 208 samples. In Figure 4.6, the original signal and the reconstructed signal are plotted for the case when the signal, Figure 4.1, is reconstructed using 224 samples. As the number of samples used for reconstruction increase, the original and the reconstructed signals come closer. The fractional mean square error verses the number of samples is plotted in Figure 4.7.

**Example 4.2** The signal analysed in this example has been shown in Figure 4.8. In Table 4.2, the fractional mean square error for various numbers of samples is presented. The various numbers of samples for which the fractional errors have been tabulated are 160, 176, 192, 208, 224, 240. For each of the numbers the reconstructed signal and the fractional mean square error are obtained. To find the mean square error, the signal is

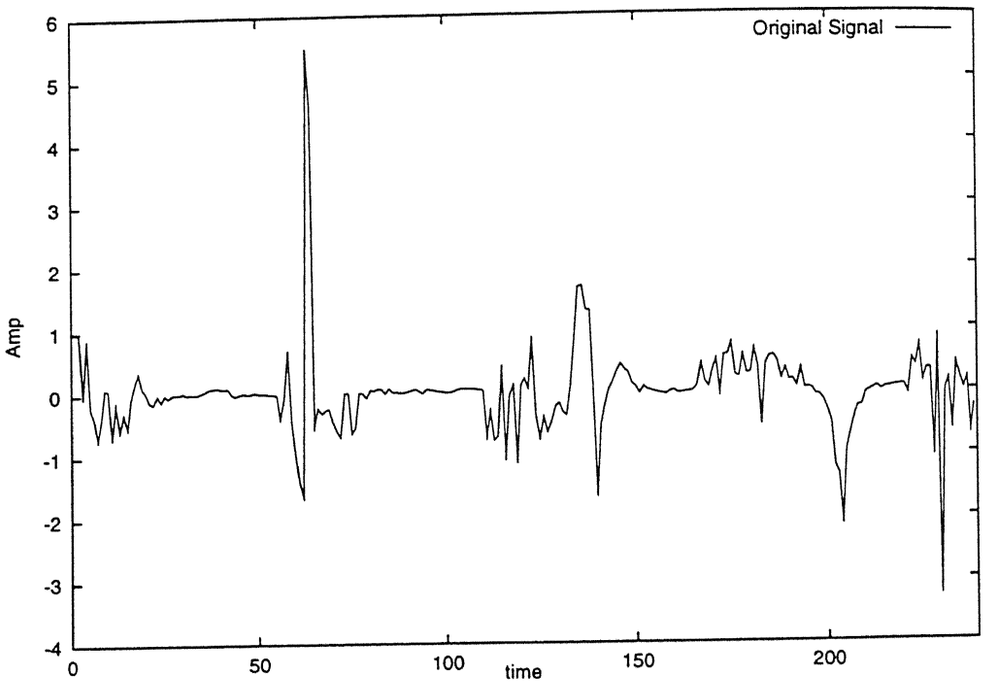


Figure 4.1: The signal analysed in the Example 4.1.

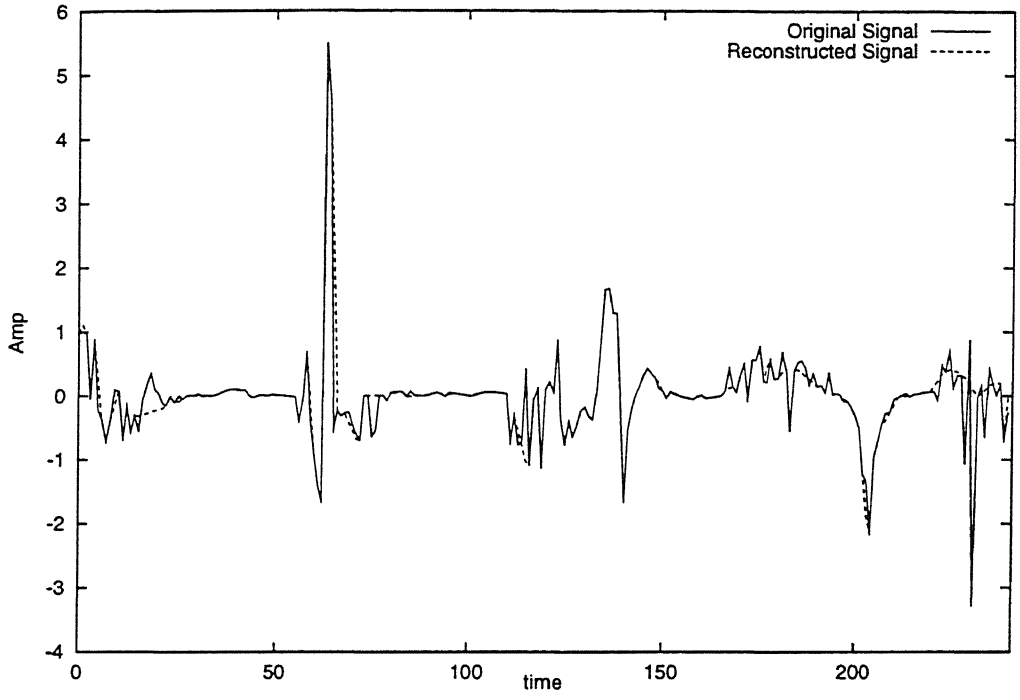


Figure 4.2: The original and the reconstructed signal for compression ratio equal to 0.6667. The original signal was sampled at 240 points, further only 160 samples are retained at nonuniform sampling instants and the signal is reconstructed at the initial 240 instants using the equation for reconstruction suggested in the section 4.1.

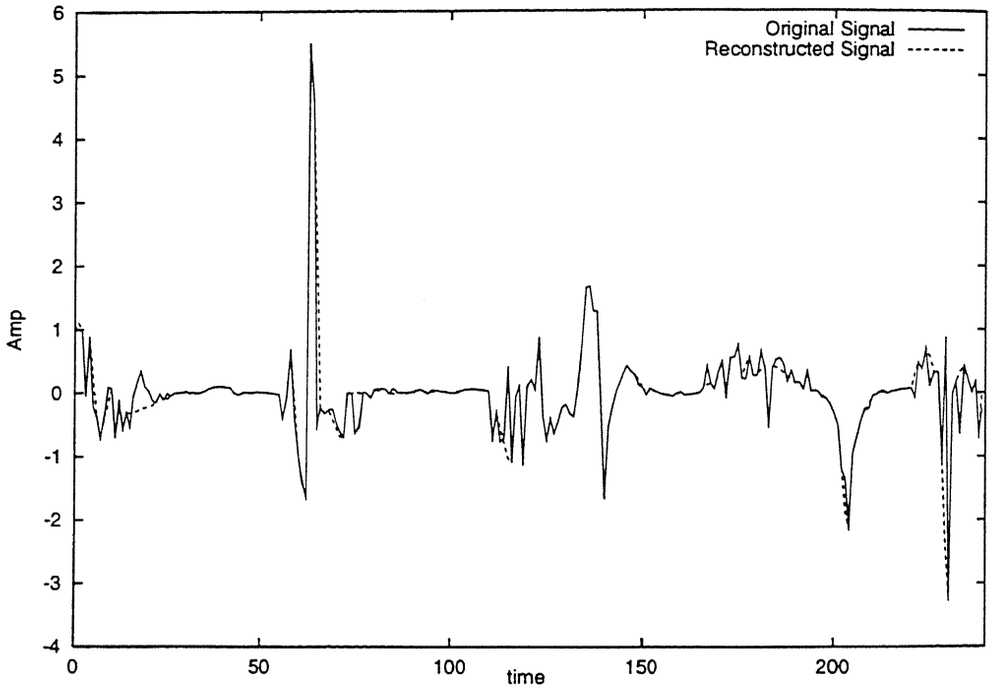


Figure 4.3: The original and the reconstructed signal for compression ratio equal to 0.7333. The original signal was sampled at 240 points, further only 176 samples are retained at nonuniform sampling instants and the signal is reconstructed at the initial 240 instants using the equation for reconstruction suggested in the section 4.1.

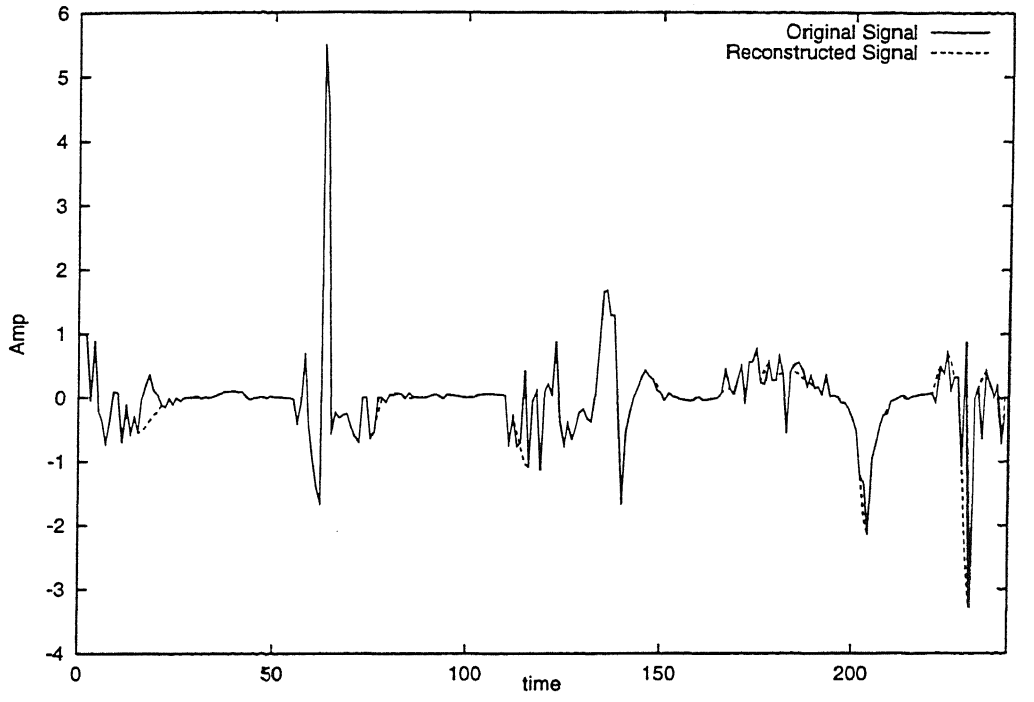


Figure 4.4: The original and the reconstructed signal for compression ratio equal to 0.8000. The original signal was sampled at 240 points, further only 192 samples are retained at nonuniform sampling instants and the signal is reconstructed at the initial 240 instants using the equation for reconstruction suggested in the section 4.1.

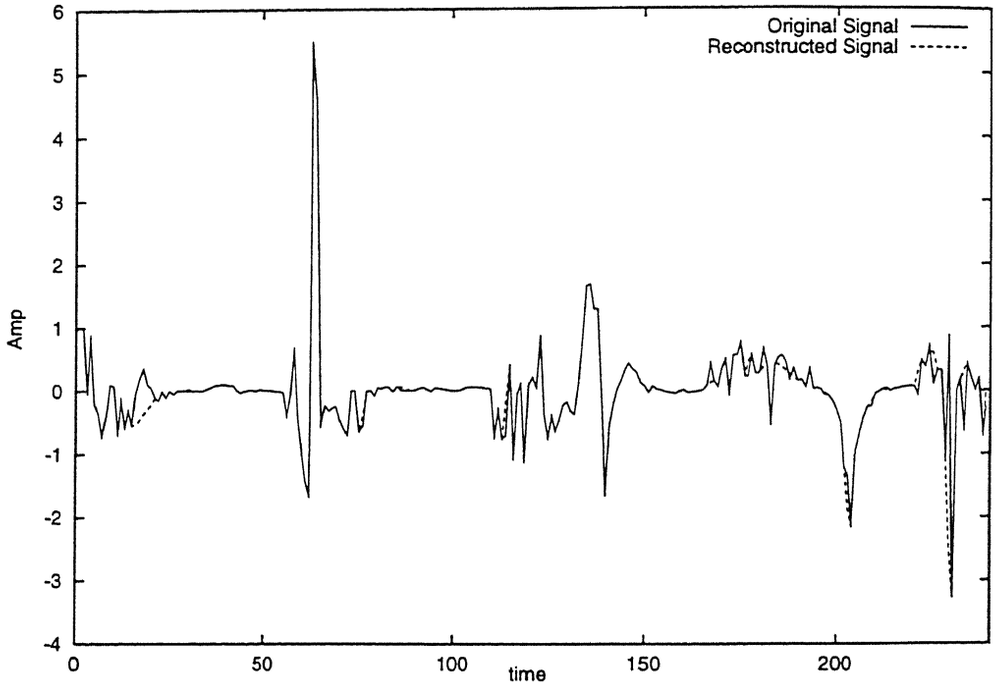


Figure 4.5: The original and the reconstructed signal for compression ratio equal to 0.8667. The original signal was sampled at 240 points, further, 208 points are retained at nonuniform sampling instants and the signal is reconstructed at the initial 240 instants using the equation for reconstruction suggested in the section 4.1.

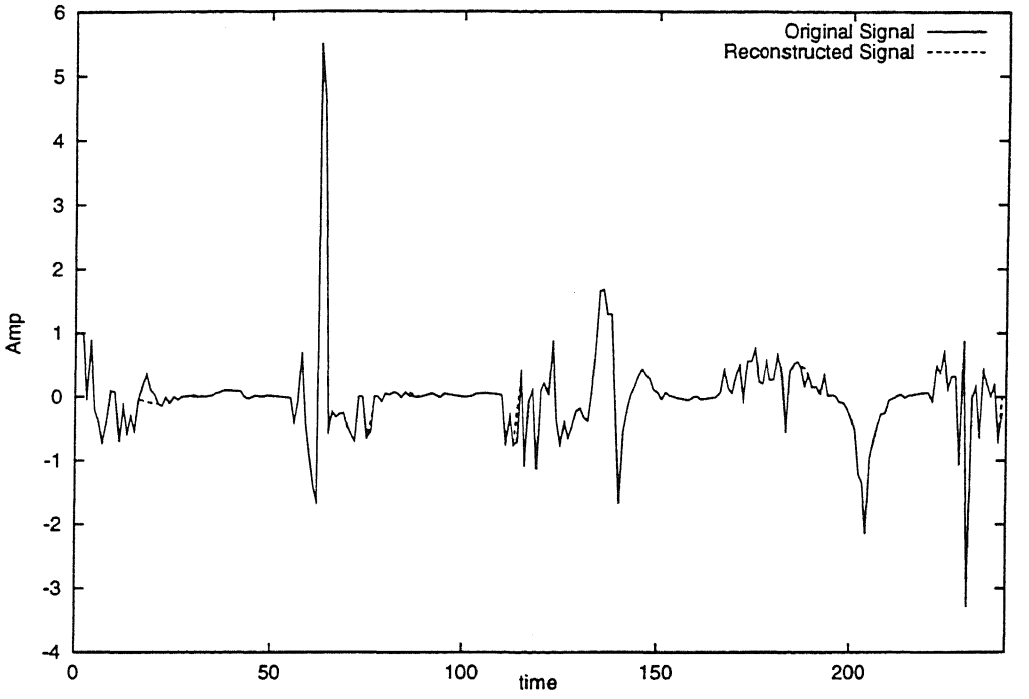


Figure 4.6: The original and the reconstructed signal for compression ratio equal to 0.9333. The original signal was sampled at 240 points, further, 224 points are retained at nonuniform sampling instants and the signal reconstructed at the initial 240 instants using the equation for reconstruction suggested in the section 4.1.

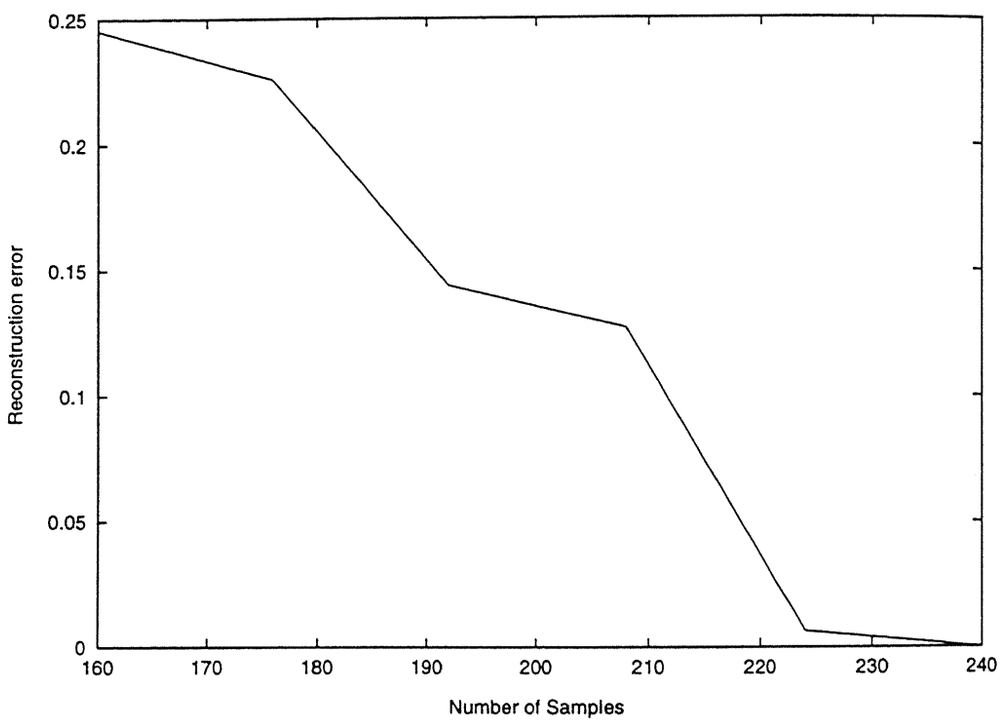


Figure 4.7: Fractional mean square reconstruction error verses the number of samples.

| Figure label | Number of samples | Fractional mean square error |
|---|---|---|
| Figure 5.9 | 160 | 0.034605 |
| Figure 5.10 | 176 | 0.025324 |
| Figure 5.11 | 192 | 0.016170 |
| Figure 5.12 | 208 | 0.016159 |
| Figure 5.13 | 224 | 0.000065 |
| | 240 | 0.0 |

Table 4.2: Error-$N$ for the original signal shown in Figure 4.8.

reconstructed at the initial set of samples. Then, using the original sample set and the reconstructed set the fractional mean square error is found. It can be observed from the table, that, the fractional mean square error reduces as the number of samples increases.

In Figure 4.9, the original signal and the reconstructed signal are plotted for the case when the signal, shown in Figure 4.8, is reconstructed using 160 samples. In Figure 4.10, the original signal and the reconstructed signal are plotted for the case when the signal,shown in Figure 4.8 is reconstructed using 176 samples. In Figure 4.11, the original signal and the reconstructed signal are plotted for the case when the signal, shown in Figure 4.8, is reconstructed using 192 samples. In Figure 4.12, the original signal and the reconstructed signal are plotted for the case when the signal, shown in Figure 4.8, is reconstructed using 208 samples. In Figure 4.13, the original signal and the reconstructed signal are plotted for the case when the signal, Figure 4.8, is reconstructed using 224 samples. As the number of samples used for reconstruction increase, the original and the reconstructed signals come closer. The fractional mean square error verses the number of samples used for signal reconstruction is plotted in Figure 4.14.

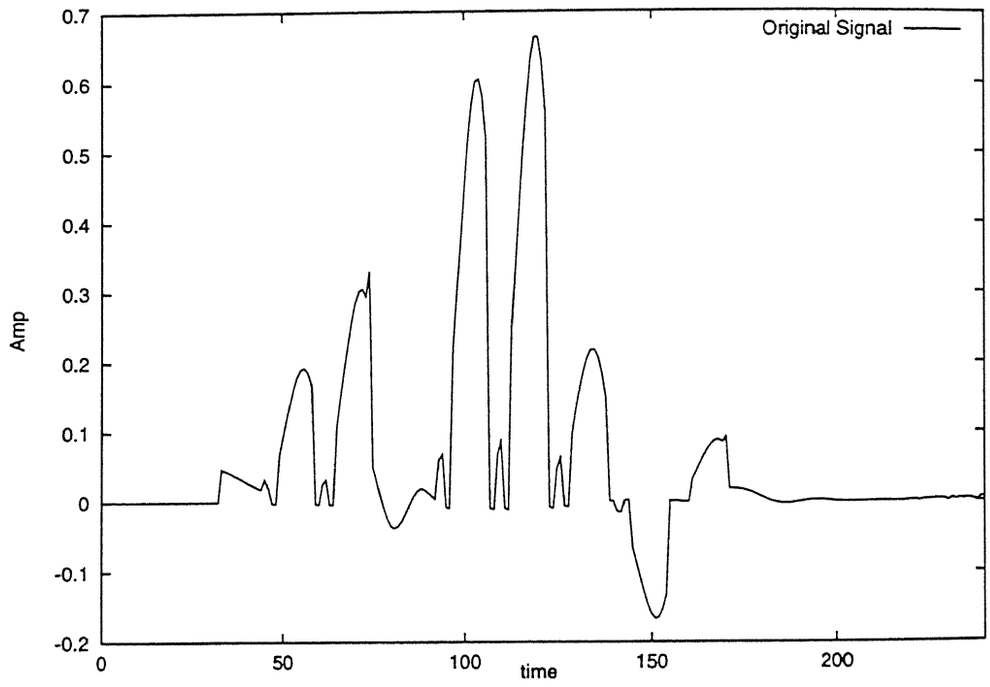


Figure 4.8: The signal analysed in Example 4.2.

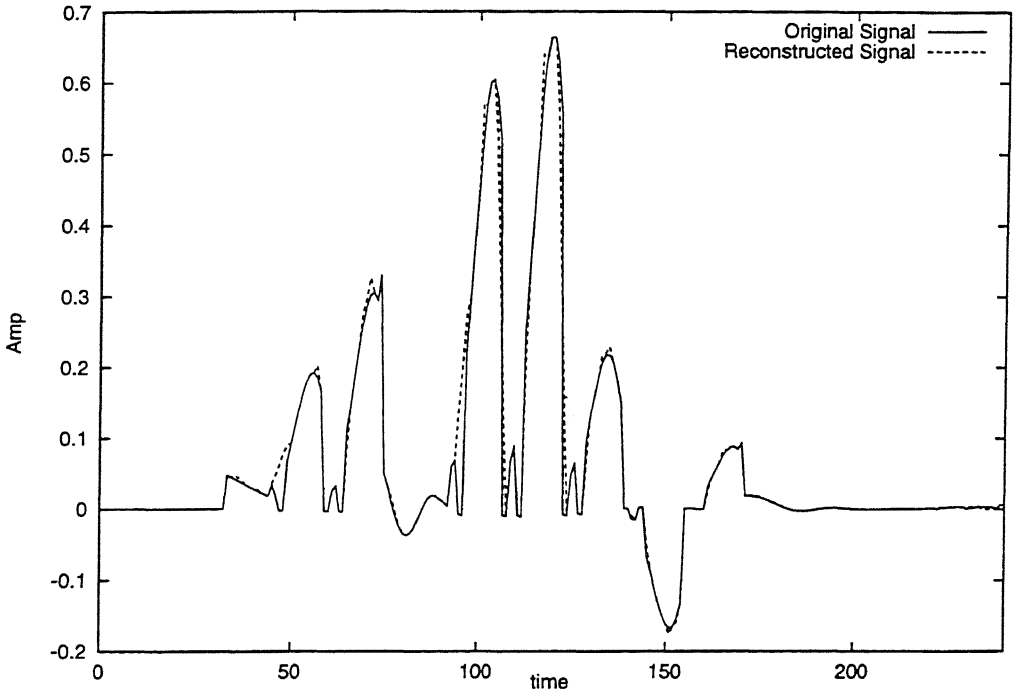


Figure 4.9: The original and the reconstructed signal for compression ratio equal to 0.6667. The original signal was sampled at 240 points, further only 160 samples are retained at nonuniform sampling instants and the signal is reconstructed at the initial 240 instants using the equation for reconstruction suggested in the section 4.1.

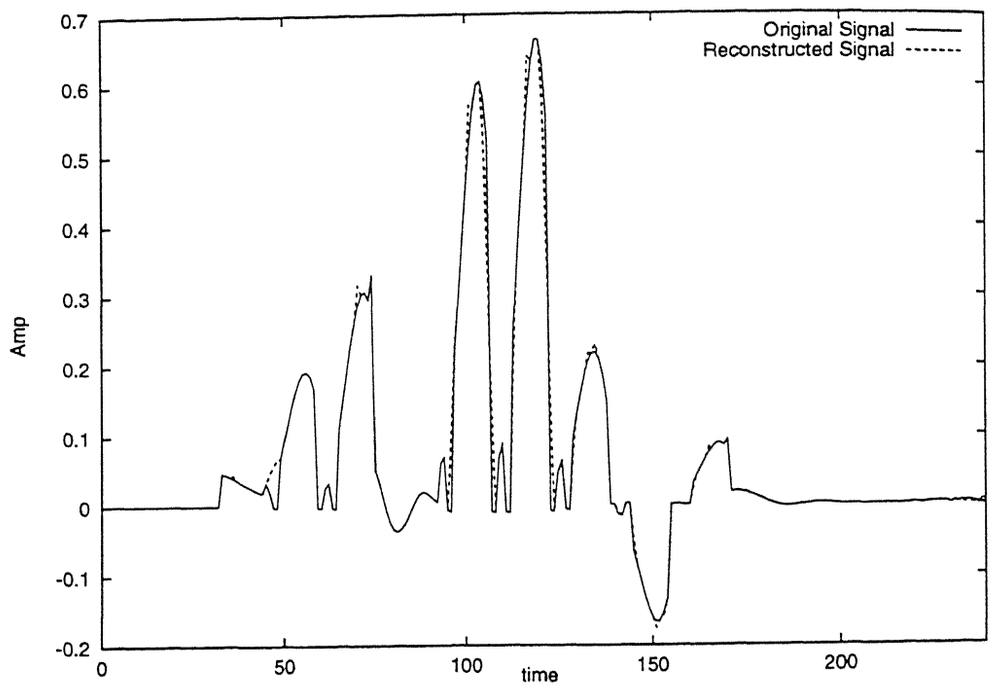


Figure 4.10: The original and the reconstructed signal for compression ratio equal to 0.7333. The original signal was sampled at 240 points, further only 176 samples are retained at nonuniform sampling instants and the signal is reconstructed at the initial 240 instants using the equation for reconstruction suggested in the section 4.1.

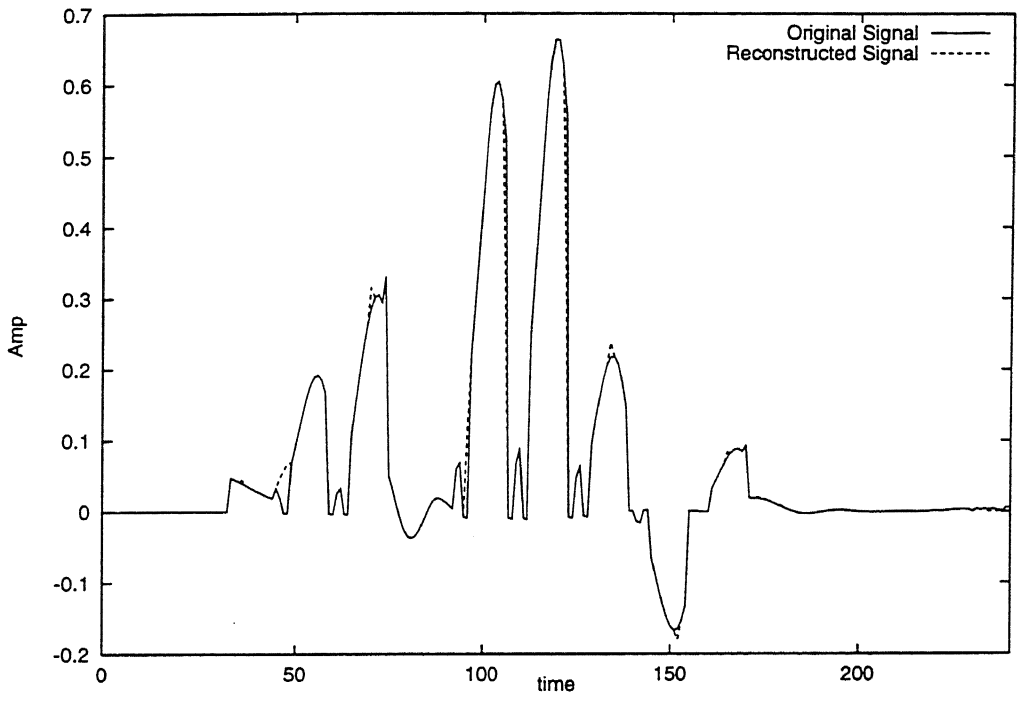


Figure 4.11: The original and the reconstructed signal for compression ratio equal to 0.8000. The original signal was sampled at 240 points, further only 192 samples are retained at nonuniform sampling instants and the signal is reconstructed at the initial 240 instants using the equation for reconstruction suggested in the section 4.1.

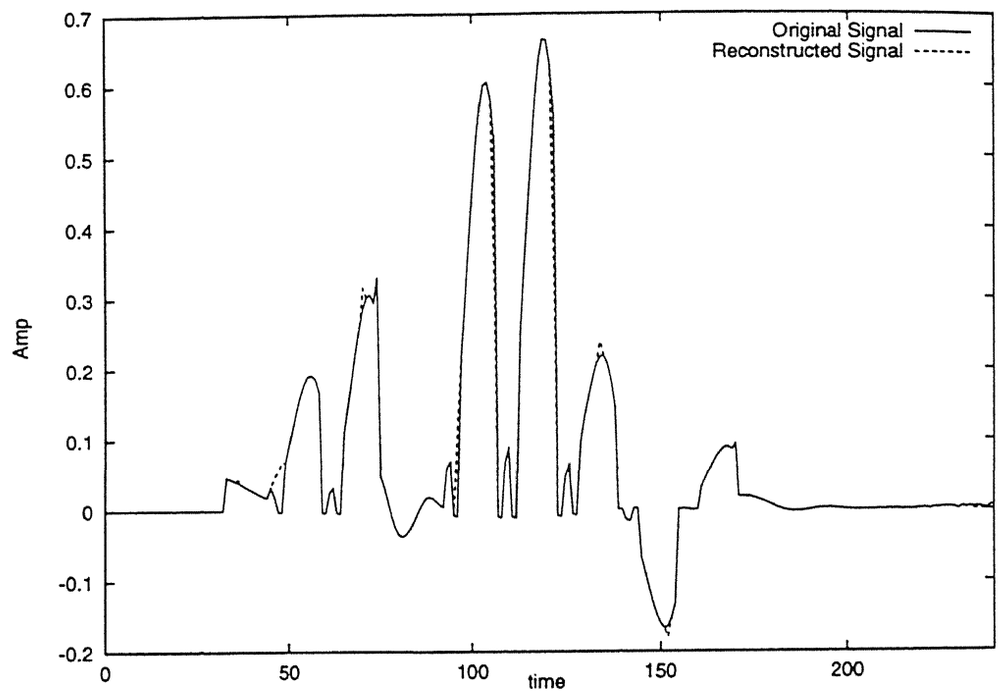


Figure 4.12: The original and the reconstructed signal for compression ratio equal to 0.8667. The original signal was sampled at 240 points, further, 208 points are retained at nonuniform sampling instants and the signal is reconstructed at the initial 240 instants using the equation for reconstruction suggested in the section 4.1.

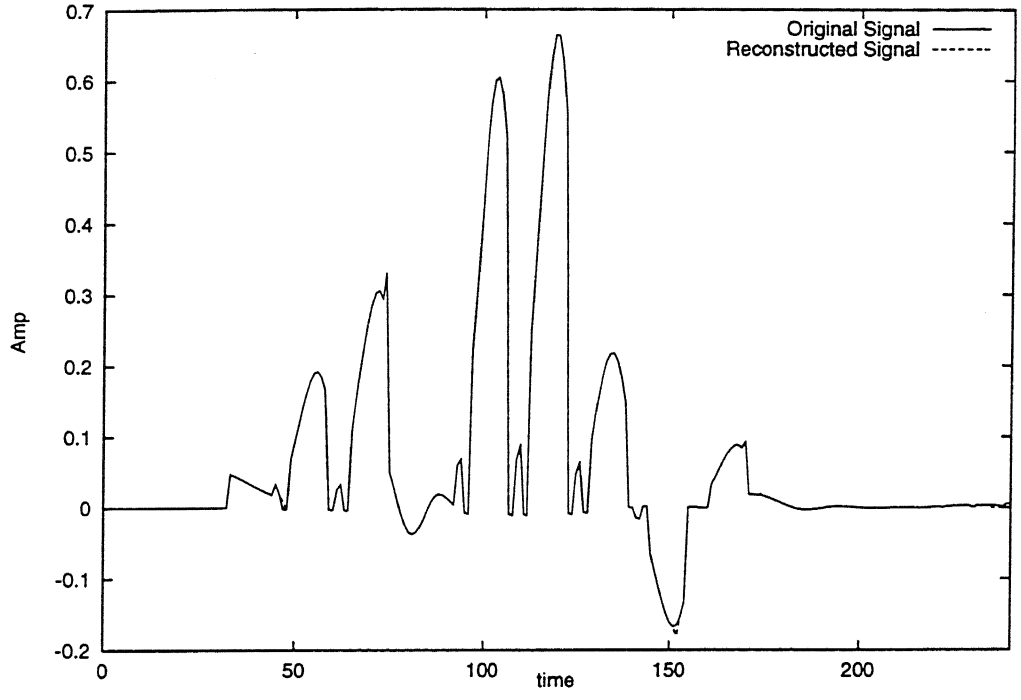


Figure 4.13: The original and the reconstructed signal for compression ratio equal to 0.9333. The original signal was sampled at 240 points, further, 224 points are retained at nonuniform sampling instants and the signal is reconstructed at the initial 240 instants using the equation for reconstruction suggested in the section 4.1.

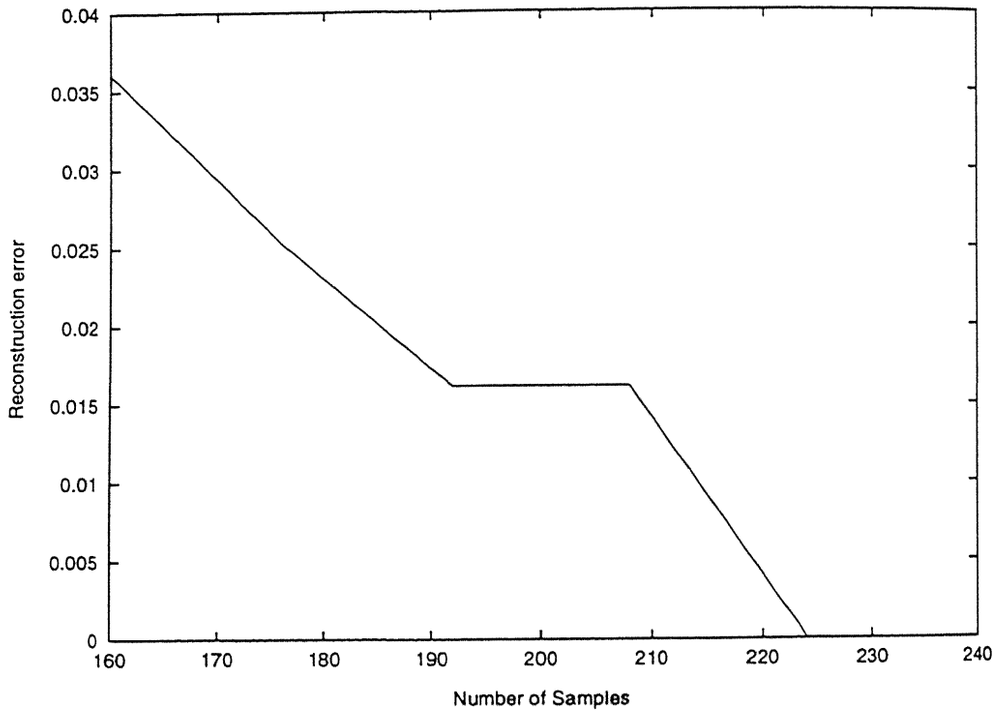


Figure 4.14: Error verses $n$ for the signal shown in Figure 4.8.

**Example 4.3** The signal analysed in this example is an ECG signal sampled at a rate of 200 samples per second and the 240 samples of this signal are shown in Figure 4.15. In Table 4.3, the fractional mean square error for various number of samples is presented. The various numbers of samples for which the fractional errors have been tabulated are 160, 176, 192, 208, 224, 240. For each of the numbers the reconstructed signal and the fractional mean square error are obtained. To find the mean square error, the signal is reconstructed at the initial set of samples. Then, using the original sample set and the reconstructed set the fractional mean square error is found. It can be observed from the table, that, the fractional mean square error reduces as the number of samples increases.

In Figure 4.16, the original signal and the reconstructed signal are plotted for the case when the signal, shown in Figure 4.15, is reconstructed using 160 samples. In Figure 4.17, the original signal and the reconstructed signal are plotted for the case when the signal, shown in Figure 4.15 is reconstructed using 176 samples. In Figure 4.18, the original signal and the reconstructed signal are plotted for the case when the signal, shown in Figure 4.15, is reconstructed using 192 samples. In Figure 4.19, the original signal and the reconstructed signal are plotted for the case when the signal, shown in Figure 4.15, is reconstructed using 208 samples. In Figure 4.20, the original signal and the reconstructed signal are plotted for the case when the signal, Figure 4.15, is reconstructed using 224 samples. As the number of samples used for reconstruction increase, the original and the reconstructed signals come closer. The fractional mean square error verses the number of samples used for signal reconstruction has been plotted in Figure 4.21.

**Example 4.4** The signal analysed in this example is an EMG signal sampled at a rate of 2000 samples per second and 240 samples of the signal are shown in Figure 4.22. In

| Figure label | Number of samples | Fractional mean square error |
|---|---|---|
| Figure 5.16 | 160 | 0.029936 |
| Figure 5.17 | 176 | 0.028127 |
| Figure 5.18 | 192 | 0.024858 |
| Figure 5.19 | 208 | 0.024396 |
| Figure 5.20 | 224 | 0.005549 |
| | 240 | 0.0 |

Table 4.3: Error-$N$ for the original shown in figure 4.15.

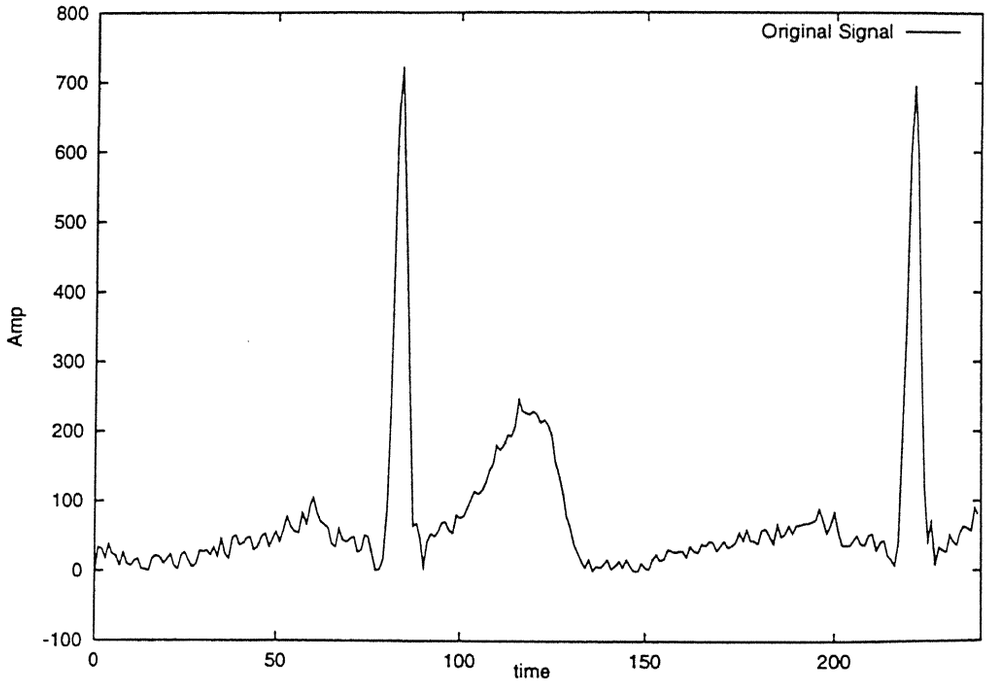


Figure 4.15: The signal analysed in example 4.3.

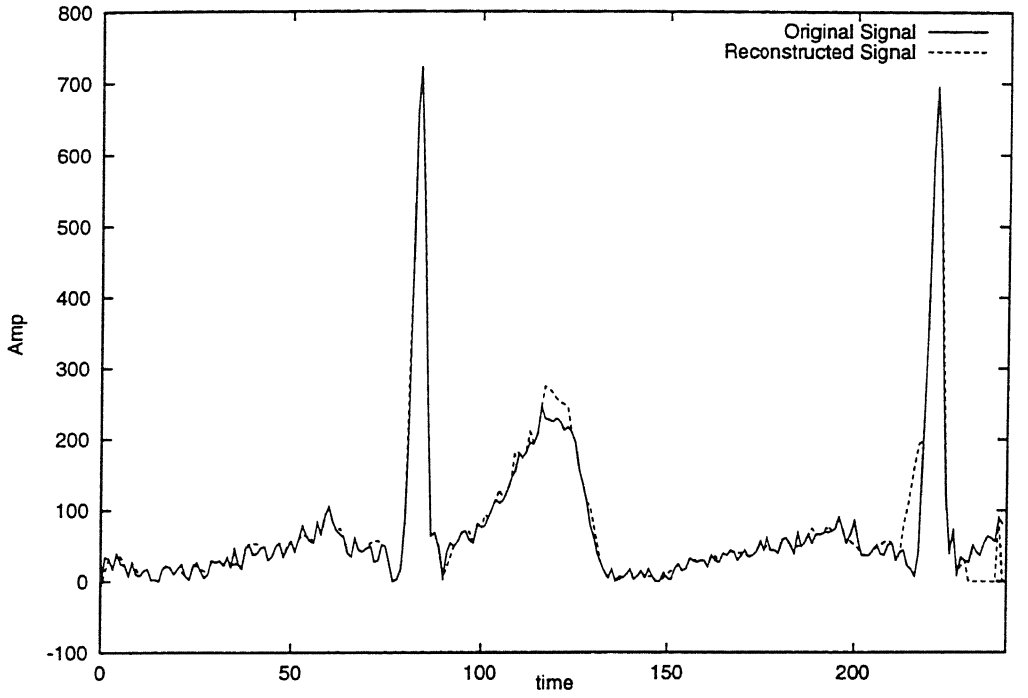


Figure 4.16: The original and the reconstructed signal for compression ratio equal to 0.6667. The original signal was sampled at 240 points, further only 160 samples are retained at nonuniform sampling instants and the signal is reconstructed at the initial 240 instants using the equation for reconstruction suggested in the section 4.1.

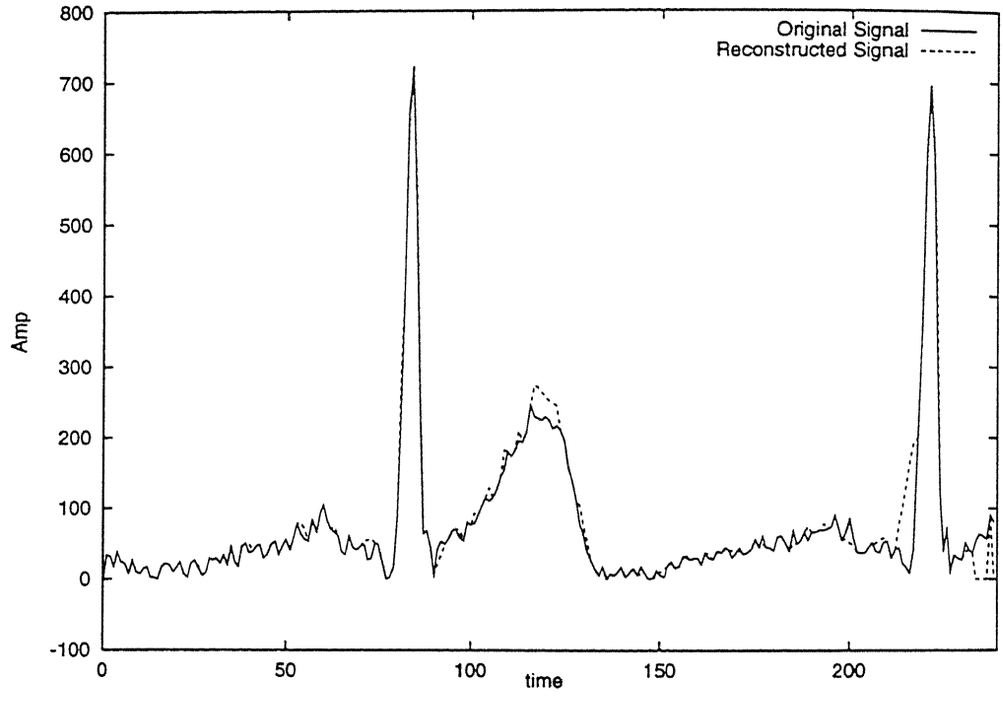


Figure 4.17: The original and the reconstructed signal for compression ratio equal to 0.7333. The original signal was sampled at 240 points, further only 176 samples are retained at nonuniform sampling instants and the signal is reconstructed at the initial 240 instants using the equation for reconstruction suggested in the section 4.1.

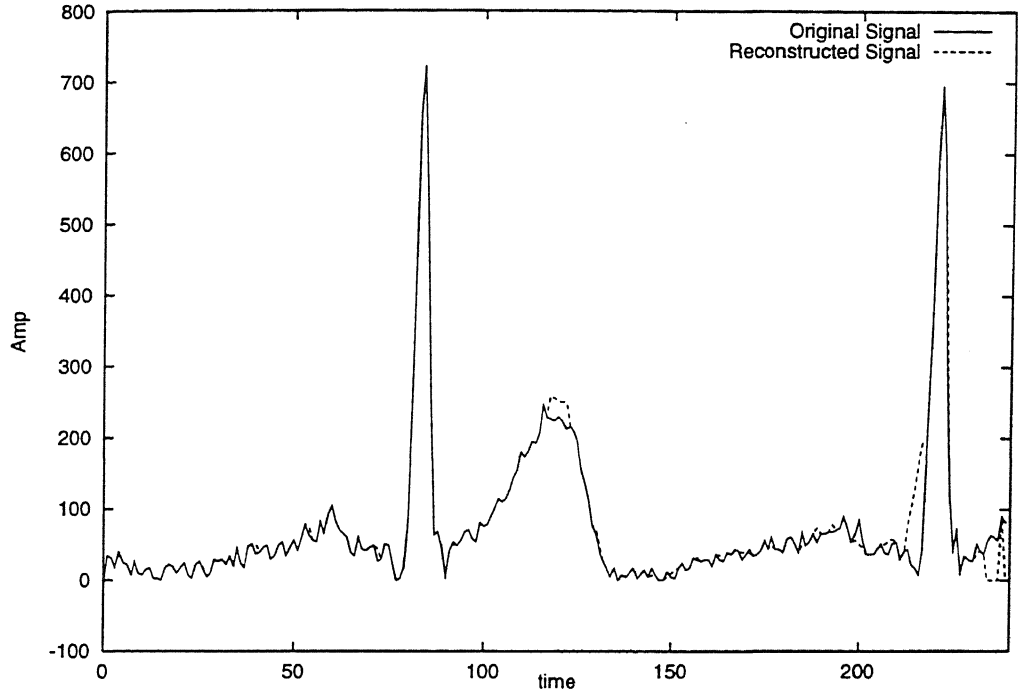


Figure 4.18: The original and the reconstructed signal for compression ratio equal to 0.8000. The original signal was sampled at 240 points, further only 192 samples are retained at nonuniform sampling instants and the signal is reconstructed at the initial 240 instants using the equation for reconstruction suggested in the section 4.1.

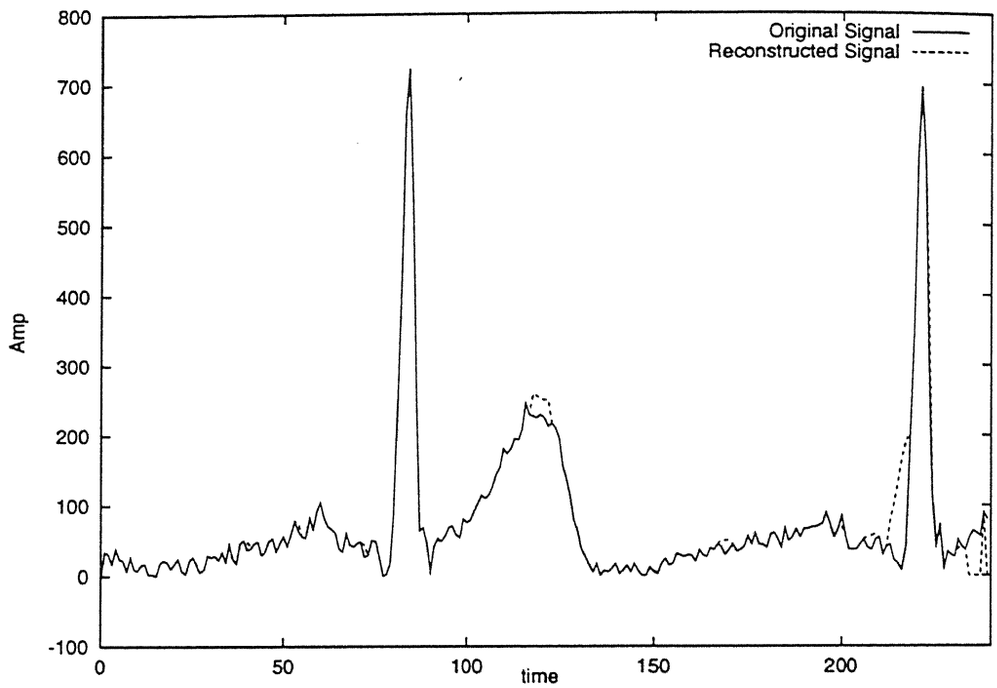


Figure 4.19: The original and the reconstructed signal for compression ratio equal to 0.8667. The original signal was sampled at 240 points, further, 208 points are retained at nonuniform sampling instants and the signal is reconstructed at the initial 240 instants using the equation for reconstruction suggested in the section 4.1.

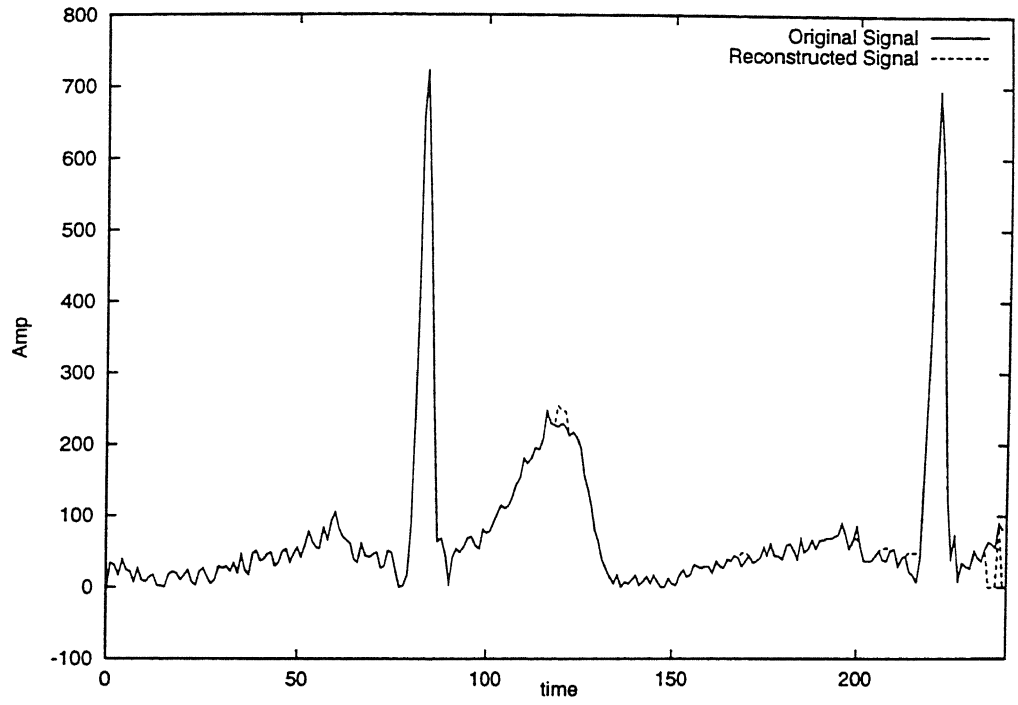


Figure 4.20: The original and the reconstructed signal for compression ratio equal to 0.9333. The original signal was sampled at 240 points, further, 224 points are retained at nonuniform sampling instants and the signal is reconstructed at the initial 240 instants using the equation for reconstruction suggested in the section 4.1.

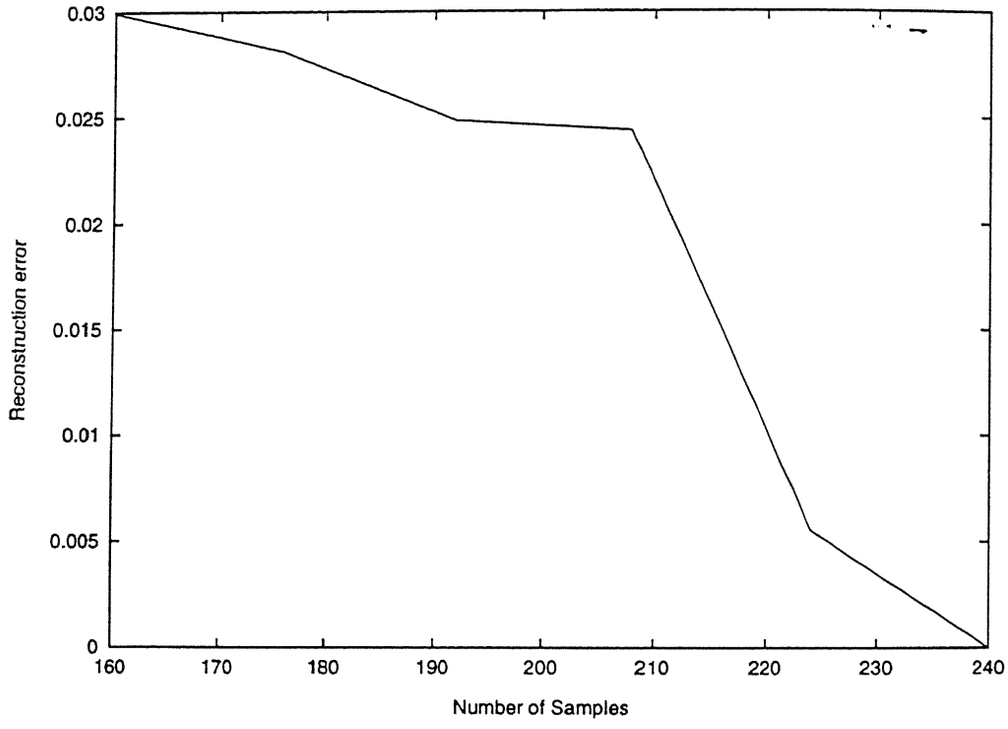


Figure 4.21: Error-$N$ for the signal in Figure 4.15.

Table 4.4, the fractional mean square error for various number of samples is presented. The various numbers of samples for which the fractional errors have been tabulated are 160, 176, 192, 208, 224, 240. For each of the numbers the reconstructed signal and the fractional mean square error are obtained. To find the mean square error, the signal is reconstructed at the initial set of samples. Then, using the original sample set and the reconstructed set the fractional mean square error is found. It can be observed from the table, that, the fractional mean square error reduces as the number of samples increases.

In Figure 4.23, the original signal and the reconstructed signal are plotted for the case when the signal, shown in Figure 4.22, is reconstructed using 160 samples. In Figure 4.24, the original signal and the reconstructed signal are plotted for the case when the signal, shown in Figure 4.22 is reconstructed using 176 samples. In Figure 4.25, the original signal and the reconstructed signal are plotted for the case when the signal, shown in Figure 4.22, is reconstructed using 192 samples. In Figure 4.26, the original signal and the reconstructed signal are plotted for the case when the signal, shown in Figure 4.22, is reconstructed using 208 samples. In Figure 4.27, the original signal and the reconstructed signal are plotted for the case when the signal, Figure 4.22, is reconstructed using 224 samples. As the number of samples used for reconstruction increase, the original and the reconstructed signals come closer. The fractional mean square error verses the number of samples used for signal reconstruction has been plotted in Figure 4.28.

| Figure label | Number of samples | Fractional mean square error |
|---|---|---|
| Figure 5.13 | 160 | 0.04919 |
| Figure 5.24 | 176 | 0.035941 |
| Figure 5.25 | 192 | 0.033553 |
| Figure 5.26 | 208 | 0.029851 |
| Figure 5.27 | 224 | 0.023691 |
| | 240 | 0.0 |

Table 4.4: Error-$N$ for the original shown in figure 4.22.

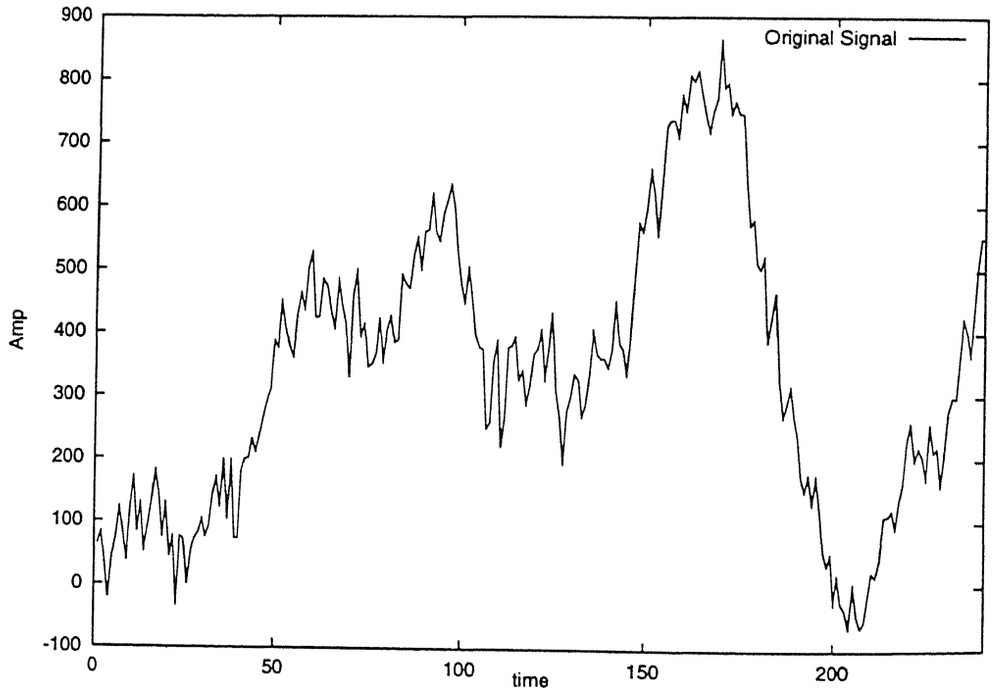


Figure 4.22: The signal analysed in example 4.4.

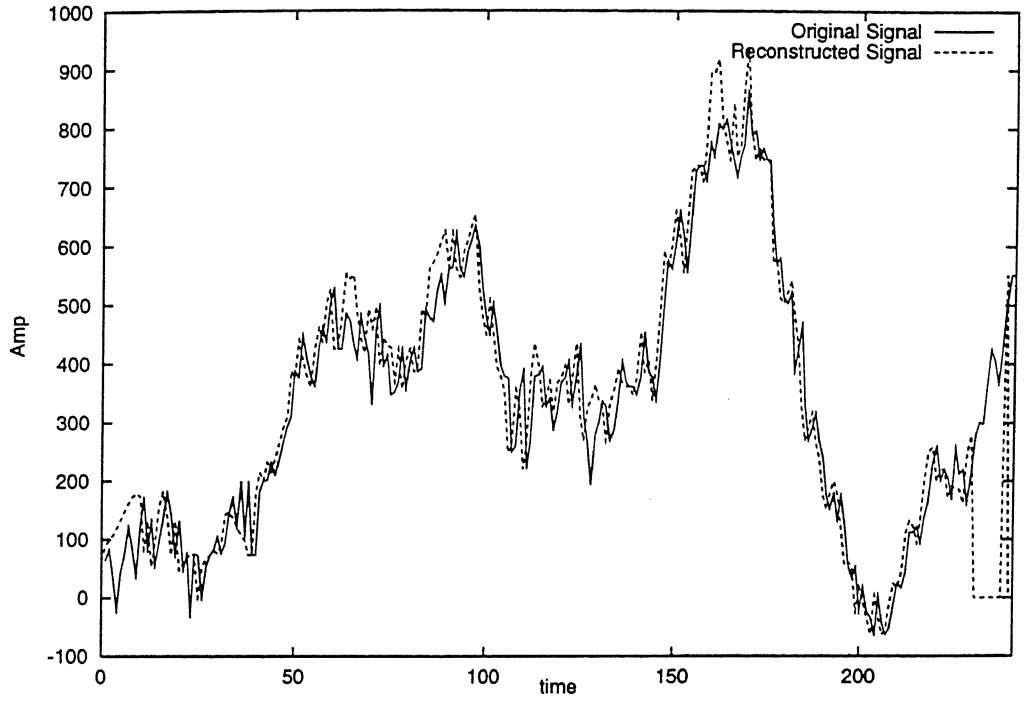


Figure 4.23: The original and the reconstructed signal for compression ratio equal to 0.6667. The original signal was sampled at 240 points, further only 160 samples are retained at nonuniform sampling instants and the signal is reconstructed at the initial 240 instants using the equation for reconstruction suggested in the section 4.1.

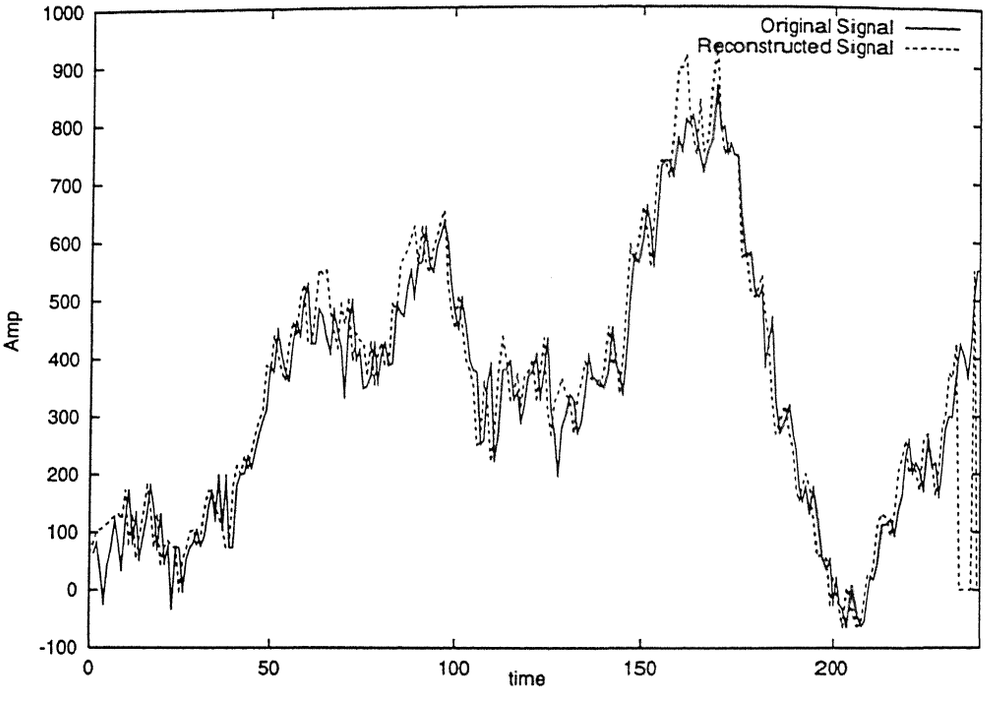


Figure 4.24: The original and the reconstructed signal for compression ratio equal to 0.7333. The original signal was sampled at 240 points, further only 176 samples are retained at nonuniform sampling instants and the signal is reconstructed at the initial 240 instants using the equation for reconstruction suggested in the section 4.1.

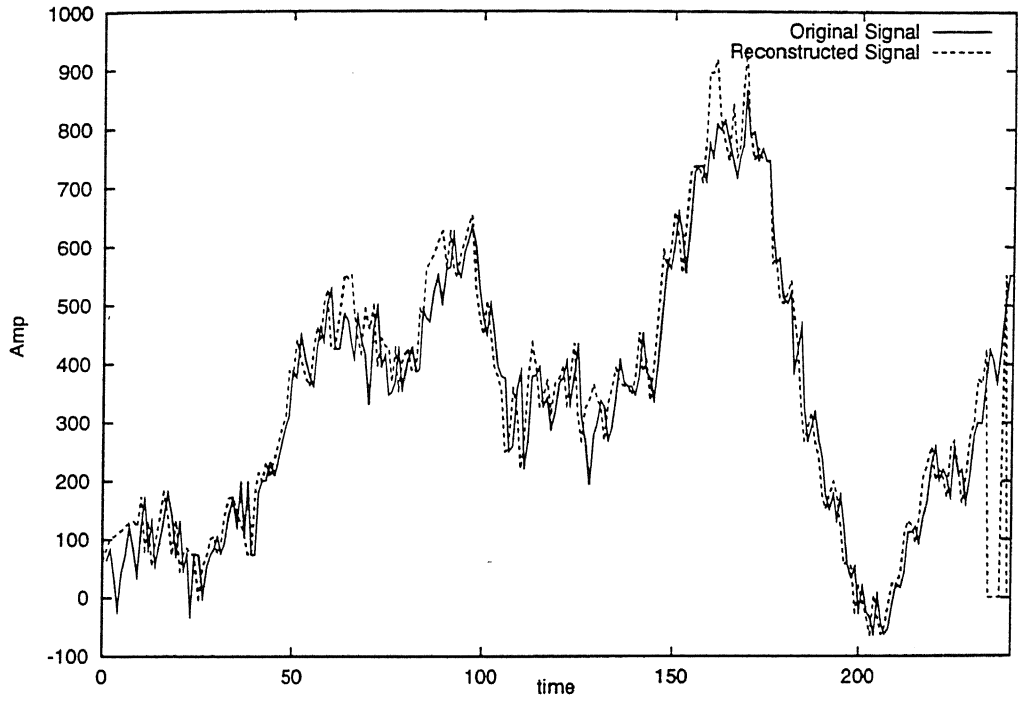


Figure 4.25: The original and the reconstructed signal for compression ratio equal to 0.8000. The original signal was sampled at 240 points, further only 192 samples are retained at nonuniform sampling instants and the signal is reconstructed at the initial 240 instants using the equation for reconstruction suggested in the section 4.1.

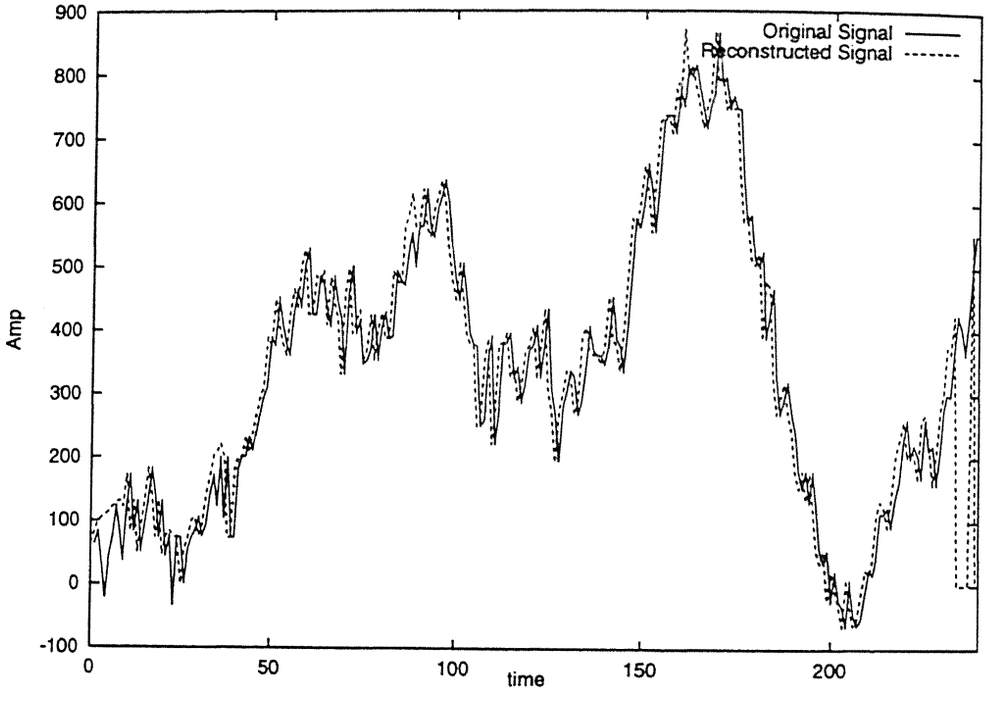


Figure 4.26: The original and the reconstructed signal for compression ratio equal to 0.8667. The original signal was sampled at 240 points, further, 208 points are retained at nonuniform sampling instants and the signal is reconstructed at the initial 240 instants using the equation for reconstruction suggested in the section 4.1.

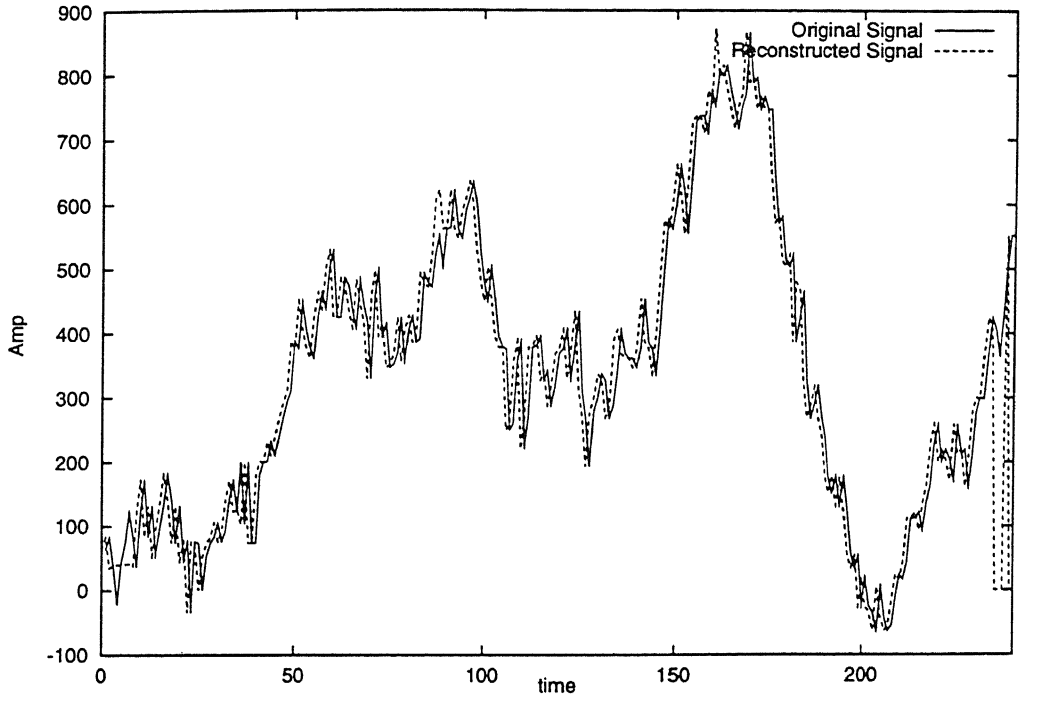


Figure 4.27: The original and the reconstructed signal for compression ratio equal to 0.9333. The original signal was sampled at 240 points, further, 224 points are retained at nonuniform sampling instants and the signal is reconstructed at the initial 240 instants using the equation for reconstruction suggested in the section 4.1.

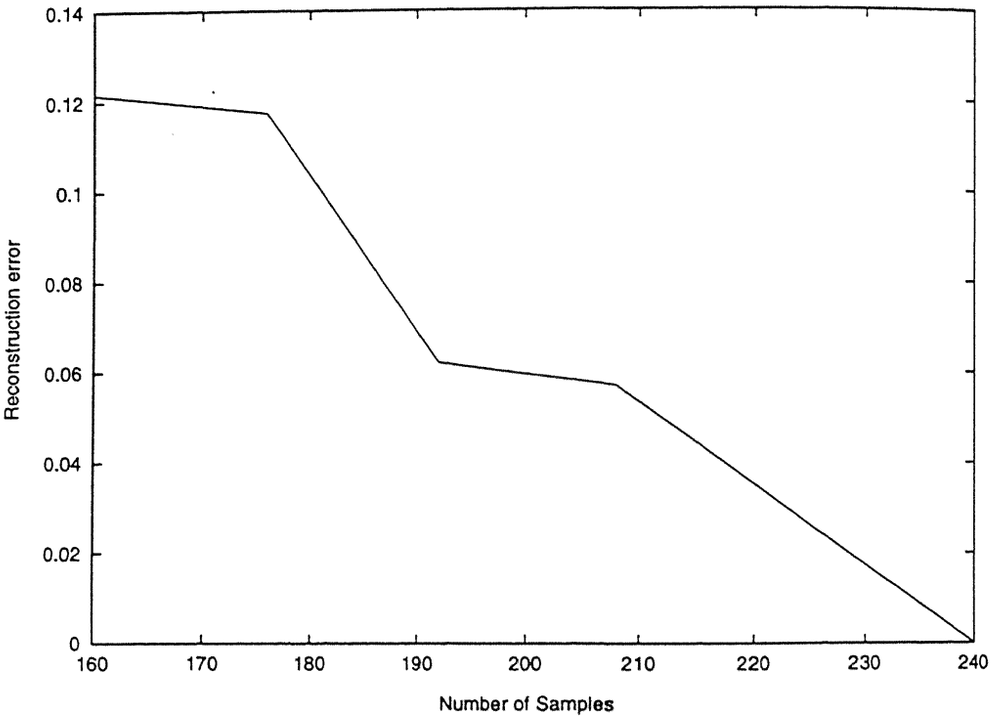


Figure 4.28: Error-$N$ for the signal in Figure 4.22.

There are time instants in the interpolated signal, when the reconstructed signal has sharp deviations from the original signal, this has been caused due to the sharp decay in the exponentials. In the simulation examples given in the chapter, the decaying exponentials are used for interpolation. Even piecewise linear interpolation can be used; the simulation result when the piecewise linear interpolation is used for the ECG signal given in Example 4.3 is given in the Appendix A. It can be observed from the simulations presented in the Appendix A, that piecewise linear interpolation is better suited than the interpolation using decaying exponentials under these conditions. However more extensive studies are needed to ascertain the combination of the best wavelet basis and best interpolation.

## 4.4 Conclusions

In this chapter an algorithm for optimal sample placement for time-limited signals is presented. The algorithm utilises the excellent time-scale localisation properties of the wavelet transforms. The sampling algorithm developed here is based on the observation that if the error in the transformed domain is bounded, then the error in the time domain also gets bounded.

In section 4.1, the problem attempted in the chapter is formulated. The conditions imposed on the type of interpolation also has been discussed. It is assumed that the interpolation has been done by functions which are local, further, the interpolation is such that the value of the interpolated signal is equal to the sample value at the sampling instant. In this chapter, the asymmetric decaying exponentials are used for interpolation. The decay of these functions are set, such that, their value is one at the sampling instant but at the neighbouring instants it is less than $\epsilon$, where $\epsilon$ is set to a

very small value.

In section 4.2, theorems have been presented, which give the bounds on the fractional mean square error. It can be inferred from the theorems, that the bound on the fractional mean square error is relatively more sensitive to the fractional mean square error in the transformed domain, at lower scales. Therefore, to make the fractional mean square error smaller the error in the transformed domain should be made relatively more small at lower scales. Another observation that has been made is that, the fractional mean square error in the transformed domain can be made small by placing the samples at those points in the transformed domain, at which the wavelet transform maxima occur. These are the guidelines using which a sampling strategy is developed in the section 4.3.

The algorithm proceeds by first sampling the signal at the highest possible rate, in our case we always take 240 samples of the signal, then the multiresolution analysis is used to find the wavelet transform of the signal. Then the samples are picked in the time domain at a value denoted by $t_i$, if the wavelet transform attains maximum in the transformed domain at $t_i$. This gives the initial set of samples, if all the maxima are exhausted and still samples can be taken then rest of the samples are taken in the neighbourhood of the samples in the initial set. Using the optimal samples the original set of samples is reconstructed using an interpolation method. Certain conditions on the interpolation methods to be used have also been placed. These condition are-

- The interpolation method should be such that, at the known values of the signal the interpolated value should come out to be same as the known value.

- The form of the interpolating function should have the following form-

$$\hat{g}(t) = \sum_k g(t_k)\, h_k\, (t - t_k, t_{k-1}, t_{k+1}).$$

For the first condition to be satisfied we require-

$$h_k(0, t_{k-1}, t_{k+1}) = 1,\ h_k(t_j - t_k, t_{k-1}, t_{k+1}) = 0,\ \text{for } j \neq k. \quad (4.15)$$

Simulation results which demonstrate the algorithm have been presented. In the optimal sampling strategy evolved here the signal to be sampled is initially at the highest possible rate, then the required number of samples are picked out of the original set of samples. The number of samples to be picked is decided by the compression ratio required.

# Chapter 5

# A Region Based Sampling Strategy Using Wavelet Transforms

In the sampling strategy proposed in the previous chapter, the samples fall nonuniformly, therefore all the sampling instants also have to be stored. To eliminate the requirement of sampling instant storage, another problem is formulated in this chapter, in which, the signal is partitioned and sampling rate is varied depending upon the local variations.

In this chapter, a sampling strategy based on the local variations is proposed. The problem formulated here consists of distributing a fixed number of samples into various segments depending upon the variations in them. The signals considered here are time-limited. The strategy proceeds by first segmenting the signal using the wavelet transformed domain description, subsequently sampling in each segment is done depending upon its scale-limit. It has been established that, under reasonable assumptions, the number of samples in any region is inversely proportional to the scale-limit.

This result has been used to develop a region based signal sampling algorithm.

## 5.1 Introduction

As already discussed in Chapter 2, in conventional signal processing, signals are sampled uniformly at twice the bandwidth[Sha49]. In the absence of any information about the bandwidth of the signal, an antialiasing filter is used and sampling is done at the Nyquist rate. However, when the estimate of the bandwidth of the antialiasing filter is not known then, it becomes very difficult to do sampling. Under these conditions arbitrarily high rates of sampling are used. However, both in the event of the availability and non-availability of the information about the bandwidth, the sampling is done uniformly. In this chapter, an alternative approach to sampling of time-limited signals is suggested. Here a sampling strategy is evolved, in which, the rate of sampling adapts to the local variations of the signal. This essentially leads to a nonuniform sampling problem.

Attempts of similar kind have been made [SA94],[MGCH88],[BdT88]. Most of these are directed towards signal and image compression applications. The problem formulated here consists of segmenting a given signal depending upon its local variations and then distributing a fixed number of samples optimally, across the segments. In the algorithm evolved here, the given signal is segmented depending upon a variation measure called scale-limitedness, and then a fixed number of samples are distributed into the partitions depending upon their respective scale-limits.

Scale-limitedness is used as a measure of variation, rather than using band-limitedness, because it has the ability to characterise local variations. The concept of scale-

limitedness with reference to wavelet transforms has already been initiated in Chapter 3. Scale-limitedness is defined as the scale value below which the wavelet transform coefficients are zero. In wavelet transform, a signal is decomposed into various scales and shifts. The coefficients corresponding to smaller scale values indicate the relatively faster varying component present in the signal. Since wavelets have energy concentrated for a finite duration, it is appropriate to use wavelet transforms for analysing practical signals (time-limited signals).

The wavelet transform of a signal is the inner product between the signal and shifted, scaled versions of a function called the mother wavelet. In practice, only the samples of the signal to be analysed are known. The approximation of the signal can be found by passing the sequence through a bank of filters[Mal89]. Algorithms based on this concept provide a method of representing a discrete sequence in terms of the wavelet transform values at scales $2^j$ and the corresponding shifts $2^j\ k$. Using the approximation sequence at any stage and the transforms (Detail signals) at the previous stages , the original sample sequence can be reconstructed.

Due to the above mentioned scheme, the algorithm for suboptimal sampling developed here starts by sampling the incoming signal at an arbitrary high rate, then retaining only the required number of samples in each partition. An algorithm for segmenting the signal is also presented.

In section 5.2, the problem has been formulated. In section 5.3, the algorithms for the segmenting and sampling are given. The simulation results are given in section 5.4. The conclusions are presented in section 5.5.

## 5.2 Problem Statement

The problem formulated in this chapter is termed as Sample number distribution problem.

Let $g(t)$ be the signal and $[0, A]$ be the interval of the signal. The interval [0, A] is partitioned into 'm' partitions. Let the $i^{th}$ partition be denoted by $[t_{i-1},\ t_i)$, so that $t_0 = 0$ and $t_m = A$. The number of samples in the $i^{th}$ partition is denoted by $n_i$. In each of the partitions uniform sampling is done.

The optimal sampling problem considered here consists of finding the sample number distribution $n_0, ..., n_{m-1}$, such that the fractional mean square error between the given signal and the reconstructed signal is minimised. Let $g(t)$ and $\hat{g}(t)$ be the original and reconstructed signals; then the optimal sampling problem is given by

$$\min_{n_0,...,n_{m-1}} \frac{\|g(t) - \hat{g}(t)\|^2}{E_g}, \tag{5.1}$$

where $E_g$ is the energy of the signal and given that $\sum_i n_i = N$, where $N$ is fixed apriori.

The sampling strategy developed here initially samples the given analog signal at an arbitrarily high rate, let the initial set of samples consists of $N_0$ samples. Then a subset of this initial sample set is selected such that an error bound between the reconstructed signal using this subset and the original signal is minimised. Let the number of samples in the subset be $N$, then $\sum_i n_i = N$.

A sampling algorithm depends upon the error norm and the interpolation method used. The error norm used here is the fractional mean square norm given by

$$\frac{\|g(t) - \hat{g}(t)\|^2}{E_g} = \frac{\int_0^A |g(t) - \hat{g}(t)|^2\, dt}{E_g}, \tag{5.2}$$

Let the reconstructed signal be

$$\hat{g}(t) \;=\; \hat{g}_i(t), \quad t \in B_i,\ i = 1,\ ...,\ m.$$

The fractional mean square reconstruction error is given by,

$$\frac{\int_0^A |g(t) - \hat{g}(t)|^2\, dt}{E_g} = \frac{\sum_i \int_{t \in B_i} |g(t) - \hat{g}_i(t)|^2\, dt}{E_g}, \tag{5.4}$$

$$= \frac{\int_b \int_a \frac{1}{a^2} |W_{g,\psi}(a,b) - W_{\hat{g},\psi}(a,b)|^2\, da\, db}{E_g}, \tag{5.5}$$

$$= \frac{\sum_{i=0}^{i=m-1} \int_{b \in B_i} \int_{a=a_{li}}^{a_{hi}} \frac{1}{a^2} |W_{g,\psi}(a,b) - W_{\hat{g},\psi}(a,b)|^2\, da\, db}{E_g} + \frac{m\,\delta_0 \;+\; Q}{E_g}, \tag{5.6}$$

where $Q$ is given by the following quantity,

$$Q \;=\; \frac{\int_{b \notin \cup B_i} \int_{a=a_{li}}^{a_{hi}} \frac{1}{a^2} |W_{g,\psi}(a,b) - W_{\hat{g},\psi}(a,b)|^2\, da\, db}{E_g}, \tag{5.7}$$

and $a'_{li}s$ are the $\delta_0$ scale-limits in the partitions.

Near the optimal distribution of the samples $Q$ is taken to be constant. The reason is that $Q$ is only a very small fraction of the overall reconstruction error and can be taken to be constant. This statement gets justified in simulations. The higher limit of the scale is taken to be $a_{lh}$, because, in practice, in the multiresolution analysis any signal is decomposed only upto a finite number of levels.

To find a bound on the fractional mean square reconstruction error, an assumption of the following kind is made-

$$\frac{|W_{g,\psi}(a,b) - W_{\hat{g},\psi}(a,b)|}{E_g} \;\leq\; \frac{C(\alpha)}{(n_i)^\alpha}, \tag{5.8}$$

for $b \in B_i$. The parameter $\alpha$ is called interpolation sensitivity. This assumption is based on the practical observation that, as the number of samples in any segment

increases the original and the reconstructed signals come close (in the sense of a norm), so that the transformed domain descriptions of the original and the reconstructed signal also come close. Therefore, the magnitude of the error can be bounded by a monotonically decreasing function. This specific form is assumed because it leads to a simpler analysis and gives an estimate of the sample distribution which can be realised easily in practice. On the right hand side of the inequality 5.8 the numerator is made dependent on $\alpha$, because for different $\alpha$ values, the constant $C(\alpha)$ has to be different, so that the assumption 5.8 gets satisfied.

Under this assumption, the error takes the following form-

$$\frac{\int_0^A |g(t) - \hat{g}(t)|^2 \, dt}{E_g} \leq \sum_{i=0}^{m-1} \int_{b \in B_i} \int_{a_{li}}^{a_{lh}} \frac{C(\alpha)}{(n_i)^\alpha} \, da \, db + m \, \delta_0 + Q \tag{5.9}$$

$$\leq \sum_{i=1}^{m} \frac{l_i \, C(\alpha)}{(n_i)^\alpha} \frac{1}{a_{li}} + m \, \delta_0 + Q \tag{5.10}$$

Next the following conjecture is made-

**Conjecture 5.3.1** *The fractional mean square error gets minimised for the same sample distribution for which the error bound 5.10 gets minimised.*

Due to this conjecture the optimal sampling problem reduces to finding the values of the parameters $n_i$, $i = 0, ..., m-1$ and $\alpha$ for which the error bound gets minimised. An optimal solution to the problem can be found by minimising the error bound with respect to the $n_i$ and $\alpha$. This error bound function is denoted by $e(n_0, ..., n_{m-1}, \alpha)$,

$$e(n_0, ..., n_{m-1}, \alpha) = \sum_{i=1}^{m} \frac{l_i \, C(\alpha)}{(n_i)^\alpha} \frac{1}{a_{li}} + m \, \delta_0 + Q \tag{5.11}$$

The constraint under which this optimisation is performed is given by

$$\sum_i n_i = N. \tag{5.12}$$

Using Lagrangian multipliers method, the following function has to be optimised-

$$e'(n_0, ..., n_{m-1}, \alpha) = \sum_{i=1}^{m} \frac{l_i\, C(\alpha)}{(n_i)^\alpha} \frac{1}{a_{l_i}} + m\, \delta_0 + Q + \lambda' \left( \sum_i n_i - N \right) \quad (5.13)$$

Differentiating $e'(n_0, ..., n_{m-1}, \alpha)$ with respect to $n_i$, $\alpha$ and $\lambda'$ independently and equating to zero leads to the following equations.

$$n_i = \left(\frac{1}{\lambda'}\right)^{\frac{1}{1+\alpha}} (C(\alpha))^{\frac{1}{1+\alpha}} \left(\frac{l_i}{a_{l_i}}\right)^{\frac{1}{1+\alpha}} \quad i = 0, ..., m-1. \quad (5.14)$$

$$\sum_i l_i \frac{C(\alpha)}{a_{li}} \frac{(-1)}{(n_i)^\alpha} ln(n_i) + \sum_i l_i \frac{1}{a_{l_i}} \frac{1}{(n_i)^\alpha} \frac{dC(\alpha)}{d\alpha} = 0 \quad (5.15)$$

$$\sum_i n_i = N \quad (5.16)$$

Solution of this system of $(m+2)$ equations requires the knowledge of $\frac{d}{d\alpha}C(\alpha)$. To eliminate the Equation 5.15, an assumption on the value of $\alpha$ is made. The parameter $\alpha$ is assumed to be close to zero. For $\alpha = 0$, the assumption is valid for $g(t)$ and $\hat{g}(t)$ in $L^2$.

Once $\alpha$ is fixed to a value close to zero (we take $\alpha$=0.0001), the $n_i$'s can be solved using Equations 5.14 and 5.16. Then $n_i$'s are used to calculate the fractional mean square reconstruction error.

A problem that arises in the implementation of the algorithm is that the optimal solution values of $n_i$ may not turn out to be integers. In that case, a decision regarding the choice of the number of samples to be distributed in the $i^{th}$ partition has to be made. The choice could be the smallest integer greater than $n_i$ or the largest integer smaller than $n_i$. We use the following notation.

$\lfloor n_i$ : The highest number less than or equal to $n_i$.

$n_i \rceil$ : The smallest number greater than or equal $n_i$.

If the $n_i$'s are real, then there are many ways in which the number of samples to be distributed in the $i^{th}$ partition can be approximated.

Case 1- If all $n_i$ are approximated to $n_i\rceil$, then the total number of samples that get distributed will turn out to be greater than $N$ but less than $N + m$.

Case 2- If all $n_i$ are approximated to $\lfloor n_i$ then the total number of samples that get distributed will turn out to be less than $N$ but greater than $N - m$.

Case 3- Another choice could, however, be to distribute $\lfloor n_i$ number of samples in the 'm' partitions and distribute the remaining $(N - \sum_i \lfloor n_i)$ samples in 'm' partitions such that at the most one sample falls in one partition. The value of $(N - \sum_i \lfloor n_i)$ is less then or equal to m; let this number be $k$. There are ${}^mC_k$ ways in which it can be done. This is highly computationally intensive.

We will shortly see that the approach given in the Case 1 is the best possible alternative. The only problem we have in this approach is that the number of samples that get distributed is more than $N$. But there is another practical phenomenon which has an opposing effect. In the computation of the wavelet transform of a signal, initially the signal is sampled at a high rate and it is assumed that the samples constitute the first approximation of the signal. This has been discussed in Chapter 3. The policy for sample distribution that we follow is, that firstly in each partition, the samples are placed uniformly and secondly the required number of samples are selected out of the samples in the first approximation. In the Case 1, the number of samples that are distributed in the $i^{th}$ partition is given by $n_i\rceil$. If $n_i\rceil$ turns out to be greater than the number of samples in the $i^{th}$ partition, in the first approximation, then there is a surplus of $(n_i\rceil - n^*)$, where $(n^* = \textit{number of samples in the } i^{th} \textit{ partition in the first approximation})$. Therefore, due to this factor as well the number of samples that get distributed turn

out to be different than than the desired. However, the two problems described above have opposing effects. Therefore the approach presented in the Case 1 has been implemented and the simulation results have been presented. In this case the number of samples that finally get distributed comes out to be less than the number of samples to be distributed.

For the practical implementation of the algorithm two issues have to be sorted out. The mean square error has to be calculated in terms of the samples of the signals $g(t)$ and $\hat{g}(t)$. The number of these samples depends on the computational ability. Let $N_0$ be the number of samples using which the fractional mean square error is to be approximated. Using the piecewise approximation, the fractional mean square error is given by-

$$e_c(n_0, ...n_{m-1}, \alpha) = \frac{\sum_{k=0}^{N_0-1}(g(k) - \hat{g}(k))^2}{\sum_{k=0}(g(k))^2}, \tag{5.17}$$

where $\hat{g}(k)$'s are the interpolated values using $N$ samples for various sample distributions. The interpolating equation used here is already discussed and is given by 5.19. Another issue is the implementation of the wavelet transform. Here for calculating the wavelet transform, the multiresolution algorithm is applied using the initial $N_0$ number of samples as the approximation in the space $V_0$. Then the wavelet decomposition is calculated for a=2, 4, 8, 16. The decomposition for scale values greater than 16 are not considered, because they contain insignificant amount of energy, and therefore have negligible contribution in deciding the sample distribution.

### 5.3.1 Segmentation Strategy

As already been described, the signal is segmented into regions of different scale-limits. For practically doing that a threshold $\theta$ is selected.

The strategy that we follow is, to assign a scale-limit of $2^{j_1}$ to an interval $[k_1 2^{j_1},\ k_2 2^{j_1}]$, for $k_1,\ k_2$ integers, if $W_{g,\psi}(a,b) \leq \theta$ for $a = 2^j$, and $b = k2^j$, forall $j \leq j_1$ and k is such that $k_1 2^{j_1} \leq k2^j \leq k_2 2^{j_1}$. This implies that any region is assigned a scale-limit of $2^{j_1}$, if for all scales less than or equal to $2^{j_1}$, the wavelet transform is zero or insignificant for 'b' (the shift parameter) lying in the interval.

The following algorithm is implemented. For $j = 1$, the coefficients $W_{g,\psi}(2^j, k2^j)$ are compared with a predecided threshold. The value of the threshold has to satisfy the following constraint

$$0 \ < \ \theta \ < \ 1 \tag{5.18}$$

The value of the threshold has to be taken close to zero. If the value of the coefficient $W_{g,\psi}(2, 2k)$ is greater than the threshold for $2k \in B_1$, and for $k2 \in B_1^c = [0,\ A] - B_1$ the coefficient is less than the threshold value then the region $B_1$ is assigned a scale-limit of 1. Next the value of $W_{g,\psi}(4, 4k)$ is compared with the threshold value. And the region $B_2 \subseteq [0,\ A] - B_1$ such that $W_{g,\psi}(4, 4k) > \theta$, for $4k \in B_2$, is assigned a scale-limit of 2. Further, a region $B_3 \subseteq ([0, A] - (B_1 \cup B_2))$ is found such that $W_{g,\psi}(8, 8k) > \theta$, for $8k \in B_3$. The region $B_3$ is assigned a scale-limit of 4. Next, a region $B_4 \subseteq ([0, A] - (B_1 \cup B_2 \cup B_3))$ is found such that $W_{g,\psi}(16, 16k) > \theta$, for $16k \in B_4$. The region $B_4$ is assigned a scale-limit of 8. Finally the region $B_5$ given by $B_5 = [0, A] - (B_1 \cup B_2 \cup B_3 \cup B_4)$ is assigned a scale-limit of 16.

### 5.3.2 Interpolation Procedure

In our derivation it has been assumed that the interpolating function used is scale-limited with the same scale value to which the original signal is scale-limited. Therefore, our problem is to find a scale-limited interpolating function. Since the functions

$\frac{1}{\sqrt{2^j}}\phi\left(\frac{t-T}{2^j}\right)$, are scale-limited hence they can be used for interpolation. Where, the function $\phi(t)$ is the scaling function of the multiresolution analysis used for analysing the signal. The interpolation used here has the following form

$$\begin{aligned} g_i(t) &= \sum_{n=0}^{n_i-1} g(nT_i)\ \frac{1}{\sqrt{a_{li}}}\phi\left(\frac{t-nT_i}{a_{li}}\right) \\ \hat{g}(t) &= g_i(t),\ \text{for}\ \ t \in [t_{i-1},\ t_i), \end{aligned} \tag{5.19}$$

where $\hat{g}_i(t)$ is the reconstruction of the signal in the $i^{th}$ region and $a_{li}$ is the scale-limit and $T_i = \frac{t_i - t_{i-1}}{n_i}$.

### 5.3.3 Algorithm

In the algorithm presented here, the values of $\theta$ are varied in steps and for each value, the optimal sample distribution is found. Using this distribution, the signal is reconstructed and the mean square error is calculated. Finally the sample distribution is selected for which the mean square error is minimum. The final algorithm has the following steps- **Begin**

**Step 1:** Choose the maximum number of iterations=$it_{max}$.

Choose the increment in $\theta = \Delta\ \theta$.

**Step 2:** Choose $\theta = \theta_0$, $N$ and $N_0$.

**Step 3:** Number of the iteration=0.

**Step 4:** Sample the given analog signal at $N_0$ number of points.

**Step 5:** Apply the multiresolution algorithm and calculate the decomposition of the signal into $W_{g,\psi}(2^j,\ k2^j)$, j=1, 2, 3, 4.

**Step 6:** Use the $W_{g,\psi}(2^j,\ k2^j)$, j=1, 2, 3, 4, to segment the signal and note down the scale-limits of the segments.

**Step 7:** Calculate the number of samples in each segment using 5.14 and 5.16.

**Step 8:** Reconstruct the original $N_0$ samples using the calculated samples in the previous step.

**Step 9:** Find the mean square reconstruction error using 5.17.

**Step 10:** $\theta = \theta + \Delta\,\theta$

*Number of iterations* = *Number of iterations* + 1.

**Step 11:** If the *Number of iterations* is equal to $it_{max}$, then select the optimal sample distribution and store the samples obtained by sampling the signal with optimal $n_i$ points in the $i^{th}$ segment for $i = 0, ..., m-1$. Else go to step 6.

**Step 12:** Stop

**End**

## 5.4 Simulation Results and Discussion

The algorithm has been tested on various signals. The original and the reconstructed signals for various $\alpha$ values have been plotted. The mean square reconstruction error has been plotted with respect to $\alpha$.

As a measure of the compression obtained, the following compression measure is

defined-

$$Compression\ ratio \quad = \quad \frac{Final\ number\ of\ the\ samples}{Initial\ number\ of\ the\ samples}$$

or,

$$Compression\ ratio \quad = \quad \frac{N}{N_0} \tag{5.20}$$

In the simulation results which are presented here, three test signals- $g_1(t)$, $g_2(t)$ and $g_3(t)$, are considered. These signals are segmented and then sampled using the algorithm presented in the previous section; the samples are again reused to reconstruct the original signal. The test signal $g_1(t)$ and its reconstructed version are plotted in Figure 5.1. The signal is segmented by using various $\theta$ and then reconstructed using the reconstruction equation given in 5.19. To find the optimal $\theta$, the error between the original and the reconstructed signal are plotted for various $\theta$. And that value of $\theta$ is picked, for which, the mean square error is minimum. The interpolation sensitivity in the transformed domain is taken to be 0.0001. The optimal $\theta$ obtained is 0.005 and the minimum mean square fractional error is given by 0.136929.

In Figure 5.2, the segmentation of the signal obtained for optimal $\theta$ is plotted along with the original signal. It can be observed that faster varying regions have relatively smaller scale-limits. In Figure 5.3, the fractional mean square error is plotted with respect to $\theta$. The mean square error with respect to $\theta$ is tabulated in Table 5.1. The compression ratio obtained for optimal $\theta$ is 0.620833. In this simulation, initially 180 samples were to be distributed in the segments, hence the expected compression ratio was 0.75, however, the compression ratio obtained is 0.620833, this compression ratio is less than the expected compression. The reason for this behaviour has already been discussed earlier.

In a certain segment if the number of the samples distributed using the algorithm is more than the number of samples in the original signal in that segment, then the number of samples allocated to that segment is taken to be the number of samples, in the original signal, in that segment. This practical step has been taken because in the first step, the original signal is replaced by its samples and it is assumed that there is no information loss in this step. Therefore, the final number of samples to be picked up from a segment should not be more than the original number of samples present in the signal in that segment. The segmentation of the signal has also been optimised with respect to the parameter $\theta$. In other words, that value of the parameter $\theta$ is chosen for which the fractional mean square error is minimum. The optimal number of partitions for the test signal $g_1(t)$ is 24.

Similarly, the test signal $g_2(t)$ and its reconstruction is plotted in Figure 5.4. The segmentation obtained for the optimal $\theta$ is plotted in Figure 5.5. In this case as well, the faster varying regions have relatively smaller scale-limits. The fractional mean square error with respect to $\theta$ is plotted in Figure 5.6. For this test signal, the optimal mean square error obtained is 0.149621. The optimal $\theta$ is 0.05. The optimal number of segments is 15. The final compression ratio obtained is 0.679166.

For the test signal $g_3(t)$, there are two optimal $\theta$ values. The first optimum is for the local minimum in the fractional mean square error versus $\theta$ plot and the second optimum is for the global minimum. For the local minimum, the test signal $g_3(t)$ and its reconstruction is plotted in Figure 5.7. For the global minimum, the test signal $g_3(t)$ and its reconstruction is plotted in Figure 5.8. The segmentation obtained for the optimal $\theta$ is plotted in Figure 5.9. In this case also the faster varying regions have relatively smaller scale-limits. The fractional mean square error with respect to $\theta$ is plotted in Figure 5.10. The mean square error with respect to $\theta$ is tabulated in Table

5.2.

For the local minimum, for the test signal $g_3(t)$, the optimal fractional mean square error obtained is 0.0007313. The optimal $\theta$ is 0.001 and the optimal number of segments is 18. The final compression ratio obtained is 0.700000.

For the global minimum, the optimal fractional mean square error obtained is 0.000037. The optimal $\theta$ is 1.0. The optimal number of segments is 1. The final compression ratio obtained is 0.745833. The mean square error with respect to $\theta$ is tabulated in Table 5.3.

From the simulation results, it can be observed that, the concept scale-limitedness can be used for partitioning the signal. The mean square error plotted with respect to $\theta$ shows many local minima, therefore, it becomes very difficult to find out, upto which value of $\theta$ the simulations have to be performed. However, within the range of $\theta$ tested in each example, the optimal fractional mean square error obtained is appreciably low. And also the signal reconstructed after partitioning and sampling using the optimal $\theta$ also matches the original signal.

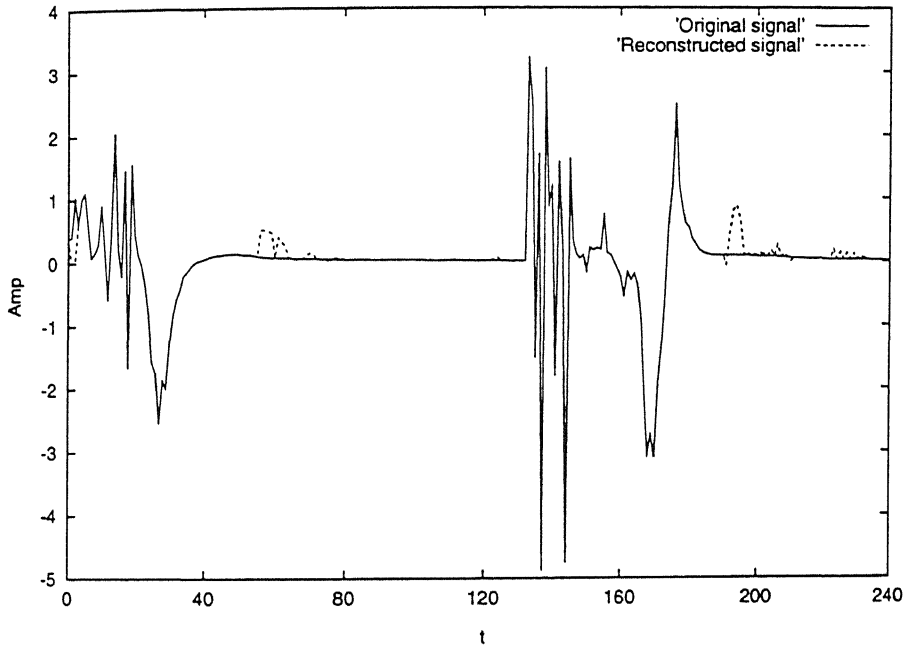


Figure 5.1: The signal $g_1(t)$ and the reconstructed signal $\hat{g}_1(t)$

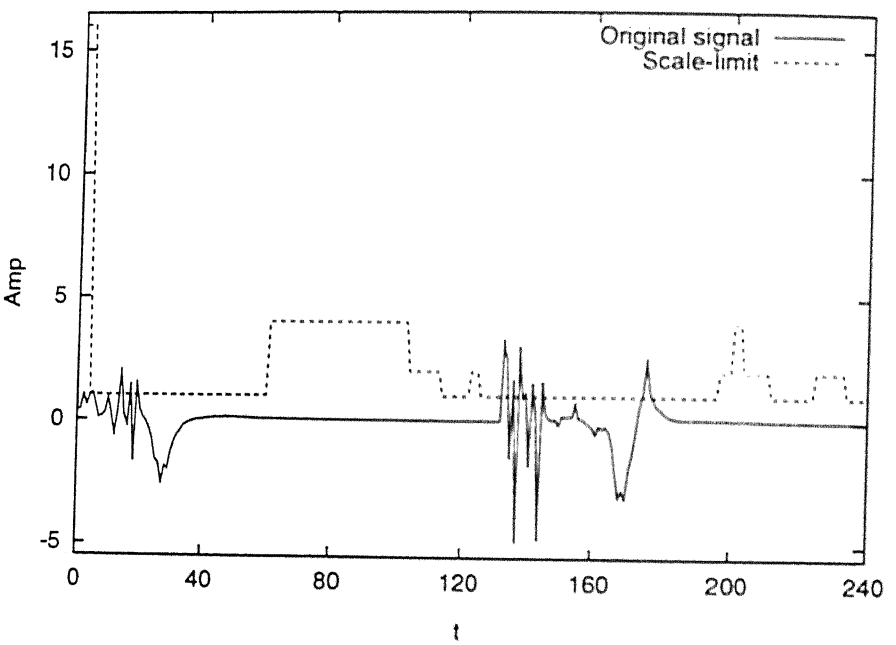


Figure 5.2: The signal $g_1(t)$ and the the partitioning obtained using the optimal choice of $\theta$.

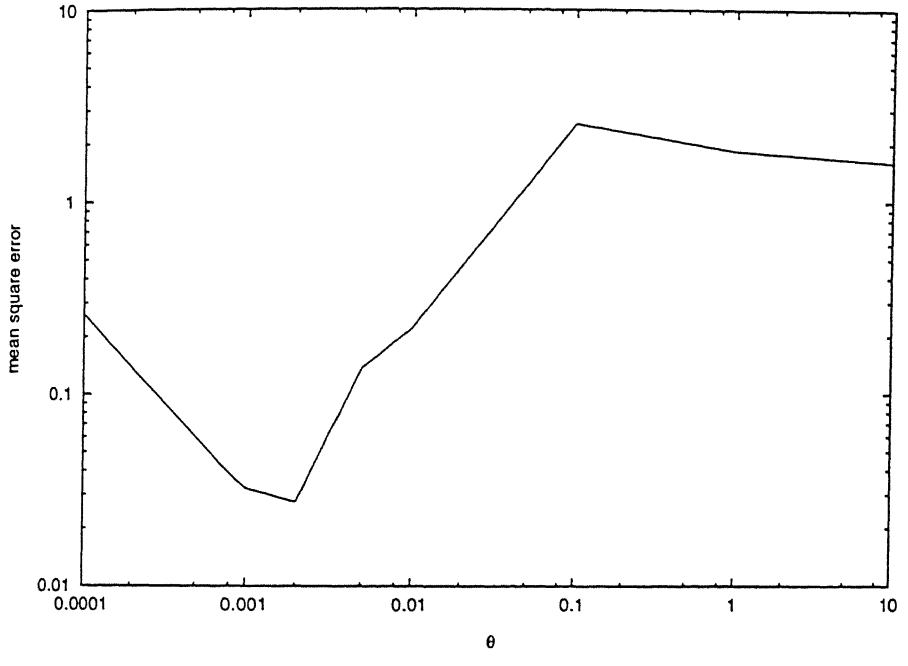


Figure 5.3: The mean square error of the signal $g_1(t)$ with respect to $\theta$ for $\alpha$ =0.0001, when the segmentation and the sampling strategy given in the section 5.3 is used.

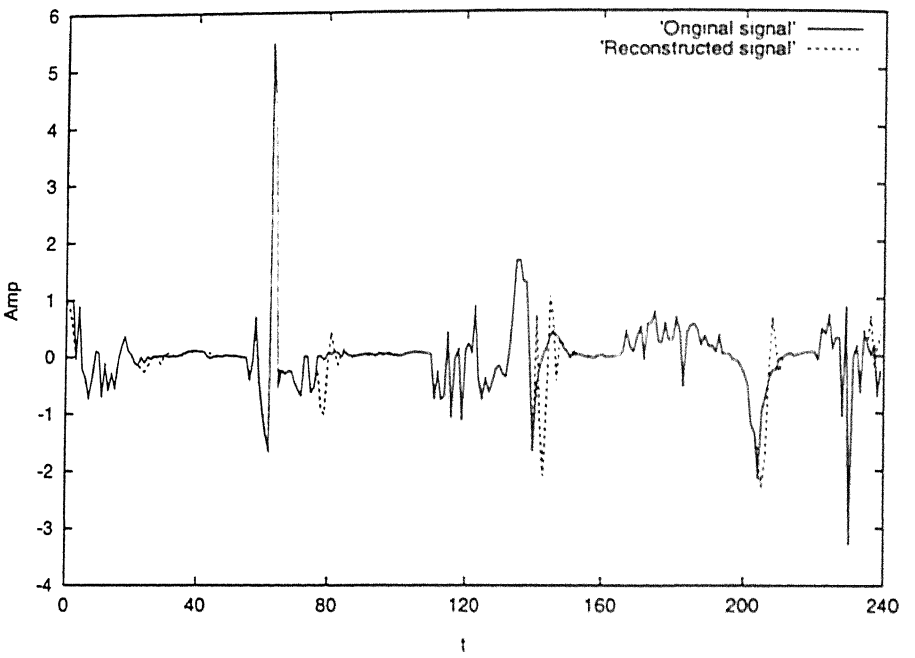


Figure 5.4: The signal $g_2(t)$ and the reconstructed signal $\hat{g}_2(t)$

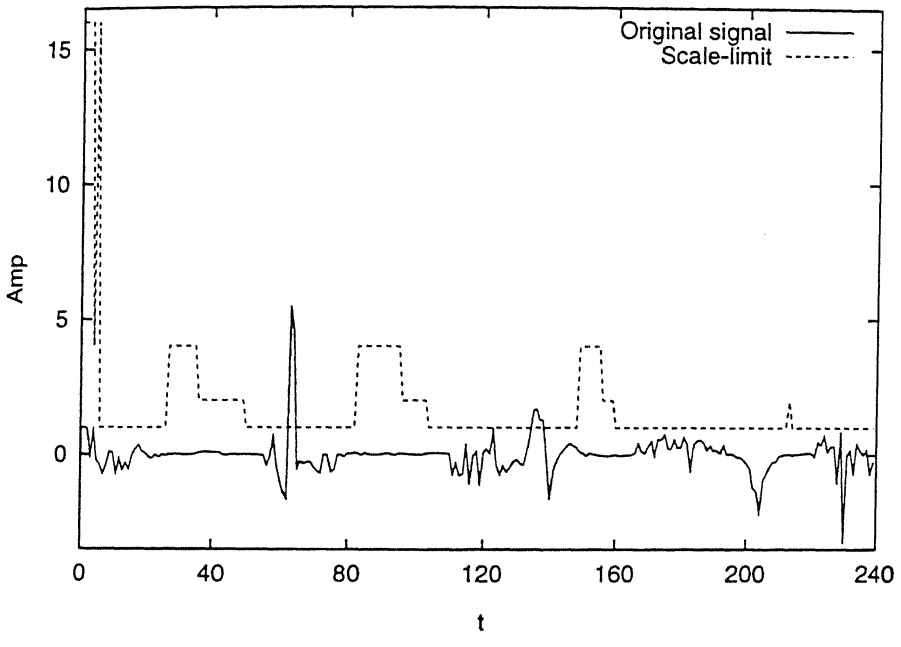


Figure 5.5: The signal $g_2(t)$ and the the partitioning obtained using the optimal choice of $\theta$.

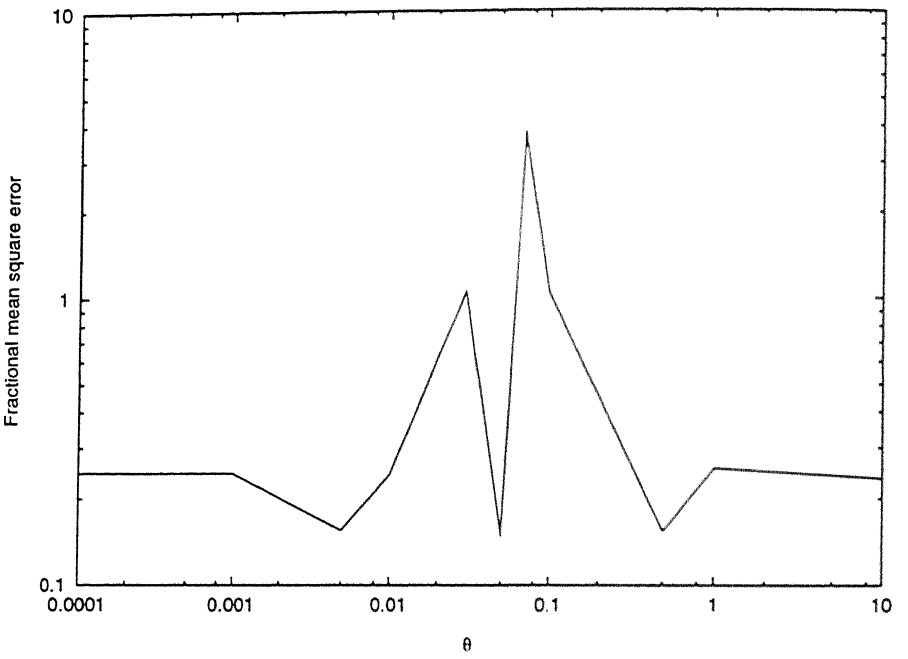


Figure 5.6: The mean square error of the signal $g_2(t)$ with respect to $\theta$ for $\alpha$ =0.0001, when the segmentation and the sampling strategy given in the section 5.3 is used.

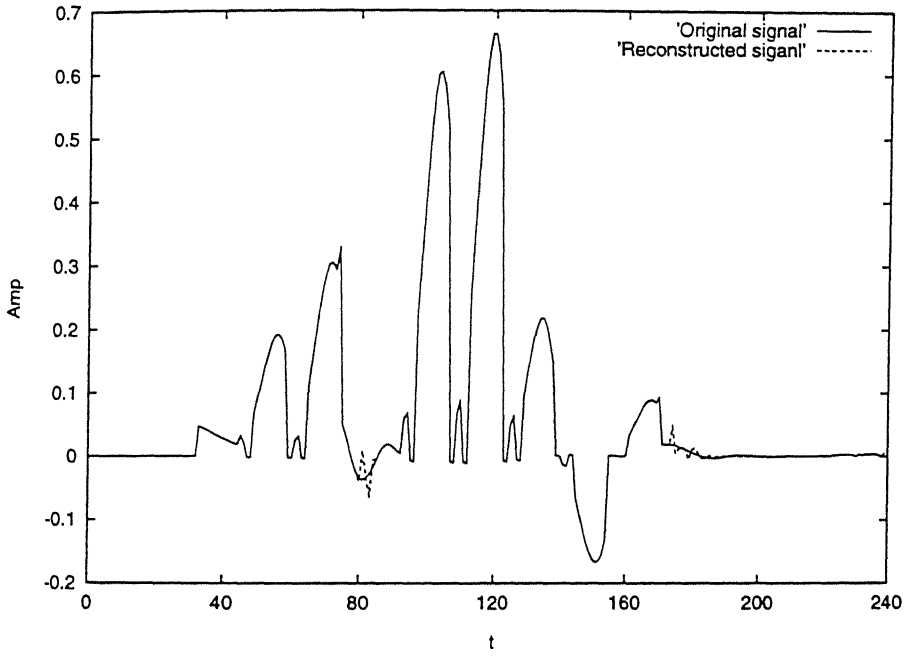


Figure 5.7: The signal $g_3(t)$ and the reconstructed signal $\hat{g}_3(t)$, for $\theta$ selected at the first local minimum of the fractional mean square error versus $\theta$ curve presented in Figure 5.10

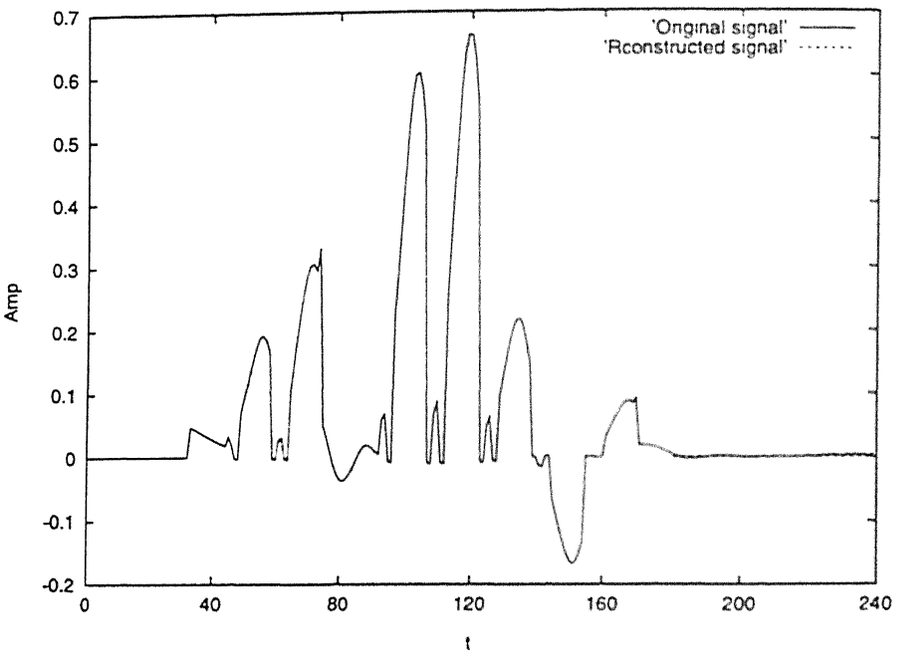


Figure 5.8: The signal $g_3(t)$ and the reconstructed signal $\tilde{g}_3(t)$, for $\theta$ selected at the global minimum of the fractional mean square error versus $\theta$ curve presented in Figure 5.10

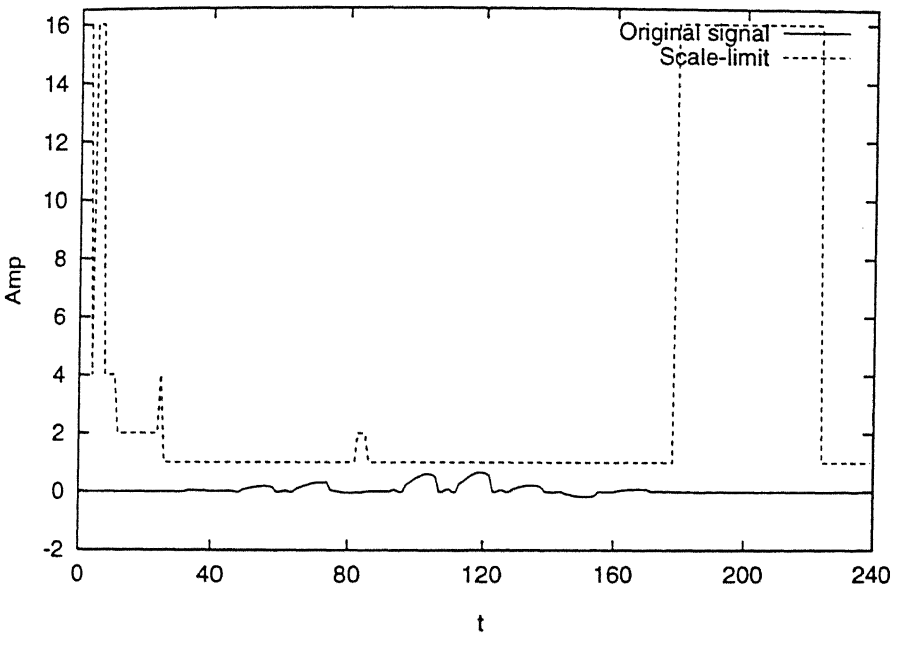


Figure 5.9: The signal $g_3(t)$ and the the partitioning obtained using the optimal choice of $\theta$.

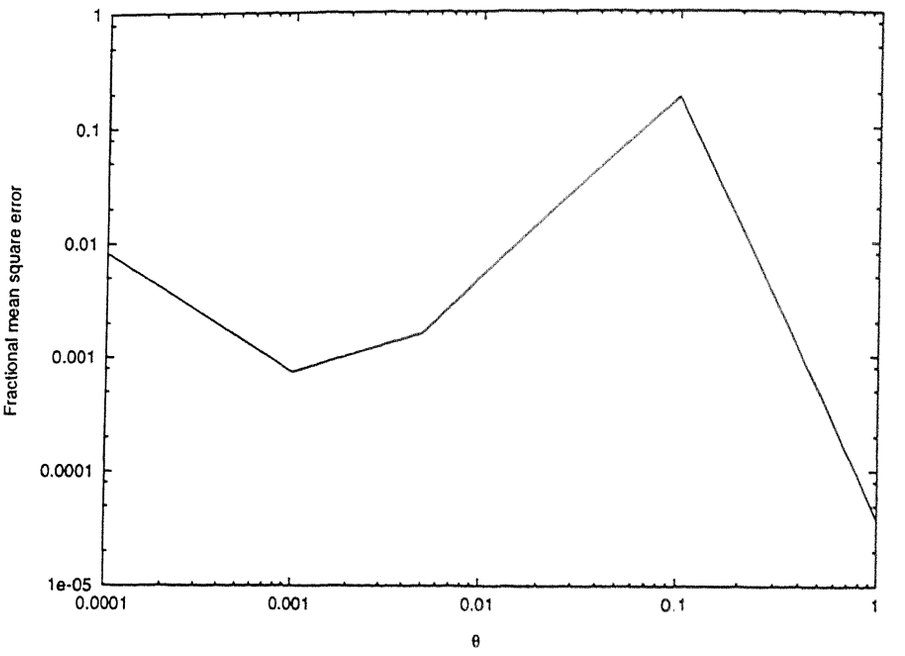


Figure 5.10: The mean square error of the signal $g_3(t)$ with respect to $\theta$ for $\alpha$ =0.0001, when the segmentation and the sampling strategy given in the section 5.3 is used.

| $\theta$ | Fractional Mean square error | Number of Partitions | Compression ratio |
|---|---|---|---|
| 0.0001 | 0.263028 | 4 | 0.733333 |
| 0.0009 | 0.034760 | 13 | 0.683333 |
| 0.001 | 0.032267 | 13 | 0.683333 |
| 0.002 | 0.027355 | 25 | 0.662500 |
| 0.005 | 0.136929 | 24 | 0.620833 |
| 0.01 | 0.220440 | 17 | 0.558333 |
| 0.1 | 2.552180 | 25 | 0.491667 |
| 1.0 | 1.845670 | 12 | 0.329167 |
| 10.0 | 1.607650 | 1 | 0.750000 |

Table 5.1: For the signal $g_1(t)$, the Fractional mean square error, number of partitions and the compression ratio along with the various values of $\theta$ are presented in this table.

## 5.5 Conclusions

The problem that has been addressed, consists of distributing a fixed number of samples optimally in the different regions of a signal. The regions are obtained by partitioning the signal depending upon local variations. In the sampling strategy, proposed here, the rate of sampling adapts to local variations. In the algorithm for sampling, proposed here, first the signal is partitioned into dissimilar regions. Each of the regions is characterised by a scale-limit, which is distinct from the values of the scale-limits of the neighbouring regions. Then, in each region the optimal number of samples are distributed, which is a fraction of the total number of samples to be distributed. This distribution is done according to the Equation 5.14.

In section 5.2, the problem has been formulated. The problem consists of distributing a fixed number of samples optimally into the partitions of a signal. Here the fractional

| $\theta$ | Fractional Mean square error | Number of Partitions | Compression ratio |
|---|---|---|---|
| 0.0001 | 0.245450 | 2 | 0.745833 |
| 0.001 | 0.245450 | 2 | 0.745833 |
| 0.005 | 0.155359 | 4 | 0.733333 |
| 0.01 | 0.242324 | 8 | 0.7041668 |
| 0.03 | 1.058120 | 11 | 0.691667 |
| 0.05 | 0.149621 | 15 | 0.679166 |
| 0.07 | 3.736660 | 16 | 0.675000 |
| 0.1 | 1.043800 | 23 | 0.666666 |
| 0.5 | 0.153883 | 19 | 0.379167 |
| 1.0 | 0.254654 | 6 | 0.337500 |
| 10.0 | 0.235071 | 1 | 0.750000 |

Table 5.2: For the signal $g_2(t)$, the Fractional mean square error, number of partitions and the compression ratio along with the various values of $\theta$ are presented in this table.

| $\theta$ | Fractional Mean square error | Number of Partitions | Compession ratio |
|---|---|---|---|
| 0.0001 | 0.008219 | 8 | 0.720833 |
| 0.001 | 0.000731 | 11 | 0.700000 |
| 0.005 | 0.001596 | 14 | 0.637500 |
| 0.01 | 0.005000 | 18 | 0.570833 |
| 0.1 | 0.183720 | 13 | 0.450000 |
| 1.0 | 0.000037 | 1 | 0.750000 |

Table 5.3: For the signal $g_3(t)$, the Fractional mean square error, number of partitions and the compression ratio along with the various values of $\theta$ are presented in this table.

mean square error is minimised by taking the number of samples in each partition as variables. The interpolation is done using functions which are scale-limited.

The segmentation and sampling algorithms have been presented in section 5.3. It has been proved that segments with smaller scale-limits should be sampled at a higher sampling rate. To segment the signal a threshold value is selected first. Next, regions of $b$ are marked out, wherein, the wavelet transform value for scale value equal to 2 is more then the threshold. The segment which is common to both this region and the domain of the signal is assigned a scale-limit of 1. Next the regions which are left over have to be classified. The regions which are common to the left over regions and the regions of the shift parameter, wherein, the wavelet transform value for scale value 2 is less than the threshold and the wavelet transform value for scale 4 is greater than the threshold value are assigned a scale-limit of 2. Similarly, any region is assigned a scale-limit of $2^j$, if the wavelet transform value for the scale in this region and the for all shifts less than equal to $2^j$ is less than the threshold.

The algorithm proposed for optimal sampling is as follows. First a low value of the threshold is set, then the optimal sample distribution is found, using this optimal distribution the signal is sampled uniformly in the different segments. Next these samples are used to reconstruct the signal back and finally the fractional mean square error is found. This is repeated for successively higher values of the threshold and that sample distribution is selected, for which, the minimum fractional mean square error is obtained. The fractional mean square error verses $\theta$ is found to have many local minima, in general, therefore, the global minimum has to be selected. The simulation results have been presented in section 4. The conclusion of this chapter is that, in order to keep the bound on the fractional mean square error low, the number of samples in any segment should be inversely proportional a positive power of the scale-limit.

Optimal sample distribution algorithm proposed in this chapter can also be used for optimal nonuniform sampling. This is possible when the number of samples to be optimally distributed in the partitions turn out to be equal to the number of partitions.

In the examples considered in this chapter the maximum number of partitions are not very high, therefore the optimal sample placement, described in the Chapter 4, cannot be done. To increase the number of partitions, the signal has to be partitioned into more number of scales. For doing that, the signal has to be decomposed into scales which fall between the diadics.

# Chapter 6

# Conclusions

The conventional approach of collecting samples of an analog signal at uniform intervals is known as uniform sampling. The uniform sampling approach is not necessarily the best or computationally most efficient. In contrast, collecting samples of an analog signal at nonuniform intervals is often more rational and optimal in the case of many practical signals. Consistent with the type of the signal, which is the best way to take the samples or at what intervals the samples are to be taken so that the whole process is efficient (requires least number of samples to represent an analog signal), may be termed as the basic problem of nonuniform sampling. The objective of this thesis is to make a contribution to the above described problem of nonuniform sampling.

## 6.1 Summary and Conclusions

In conventional signal processing, signals are sampled uniformly. This is based on Shannon's sampling theorem. In uniform sampling the signal is sampled at a rate

equal to the twice of the bandwidth. This technique is not suitable for the following cases- (a) When the signal is not band-limited, (2) When an estimate of the bandwidth of the signal is not available. It is for these cases the nonuniform sampling can serve as an alternative. In this thesis, two nonuniform sampling problems for time-limited signals have been formulated. In the first problem, a finite number of samples are placed in the domain of the signal such that the fractional mean square reconstruction error is minimised. Here the fractional mean square error is the ratio of the mean square error to the energy of the original signal. In the second problem, a finite number of samples are distributed optimally in the partitions of a time-limited signal.

In the first problem, a finite number of samples are distributed in the domain of the signal such that the fractional mean square reconstruction error is minimised. In Chapter 4 this problem has been analysed and simulation results are presented. It has been shown that if the interpolation is done using functions which are shifted to sample point and multiplied by the sample value and further these functions are local (Most of the energy is concentrated around the origin.), then, the samples should fall in the same regions, in which, the wavelet transform values are relatively large in the domain of the shift parameter. Another constraint on the sample point is that it should be in the domain of the original signal. Using the above mentioned properties of the optimal sampling instants, an algorithm for optimal sampling has been proposed.

In the case of the problem proposed in Chapter 4 the samples fall nonuniformly, therefore all the sampling instants also have to be stored. To eliminate the requirement of sampling instant storage, another problem is formulated, in which, the signal is partitioned and sampling rate is varied depending upon the local variations. This is the second problem attempted in this thesis.

In the second problem, which has been formulated in Chapter 5, a finite number of samples are distributed optimally in the partitions of a signal such that the fractional mean square reconstruction error is minimised. It is assumed that in each of the partitions the samples are distributed uniformly and reconstruction is done using functions which are scale-limited. Under these conditions it has been shown that, the optimal number of samples in a partition is inversely proportional to a positive power of the scale-limit of the partition. To partition the signal into dissimilar regions, a new concept of scale-limitedness is introduced and utilised. The algorithm for sampling and the simulations results are also presented in the same chapter.

In Chapter 3, the concept of scale-limitedness with reference to wavelet transforms has been introduced. This concept has been used to characterise variations in a signal. A signal is said to be scale-imited to a certain value if the wavelet transform is zero for the scale parameter below that value and for all shifts. It has been shown through simulations that signals with smaller scale-limits are faster varying. In the same chapter it has been shown that, for the same reconstruction error, signals with smaller scale-limits should be sampled at a relatively faster rate.

It is important to note, that the approach of nonuniform sampling followed in Chapter 5 is similar to subband coding of speech signals. In subband coding proposed by Crochiere et. al. [Cro77], the speech signal is partitioned in frequency domain into subbands and then encoding the bands are individually done. In subband coding, at lower bands, where pitch and formant structure must be accurately preserved, a larger number of bits per sample are used for encoding, whereas in upper bands noise-like sounds occur in speech, fewer bits per sample are used. In our approach, the incoming signal is partitioned in the time domain itself and the rate of sampling in each partition is varied depending upon the scale-limit of each partition. To summerise these are the

conclusions of this thesis.

- The concept of scale-limitedness can be used for characterisation of signal variations. Scale-limited signals have the following properties-
  - A band-limited signal is also scale-limited with respect to a certain wavelet family.
  - The $n^{th}$ differential is inversely proportional to the $n^{th}$ power of the scale-limit of the signal.
  - There exist time-limited signals which are scale-limited as well.
  - The Lagrangian interpolating function is $\delta_0$-practically scale-limited.
  - A signal in $V_j$ is scale-limited to $2^j$, where, $V_j$ is space associated to the multiresolution analysis.

  It has been shown through simulations that signals with smaller scale-limits are faster varying. Further it has been shown that signals with smaller scale-limits should be sampled at a relatively faster rate for the same reconstruction error.

- If a signal is partitioned into regions of different scale-limits, then regions with smaller scale-limits should be sampled at a relatively higher rate to minimise the overall fractional mean square reconstruction error. The reconstruction in any partition is done using functions which are scale-limited to the scale-limit of the partition.

- The optimal nonuniform sampling strategy is one in which, the samples are placed in regions, in which, the wavelet transform has relatively large magnitude with respect to the shift parameter over different scales. It has been assumed that the

reconstruction is done using local functions. Using this result, an algorithm for nonuniform sampling of a finite duration signal is proposed.

## 6.2 Scope for Future Work

The possible directions for future work are as follows.

- This thesis has proposed novel techniques for optimal sampling of time-limited signals. The signals considered are one dimensional, however, the theory proposed here can be applied for higher dimensional signals. For example, this theory can be reformulated for images and images can be nonuniformly sampled.

- In the case of region based sampling strategy proposed in the thesis, for segmenting the signal, same threshold values have been used for all scales, however, the performance of the algorithm can be studied for case when different threshold values are used for different scales.

- The processing of nonuniform samples also has to be thoroughly studied. There has been some work done in the area of spectral estimation and system identification using nonuniform samples [Sir87], [SS88], however, there are many subfields of processing, in which work has to be done. For example, filtering of nonuniform samples and interpolation of signals using nonuniform samples.

- Using the algorithm for region based sampling proposed in Chapter 5, optimal nonuniform sampling discussed in Chapter 4 can be done. For doing that, the number of partitions should be equal to the number of samples to be distributed. To increase the number of partitions, there can be two ways- one is to increase

the number of scales into which the signal is partitioned and another way is to have different threshold values for different scales.

- In this thesis, only $8^{\psi}$ wavelets are used, however the same algorithms can be tried out with other wavelets and the wavelet basis which gives the minimum reconstruction error can be found out. Similarly, different interpolation methods can also be tried out and the best interpolation method can be ascertained.

# Appendix A- Simulation results when linear interpolation is used for ECG signals

First we show that linear interpolation also falls in the class of interpolations, in which, the interpolation is done in terms of local functions and the samples. Because the theory developed in the Chapter 4 is applicable only for the case when interpolation is done using shifted local functions.

For linear interpolation $h_k(t, t_{k-1}, t_{k+1})$ takes the following form,

$$h_k(t - t_k, t_{k-1}, t_k) = \begin{cases} 0, \ t < t_{k-1} \\ g(t_k)\frac{(t-t_k)+(t_k-t_{k-1})}{(t_k-t_{k-1})}, & t < t_k \\ g(t_k)\frac{(t_{k+1}-t_k)-(t-t_k)}{t_{k+1}-t_k}, & t_k < t \\ 0, \ t > t_{k+1} \end{cases} \tag{7.1}$$

**Example** The signal analysed in this example is an ECG signal sampled at a rate of 200 samples per second and the 240 samples of this signal are shown in Figure 4.15. In Table 7.1, the fractional mean square error for various number of samples is presented. The various numbers of samples for which the fractional errors have been tabulated are 160, 176, 192, 208, 224, 240. For each of the numbers the reconstructed signal and the

fractional mean square error are obtained. To find the mean square error, the signal is reconstructed at the initial set of samples. Then, using the original sample set and the reconstructed set the fractional mean square error is found. It can be observed from the table, that, the fractional mean square error reduces as the number of samples increases.

In Figure 7.1, the original signal and the reconstructed signal are plotted for the case when the signal, shown in Figure 4.15, is reconstructed using 160 samples. In Figure 7.2, the original signal and the reconstructed signal are plotted for the case when the signal, shown in Figure 4.15 is reconstructed using 176 samples. In Figure 7.3, the original signal and the reconstructed signal are plotted for the case when the signal, shown in Figure 4.15, is reconstructed using 192 samples. In Figure 7.4, the original signal and the reconstructed signal are plotted for the case when the signal, shown in Figure 4.15, is reconstructed using 208 samples. In Figure 7.5, the original signal and the reconstructed signal are plotted for the case when the signal, Figure 4.15, is reconstructed using 224 samples. As the number of samples used for reconstruction increase, the original and the reconstructed signals come closer. The fractional mean square error verses the number of samples used for signal reconstruction has been plotted in Figure 7.6.

From the simulation results, it can be observed that the linear interpolation can also be used.

| Figure label | Number of samples | fractional mean square error |
|---|---|---|
| Figure 0.1 | 160 | 0.021332 |
| Figure 0.2 | 176 | 0.019385 |
| Figure 0.3 | 192 | 0.018330 |
| Figure 0.4 | 208 | 0.017669 |
| Figure 0.5 | 224 | 0.004882 |
| | 240 | 0.000000 |

Table 7.1: Error-$N$ for the original shown in figure 4.15.

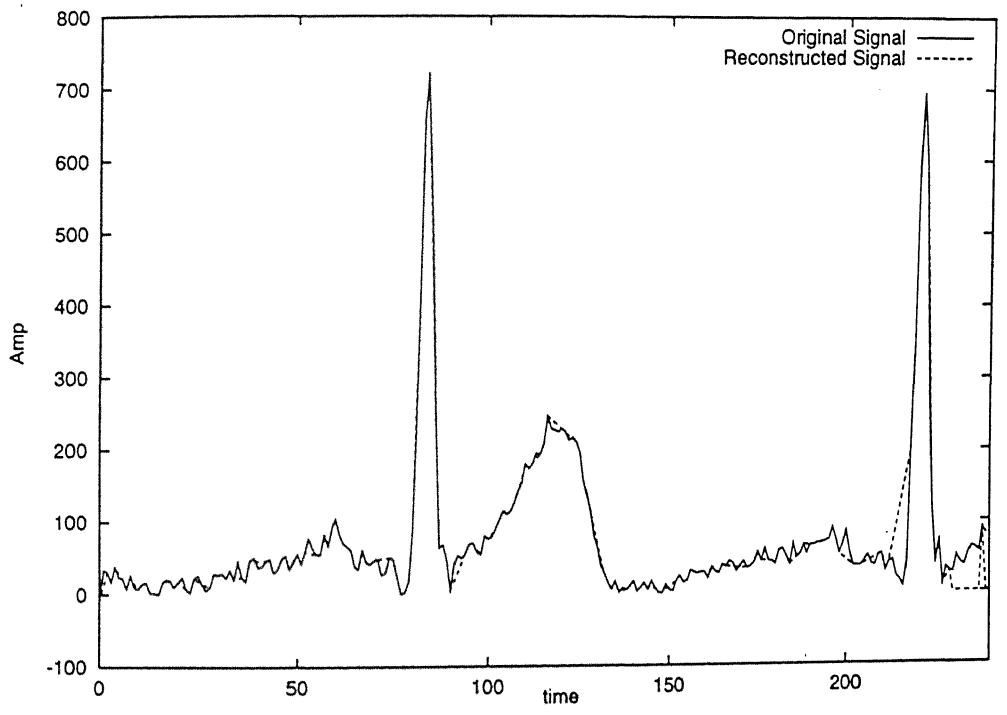


Figure 7.1: The original and the reconstructed signal for compression ratio equal to 0.6667. The original signal was sampled at 240 points, further only 160 samples are retained at nonuniform sampling instants and the signal is reconstructed at the initial 240 instants using linear interpolation.

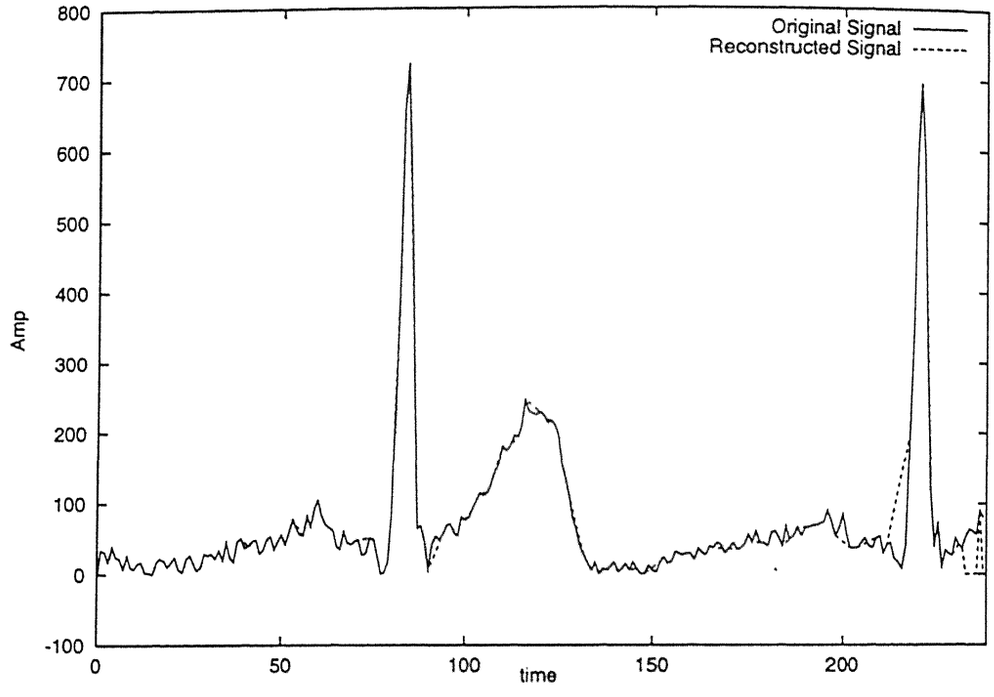


Figure 7.2: The original and the reconstructed signal for compression ratio equal to 0.7333. The original signal was sampled at 240 points, further only 176 samples are retained at nonuniform sampling instants and the signal is reconstructed at the initial 240 instants using linear interpolation.

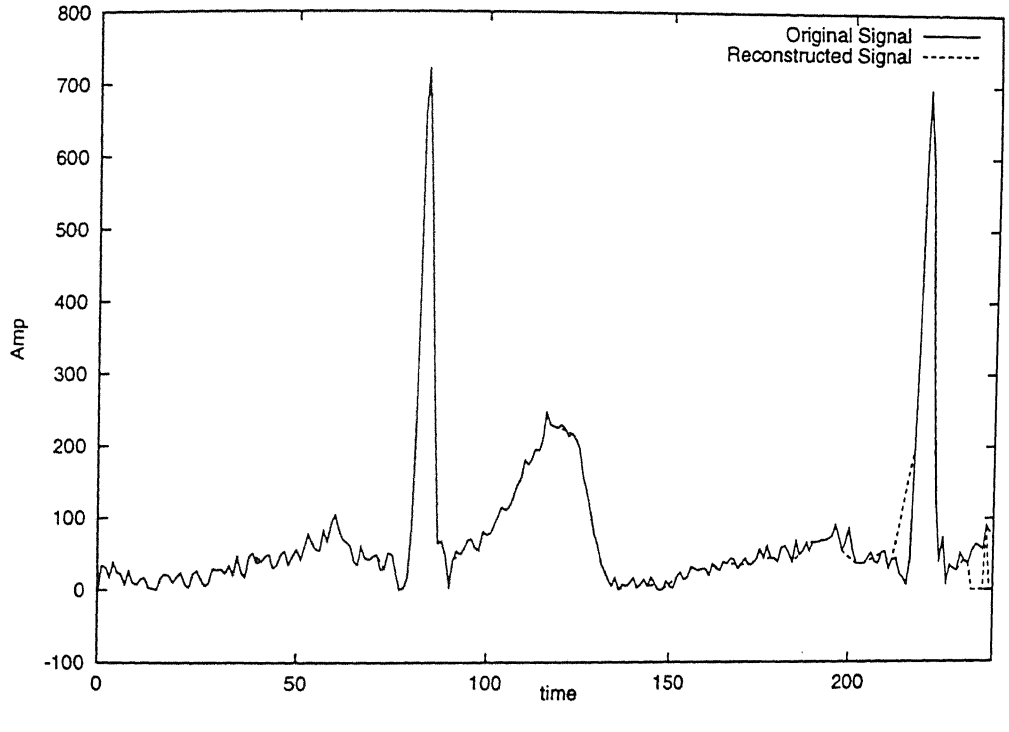


Figure 7.3: The original and the reconstructed signal for compression ratio equal to 0.8000. The original signal was sampled at 240 points, further only 192 samples are retained at nonuniform sampling instants and the signal is reconstructed at the initial 240 instants using linear interpolation.

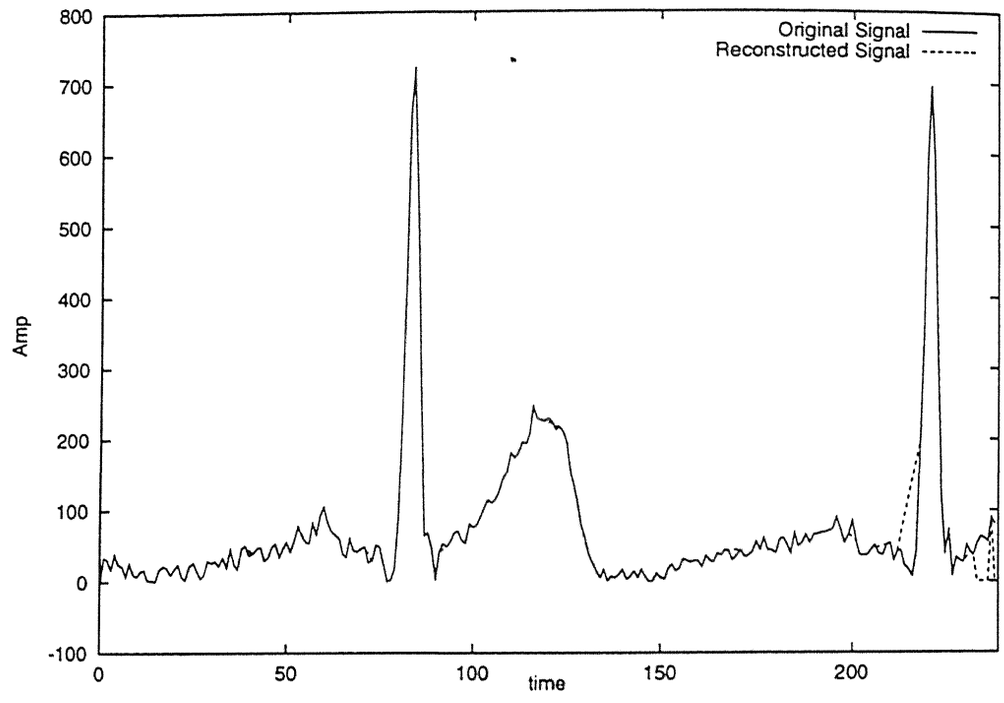


Figure 7.4: The original and the reconstructed signal for compression ratio equal to 0.8667. The original signal was sampled at 240 points, further, 208 points are retained at nonuniform sampling instants and the signal is reconstructed at the initial 240 instants using linear interpolation.

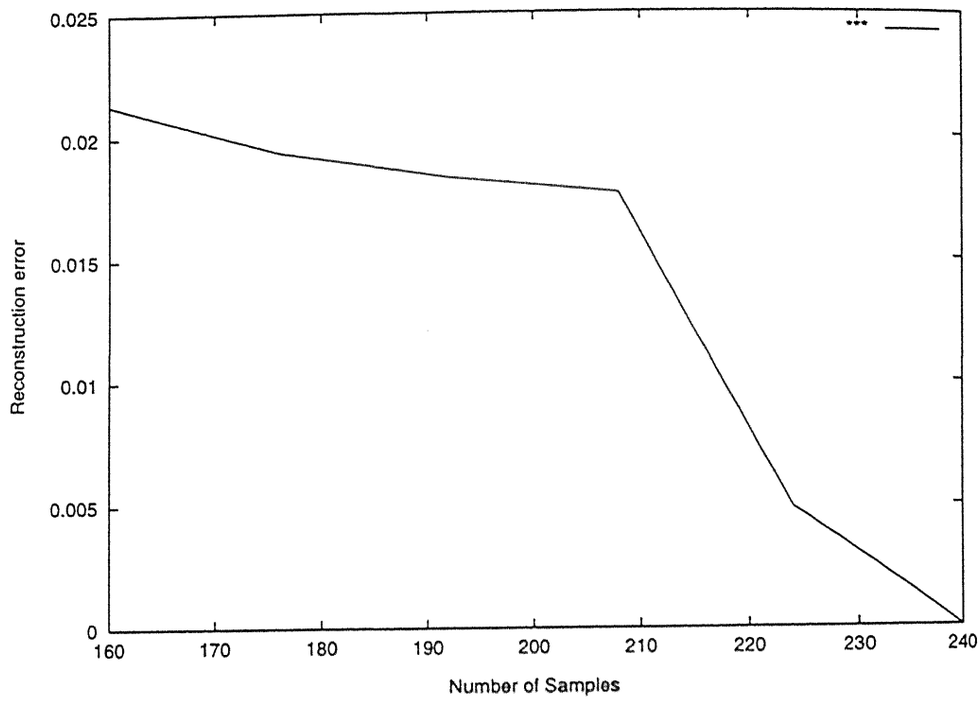


Figure 7.6: Error-$N$ for the signal in Figure 4.15.

# References


[AHT95] Hehong Zou Ahmed H. Tewfik. Completeness of arbitrarily sampled discrete time wavelet transform. *IEEE Trans. Signal Processing*, 43(11):2570–2581, Nov. 1995.

[BC58] F. E. Bond and C. R. Cahn. On sampling the zeros of the bandwidth limited signals. *IEEE Trans. Inform. Theory*, IT-4:110–113, 1958.

[BD74] I. Bar-David. An implicit sampling theorem for bounded bandlimited functions. *Inform. Contr.*, 24:36–44, Jan. 1974.

[BdT88] M. Bozzini and F. de Tisi. An algorithm for knot location in bivariate least squares spline approximation. *Algorithms for Approximation II, Proceedings of second international conference on Algorithms for approximation, held at Royal Military College of science, Srevanham, Chapman and Hall Mathematics*, July 1988.

[Ber92] A. Berman. A reconstruction set of a discrete wavelet transform representation. *Proc. 1992 IEEE Int. Conf. Acoust. Speech Signal Processing, San Fransisco*, pages IV629–IV632, March 1992.

[Beu61] F. J. Beutler. Sampling theorems and bases in hilbert space. *Inform. Contr.*, 4:97–117, 1961.

[Beu66] F. J. Beutler. Error free recovery of signals from irregularly spaced samples. *SIAM REV.*, 8(3):328–335, July 1966.

[Beu76] F. J. Beutler. On the truncation error of cardinal sampling expansion. *IEEE Trans. Inform. theory*, 22(5):568–573, Sept. 1976.

[BM92] I. Bilinskis and A. Mikelsons. Randomised signal processing. *Prentice hall international Series in Acoustics, Speech and Signal Processing*, 1992.

[Coh89] L. Cohen. Time frequency distributions- a review. *Proc. IEEE*, 77(7):94–981, 1989.

[Cro77] R. E. Crochiere. On the design of sub-band coders for low-bit-rate speech communication. *the Bell System Technical Journal*, 56(5):747–779, May-June 1977.

[Dau92] I. Daubechies. Ten lectures on wavelets. *Industrial and Applied mathematics, Philadelphia , Pennsylvania*, 1992.

[deF67] S. deFrancesco. An estimate of Shannon's sample series partial summation inaccuracy. *Presented at 15th Int. Commun. Conv. Int. Inst. Commun., Geneva*, Oct. 1967.

[DJ94] D. L. Donoho and I. M. Johnstone. Ideal spatial adaption by wavelet shrinkage. *Biometrika*, 81(3):425–455, 1994. Printed in Britain.

[DS] R. J. Duffin and A. C. Schaeffer. A class of non-harmonic fourier series. *Trans. of the Amer. Math. Society*, 72:341–366.

[ea94] R. A. Gopinath et al. Optimal wavelet representation of signals and the wavelet sampling theorem. *IEEE Trans. Circuits and Systems-II: Analog and Digital Signal processing*, 41(4):262–277, April 1994.

[Gam89] M. Gamshadzahi. Bandwidth reduction in delta modulation systems using an iterative reconstruction scheme. *Master's thesis, Dept. of ECE, Illinois Institute of Technology, Chicago*, Dec. 1989.

[Hig76] J. R. Higgins. A sampling theorem form irregularly spaced sampling points. *IEEE Trans. Inform. theory*, IT-22:621–622, Sept. 1976.

[HT62] H. D. Helms and J. B. Thomas. Truncation error of sampling theorem expansion. *Proc. IRE*, 50:179–184, Feb. 1962.

[Jer77] Abdul J. Jerri. The Shannon's sampling theorem-its various extensions and applications: A tutorial review. *Proc. IEEE*, 65(11):1565–1596, Nov. 1977.

[JJCL85] M. R. Palmer J. J. Clark and P. D. Lawrence. A transformation method for the reconstruction of functions from nonuniformly spaced samples. *IEEE Trans. Acoust. Speech Signal Processing*, ASSP-33:1151–1165, 1985.

[JLB67] Jr. J. L. Brown. On the error arising in reconstructing a nonbandlimited function by means of band pass sampling theorem. *J. Math. Anal. Appl.*, 18:75–84, 1967.

[Jor61] K. L. Jordan. Discrete representation of random signals. *M.I.T., Cambridge, MA, Tech. Rep.*, (378), July 1961.

[Kon89] R. Konoun. Ppm reconstruction using iterative techniques. *Project report, Technical report, Dept. of ECE, Illinois Institute of Technology, Chicago,* Sept. 1989.

[Kra59] H. P. Kramer. A generalised sampling theorem. *J. Math. Phy.*, 38:68–72, 1959.

[LA60] D. A. Linden and N. M. Abramson. A generalisation of the sampling theorem. *Inform. Contr.*, 3:26–31, 1960.

[Lan67] H. J. Landau. Sampling, data transmission and Nyquist rate. *Proc. IEEE,* 55:1701–1706, 1967.

[Mal89] S. G. Mallat. A theory for multiresolution signal decomposition, the wavelet representation. *IEEE Trans. Pattern Analysis and Machine Intelligence*, 2:674–493, July 1989.

[Mal91] S. Mallat. Zero crossings of a wavelet transform. *IEEE Trans. Inform. Theory*, 37:1019–1034, July 1991.

[Mar90] F. A. Marvasti. Over sampling as an alternative to error correcting codes. *Minisymposium on sampling theory and practice, SIAM Annual Meeting , Chicago, IL*, July 1990.

[Mar92] F. A. Marvasti. Nonuniform sampling. *Advanced Topics in Shannon Sampling and Interpolation Theory, Editor R. J. Marks II, Springer-Verlag,* 1992.

[Mar93] Robert J. Marks. Advanced topics of Shannon's sampling theory. *Springer Verlag, New York*, 1993.

[Mey91] Y. Meyer. Orthonormal wavelets. *Wavelets: Time-Frequency Methods and Phase Space, J. M. Combes, A. Grossman, and Ph. Tchamitchian, (editors), Second Edition, Springer-Verlag, New York*, (66-168), 1991.

[MGCH88] P. M. Harris M. G. Cox and H.M.Jones. A knot placement strategy for least squares spline fitting based on the use of local polynomial approximations. *Algorithms for Approximation II, Proceedings of second international conference on Algorithms for approximation, held at Royal Military College of science, Srevanham, Chapman and Hall Mathematics*, July 1988.

[MH92] S. Mallat and W. L. Hwang. Singularity detection and processing with wavelets. *IEEE Trans. Inform. theory*, 38(2):617–645, March 1992.

[Mie79] D. D. Miesel. Fourier transforms of data sampled in unequally spaced segments. *Astronomical Journal*, 84:116–126, 1979.

[ML92] F. A. Marvasti and T. J. Lee. Analysis and recovery of sample and hold and linearly interpolated signals with irregular samples. *IEEE Trans. Signal Processing*, 40(8):1884–1891, 1992.

[MZ92] S. Mallat and S. Zhong. Characterisation of signals from multiscale edges. *IEEE Trans. Pattern Analysis and Machine Intelligence*, 14(7):710–732, July 1992.

[Pon] T. Ponman. The analysis of periodicities in irregularly sampled data.

[Pou66] A. Poupolis. Error analysis in sampling theory. *Proc. IEEE*, 54(7):947–955, July 1966.

[Pou68] A. Poupolis. Systems and transforms with applications in optics. *New York: McGraw-Hill*, 1968.

[Pou77] A. Poupolis. Signal analysis. *McGraw Hill. New York*, 1977.

[Raw89] M. D. Rawn. A stable nonuniform sampling expansion involving derivatives. *IEEE Trans. Inform. Theory*, 35(6), 1989.

[RB72] R. Radzyner and P. T. Bason. An error bound for Lagrange interpolation of low pass functions. *IEEE Trans. Inform. Theory*, IT-18:669–671, Sept. 1972.

[Req80] A. Requicha. The zeros of entire functions: Theory and engineering applications. *Proc. IEEE*, 68(3):308–328, March 1980.

[RGWW77] H. Schwarzlander R. G. Wiley and D. D. Weiner. Demodulation procedure for very wide band fm. *IEEE Trans. Communications*, COM-25:318–327, March 1977.

[Ric45] S. O. Rice. Mathematical analysis of random noise. *Bell System Technical J.*, 24:46–156, 1945.

[RSC87] Y. Rahmat-Samii and R. L. Cheung. Nonuniform sampling techniques for antenna applications. *IEEE Trans. Antennas and Propagat.*, Ap-35:268–279, 1987.

[SA94] H. I. Shahein and H. M. Abbas. ECG data compression via cubic-splines and scan along polygonal approximation. *Signal Processing*, 35:269–283, 1994.

[Sha49] C. E. Shannon. Communications in the presence of noise. *Proc. IRE*, 37:10–21, Jan. 1949.

[Sir87] P. Sircar. Accurate parameter estimation of damped sinusoidal signals sampled at non-uniform spacings. *Ph D Thesis, Syracuse University, Syracuse, N. Y., December*, Dec. 1987.

[Sou88] M. Soumekh. Band-limited interpolation from unevenly spaced sampled data. *IEEE Trans. Acoust. Speech Signal processing*, ASSP-36:110–122, 1988.

[Sou89] M. Soumekh. Reconstruction and sampling constraints for spiral data. *IEEE Trans. Acoust., Speech, Signal Processing*, ASSP-37:882–891, 1989.

[SS] H. S. Shapiro and R. A. Silverman. Alias-free sampling of random noise. *SIAM J. Appl. Math.*, 8(2):245–248.

[SS88] P. Sircar and T. K. Sarkar. System identification from non-uniformly spaced signal measurements. *Signal Processing*, 14:253–268, 1988.

[SS93] J. Segman and Walter Schempp. Two ways to incorporate scale in the Heisenberg group with an intertwining operator. *J. Math. Image Vis.*, (3):79–94, 1993.

[SS94] J. Segman and Walter Schempp. On the extension of the Heisenberg group to incorporate multiscale resolution. *Wavelets and Their Applications, Kluwer Academic Publishers*, pages 347–361, 1994.

[Sta67] J. Standish. Two remarks on the reconstruction of sampled non-bandlimited functions. *IBM J. Res. Develop.*, 11(6):648, 1967.

[Sti67] D. C. Stickler. An upper bound on aliasing error. *Proc. IEEE (Lett.)*, 55:418–419, 1967.

[Stu83] R. Sturges. On interpolating gappy records for time-series analysis. *J. Geophys. Res.*, 88:9736–9740, 1983.

[TI59] B. S. Tsybakov and V. P. Iakovlev. On the accuracy of restoring a function with a finite number of terms of Kotel'nikov series. *Radio Eng. Electron. (Phys.)*, 4(3):274–275, March 1959.

[Tit39] E. C. Titchmarsh. The theory of functions. *2nd ed. The University Press, London*, 1939.

[TL64] J. B. Thomas and B. Liu. Error problems in sampling representation. *IEEE Int. Conv. Rec. (USA)*, 12(5):269–277, 1964.

[Wei63] P. Weiss. An estimate of the error arising from the misapplication of the sampling theorem. *Amer. Math. Soc. Notices*, 10.351, 1963. abstract No. 601-54.

[Wil78] R. G. Wiley. Recovery of bandlimited signals from unequally spaced samples. *IEEE Trans. Communications*, COM-26(1), Jan. 1978.

[Yen56] J. L. Yen. On the nonuniform sampling of band width limited signals. *IRE Trans. Circuit Theory*, CT-3:251–257, 1956.

[Yen57] J. L. Yen. On the synthesis of line sources and infinite strip sources. *IRE Trans. Antennas and Propagat.*, pages 40–46, Jan. 1957.

[YS87] E. Yudilevich and H. Stark. Interpolation from samples on a linear spiral scan. *IEEE Trans. Med. Imaging*, MI-6:193–200, 1987.

[YT67] K. Yao and J. B. Thomas. On some stability and interpolatory properties of nonuniform sampling expansions. *IEEE Trans. Circuit theory*, CT-14:404–408, 1967.

[Sti67]

[Stu83]

[TI59]

[Tit39]

[TL64]

[Wei63]

[Wil78]

[Yen56]

[Yen57]

[YS87] I

s

# Errata

| Location | Correction |
|---|---|
| Page 103 last line | Add $S \subset R$. |
| Page 105 first line | Add $S \subset R$. |
| Page 109 line 11 from bottom | replace $\frac{7N}{16}$ by $\frac{9N}{16}$. |
| Page 197 line 3 from bottom | Add "taken from I. Bilinskis and A. Mikelsons, Randomised signal processing. *Prentice Hall, International Series in Acoustics,Speech and Signal Processing, 1992.*" |

**Date Slip**

This book is to be returned on the date last stamped.



| | |
|---|---|
| | |
| | |
| | |
| | |
| | |
| | |
| | |
| | |
| | |
| | |
| | |